A STUDY OF SECA, THE MOTOR OF THE BACTERIAL SECRETION SYSTEM, BY SITE-DIRECTED SPIN LABELING AND EPR

A Thesis
presented to
the Faculty of the Graduate School
University of Missouri

In Partial Fulfillment
Of the Requirements for the Degree

Master of Science

---

by
DYLAN BENJAMIN JONES COOPER

Dr. Linda L. Randall, Thesis Supervisor

MAY 2008

The undersigned, appointed by the Dean of the Graduate School, have examined the thesis entitled

A STUDY OF SECA, THE MOTOR OF THE BACTERIAL SECRETION SYSTEM BY SITE-DIRECTED SPIN LABELING AND EPR

presented by Dylan Benjamin Jones Cooper

a candidate for the degree of Master of Science

and hereby certify that in their opinion it is worthy of acceptance.

_____
Linda L. Randall

_____
Michael Henzl

_____
John J. Tanner

_____
Peter A. Tipton

ACKNOWLEDGEMENTS

This work is the tangible product of the scientific method. As its contents are added to the body of scientific knowledge I wish to thank those who contributed to my success in ways both concrete and abstract. I thank Lin Randall, my mentor, for providing an environment in which both my scientific and cultural development were encouraged. The laboratory she and Jerry Hazelbauer have created is a wonderful example of how science and the arts complement one another. Knowledge is threadbare without enlightenment.

I thank the members of my committee: Mike Henzl, Peter Tipton, and Jack Tanner for welcoming me into the program and exposing nuance in biochemistry through their lectures.

I thank the members of the Membrane Group for their camaraderie and contributions to this work: Divya Amin, Jennine Crane, Simon Hardy, Wing-Cheung Lai, Mingshan Li, Angie Lilly, Chunfeng Mao, Hilary Roth, Virginia Smith, Mary Belle Streit, Yuying Suo.

TABLE OF CONTENTS

ACKNOWLEDGEMENTS ii

LIST OF FIGURES iv

LIST OF TABLES v

ABSTRACT vi

CHAPTER

1. INTRODUCTION 1
2. MATERIALS AND METHODS 9
3. RESULTS 15
4. DISCUSSION 50

APPENDIX 72

REFERENCES 79

LIST OF FIGURES

Figure Page

1. Protein labeling and spectral characteristics 17
2. Analysis of SecA by size exclusion chromatography and SDS-PAGE 21
3. Venn diagram of SecA residues and changes observed 24
4. Structure of E. coli SecA protomer 25
5. Representative EPR spectra showing constraint on SecA 29
6. EPR spectra of SecA residues showing constraint with precursor 33
7. Summary of constraints on the surface of SecA with precursor 37
8. EPR spectra of SecA residues showing constraint with SecA 38
9. Summary of constraints on the surface of SecA with SecB 41
10. EPR spectra of SecA residues showing constraint with SecYEG 42
11. Summary of constraints on the surface of SecA with SecYEG 48
12. Summary of constraints on the surface of SecA 49
13. Summary of precursor protein signal binding data 52
14. EPR spectra of SecA residues showing mobilility with SecB 59
15. EPR spectra of SecA residues showing mobility with SecYEG 61
16. EPR spectra of SecA residues showing mobility with liposomes 65
17. Summary of mobilization on the surface of SecA 71

LIST OF TABLES

Table Page

1. Summary of EPR data 30

A STUDY OF SECA, THE MOTOR OF THE BACTERIAL SECRETION SYSTEM, BY SITE-DIRECTED SPIN LABELING AND EPR

Dylan Benjamin Jones Cooper

Dr. Linda L. Randall, Thesis Advisor

ABSTRACT

For more than 3 decades, the genetic and biochemical details of the Sec system of protein export have been teased out of the Gram-negative bacterium, *Escherichia coli*. It is through these arduous efforts we know that SecA, the ATPase of the Sec system, interacts with several entities as it functions in protein translocation: unfolded precursor polypeptides, the molecular chaperone SecB, membrane phospholipids, and the membrane-embedded translocase SecYEG. Functional studies implied that some of these interactions occurred simultaneously, i.e., binding to precursor polypeptide and its chaperone SecB or to precursor polypeptide and the translocase. However, very little is known about the details of these binding sites, and it was not clear to what extent SecA interacted with these diverse ligands at distinct, adjacent or overlapping surfaces along its extended and mobile structure.

We investigated these issues using electron paramagnetic resonance (EPR) spectroscopy and site-directed spin labels at a multitude of sites on the surface of the 102 kDa SecA protein. EPR spectroscopy is very sensitive to changes in the local environment of the spin label, and thus our extensive survey of the SecA surface provided a map of interaction sites with all of its partners involved in the Sec pathway of protein export. Strikingly, we found that SecA utilizes a single interactive surface to bind its multiple partners during protein export. The locations of the residues specific for each binding partner on the common surface of SecA reveal characteristic patterns that permit

simultaneous binding of precursor and either SecB or the translocon to facilitate transfer. In addition, we have identified movement of structural elements that are likely to be involved in the transduction of chemical energy to the mechanical work that moves the polypeptide through the translocon.

Knowing the locations and relationships of these binding sites on the surface of SecA represents significant progress in revealing the mechanistic steps in the progression of passing an unfolded polypeptide chain from SecB to SecA and ultimately driving it through the secretion pore.

Chapter One

Introduction

Introduction

The diversity of life's morphological forms, from single cell organisms to multicellular plants and animals, is immediately apparent to even the most casual observer. In contrast to these outward differences is the unity found in life by the molecular sciences. The universality of fundamental physical and chemical properties gives rise to similarity between the molecules, processes and cellular organization of different organisms, each needing to perform similar functions of life.

Of these common biochemical constructs found in life, the semi-permeable lipid bilayer is the cornerstone, separating the contents of a cell from the environment or dividing it into functional compartments. With this most basic of functions, the membrane provides for the sequestration of molecules, the forming chemical and electrical gradients, and compartmentalization of biochemical reactions and processes. To carry out such functions, transmission machinery is necessary, whether it be a membrane-bound receptor that transduces a signal across the membrane or a pore that conducts molecules.

Membrane-enclosed organelles found in eukaryotic cells, such as the nucleus, endoplasmic reticulum or chloroplast, organize different cellular processes into compartments. Although membrane-enclosed organelles are absent in prokaryotes, they do have distinct compartments. In the Gram-negative bacterium, *Escherichia coli*, there are four functional compartments: two aqueous compartments and two membranous. The cytoplasm is the central compartment and is bounded by the cytoplasmic membrane, also known as the inner membrane. These compartments are further enveloped by an outer

membrane and the space defined by the inner and outer membranes is called the periplasm.

Targeting and trafficking proteins to and across membranes are ubiquitous features in life, and have dedicated machinery that accomplishes this function. A bacterium is an ideal model to use when studying this phenomenon because it offers the investigator a tractable system to work with, yet it still contains the fundamental mechanisms within the pathway.

Protein Secretion

In *E. coli*, there are 2 primary mechanisms by which proteins are inserted into or translocated across the inner membrane. Precursor proteins targeted for entry into a secretion pathway have some common characteristics, namely a hydrophobic signal sequence and a mature region from which the signal sequence is cleaved proteolytically once translocation across the inner membrane occurs.

The twin-arginine translocation (Tat) system is composed of four membrane proteins that transport precursor proteins already folded in their native state across the membrane. Precursor proteins destined for the Tat system of export have a conserved leader sequence containing a distinctive twin-arginine motif, are often accompanied by red-ox cofactors (Sargent et al. 2007; Brüser 2007), and their interaction with the translocation machinery is not mediated by soluble proteins that target them for the Tat pathway (Brink et al. 1998). In contrast to proteins exported by the Tat system, a majority of the precursor proteins destined for export do so by the general secretory (Sec) system and must be translocated while in a nonnative conformation. The Sec system is unable to translocate precursor proteins with stable tertiary structure, so the precursors

must be captured before they fold by a family of soluble proteins called chaperones (Randall and Hardy 1986). Precursor proteins in binary complex with the chaperone are then delivered to the translocon in ternary complex with the SecA ATPase. The research presented covers the Sec system, centered around SecA.

Sec Translocon

The function of the Sec translocon is to transport periplasmic and outer membrane proteins across the cytoplasmic membreane. The Sec translocon comprises a multisubunit protein complex including the integral membrane proteins SecY, SecE, SecG, and the peripheral membrane protein, SecA (Brundage et al. 1990; Akimaru et al. 1991). The core of the translocon, the SecYEG complex, is highly conserved across all organisms. SecY and SecE are homologous to the α-subunit and β-subunit of the eukaryotic Sec61p translocation channel found in the membrane of the endoplasmic reticulum (Hartmann et al. 1994; Walter and Johnson 1994). Although the exact role of the complex is not yet understood, SecD, SecF, and YajC form an accessory heterotrimer complex that supports translocation (Economou et al. 1995). Leader peptidase, a membrane-bound endopeptidase, removes the N-terminal amino acids identified as the leader sequence, once translocation of the precursor is partially complete (Dalbey et al. 1997).

Precursor Proteins

Precursor polypeptides are characterized by two regions, the leader sequence and mature domain. Although the length and sequence of the leader varies, it is typically between 15 and 30 amino acids in length and can be subdivided into 3 regions: a hydrophobic central region, bounded by a positively charged N-terminal region and polar

C-terminal region. Changing these leader sequence characteristics can have effects on the efficiency of precursor translocation. When one considers the hydrophobic center region of the leader sequence, there are two changes that increase translocation efficiency: an increase in length or an increase in hydrophobicity (Chou 1990). Although it has been demonstrated that the positively charged N-terminal region of the signal sequence is not required for translocation, changing the region to be negatively charged, or even neutral, decreased the rate of precursor export (Gennity et al. 1990). It is possible that changes to this region of the leader sequence interfere with the specific interaction between SecA and the precursor (Akita et al. 1990; Gelis et al. 2007). The export defects caused by decreasing the positive charge on the N-terminal region can be compensated by an increase of hydrophobicity in the middle region of the leader (Hikita and Mizushima 1992). The recognition site for leader peptidase, the endopeptidase that proteolytically cleaves the leader sequence from the mature domain (Zwizinski and Wickner 1980; Kuhn and Wickner 1985), is located in the C-terminal end of the leader sequence, but this region of the leader sequence is not necessary for translocation (Dalbey and Wickner 1985).

Although some precursor polypeptides enter a translocation pathway by means of signal sequence recognition, as is the case with SRP, entry into the Sec system by way of SecB requires interaction with the mature region of the protein in a nonnative state (Randall and Hardy 1986; Randall et al. 1990; Smith et al. 1996; Crane et al. 2006). In this case, the leader of the precursor polypeptide plays an indirect role by retarding the folding of the mature region, thus promoting interaction between precursor and SecB (Park et al. 1988; Liu et al. 1989).

SecB

In *E. coli*, translocation of precursor proteins by the Sec system may occur either post-translationally or co-translationally, because elongation and translocation are uncoupled (Randall 1983). These peptides are maintained as unfolded precursors with the aid of molecular chaperones. Found in Gram-negative bacteria, SecB is one such cytosolic chaperone dedicated to capture of precursor proteins, targeting them for translocation. SecB binds promiscuously to proteins in nonnative structure and maintains precursor proteins in an unfolded state through a kinetic partitioning between association with SecB and a folded state (Hardy and Randall 1991). In solution, SecB exists as a 69 kDa homotetramer, organized as a dimer of dimers (Múren et al.; Topping et al. 2001; Dekker et al. 2003).

SecA

SecA is an extended multidomain protein that is central to the Sec export pathway. SecA is essential to cell viability, and modulates protein export in a cell by regulating its own expression (Oliver et al. 1990). *In vivo*, SecA is found in the cytoplasm and in the membrane, divided nearly equally between both compartments (Cabelli et al. 1988; Chun and Randall 1994). SecA is a homodimer with a protomer molecular weight of 102 kDa (Schmidt et al. 1988; Driessen 1993). The SecA protomer has two primary structural domains: an N-terminal domain of 65 kDa, and a C-terminal domain of 30 kDa (Price et al. 1996; Karamanou et al. 1999). The N-terminal domain contains two nucleotide-binding folds, which form a high-affinity nucleotide binding site (Mitchell and Oliver 1993; Keramisanou et al. 2006; Papanikolau et al. 2007), as well as binding sites for precursor polypeptide and its leader sequences (Kimura et al. 1991;

Chou and Gierasch 2005; Gelis et al. 2007). The C-terminal domain of SecA has been shown to contain a zinc binding site (Fekkes et al. 1999) and binds both SecB (Breukink et al. 1995; Fekkes et al. 1997; Crane et al. 2005) and acidic phospholipids (Lill et al. 1990; Breukink et al. 1995). In solution, SecA is in equilibrium between monomer and dimer states, with an approximately micromolar equilibrium constant (Woodbury et al. 2000). The oligomeric state of SecA, while associated with SecYEG and performing translocation, is presently under debate. It is still not clear if a dimeric state is essential for SecA function (Jilaveanu et al. 2005; Jilaveanu and Oliver 2006) or a monomeric state is sufficient (Or et al. 2002; Or et al. 2005; Or and Rapoport 2007). The X-ray crystal structure for SecA has been solved in *Bacillus subtilis* (Hunt et al. 2002), *Mycobacterium tuberculosis* (Sharma et al. 2003), *Thermus thermophilus* (Vassylyev et al. 2006), and *Escherichia coli* (Papanikolau et al. 2007). The figures in this work were produced using the crystal structure from *E. coli*.

SecA is a dynamic protein that has been shown to interact with nearly all components of the Sec export pathway. Cunningham and Wickner first demonstrated that SecA interacts with precursor proteins early in the export pathway (Cunningham and Wickner 1989). This interaction is known to occur with both the leader sequence and mature domain of the precursor protein (Akita et al. 1990; Lill et al. 1990; Gelis et al. 2007). In solution, and in the absence of precursor, interaction between SecA and SecB is characterized by a dissociation constant (K_d) that is approximately micromolar (den Blaauwen et al. 1997), with at least three sites of interaction (Patel et al. 2006). This interaction is of lower affinity than when SecB is already in complex with precursor and subsequently forms a complex with SecA ($K_d \sim 10$ nM) (Fekkes et al. 1997).

SecA binding to the membrane is accomplished in two ways: 1) a low-affinity interaction with acidic phospholipids (Lill et al. 1990; Chen et al. 1996), and 2) a high-affinity interaction with the Sec translocon, through SecY (Matsumoto et al. 1997). Protein translocation begins when SecA interacts with the heterotrimer SecYEG, precursor protein, and ATP. A conformational change by SecA to a more open state is achieved when SecA binds ATP. During this conformational change, the membrane-bound face of SecA is exposed to the periplasm (Kim et al. 1994; van der Does et al. 1996). When this occurs, 20 to 30 amino acids of the precursor protein are inserted into the membrane (Schiebel et al. 1991; Joly and Wickner 1993; Economou and Wickner 1994; van der Wolk et al. 1997) and SecB is released from the complex (Fekkes et al. 1997; Fekkes et al. 1998). Cycles of insertion and deinsertion of SecA are driven by ATP binding and hydrolysis, continuing precursor translocation across the membrane (Economou and Wickner 1994; Kim et al. 1994; Economou et al. 1995).

Chapter Two

Materials and Methods

Materials and Methods

Strains and Mutagenesis

The strategy of site-directed spin labeling requires that a reactive cysteine residue at the site of interest be the only residue available for modification by the nitroxide reagent via sulfhydryl chemistry. SecA contains 4 native cysteines, which we replaced with serine to create our base protein. The plasmid pT7SecAC4 (from D. Oliver, Wesleyan University) carrying the gene for the base protein driven by the T7 promoter was modified by standard recombinant DNA techniques (Quickchange, Stratagene) to generate the cysteine variants used here. The plasmids were transformed into the BL21(DE3) strain of *E. coli*.

SecA Purification

BL21(DE3) cells containing a derivative pT7SecAC4 plasmid were grown in Luria Broth with 100 μg / ml ampicillin at 35 °C. SecA expression was induced by addition of isopropyl-1-thio-β-D-galactopyranoside to 0.1 mM at an optical density of 0.6 at 560 nm and growth was continued 2.5 hours. Cells were harvested, washed and suspended to 2 g / mL in 20 mM HEPES-KOH (pH 7.6). The cell suspension was frozen by drop-wise addition into liquid nitrogen and stored at -80 °C. The cell suspension was thawed on ice and dithiothreitol (DTT) and phenylmethylsulfonylfluoride (PMSF) were added to 2 mM and 1 mM final concentrations, respectively. Cells were mechanically disrupted using a French pressure cell at 8000 psi in two successive passes. Between the first and second pass, DTT and PMSF were added to the cell lysate to 4 mM and 2 mM, respectively. The cell lysate was subjected to centrifugation using the Optima L-90K ultracentrifuge (Beckman Instruments) and the Ty65 rotor for 2 hours, 65,000 rpm, 4 °C.

The supernatant was passed through a syringe filter containing a polyethersulfone membrane with a pore size 0.45 μm. The filtrate was then frozen by drop-wise addition into liquid nitrogen and stored at -80 °C.

The filtered lysate was loaded at 0.5 mL / min onto a 5 mL HiTrap Blue HP affinity column (GE Healthcare) equilibrated in 10 mM HEPES-KOH, 2 mM DTT (pH 7.6). at 0.5 mL / min. The column was washed successively with column buffer, 0.4 M NaCl in column buffer, and then eluted with 10 mM HEPES-KOH, 50% (v/v) ethylene glycol, 1.5 M NaCl, 2 mM DTT (pH 7.6). Fractions containing SecA were pooled and concentrated to a volume ≤ 1.0 mL using a Centriprep centrifugal filter device with Ultracel membrane, 50K MWCO (Millipore). The concentrated proteins were stored at -80 °C until spin-labeling.

Inner Membrane Vesicles and Liposomes

Inner membrane vesicles were prapared as described previously (Woodbury, JBC 2000). Liposomes were prepared from *E. coli* polar lipids (Avanti Polar Lipids, Inc.) by extrusion using a LiposoFast apparatus (Avestin, Inc.) with a polycarbonate membrane of 100 nm pore size. The lipid concentration in both vesicles and liposomes was determined using the following method and used at a final concentration of 7.5 mM. To sample tubes containing liposomes, inner membrane vesicles or a phosphorus standard solution, 0.45 ml of a 8.9 N H_2SO_4 solution was added and heated to 200-215 °C for 25 minutes. The sample tubes were removed from the heat source and allowed to cool for 5 minutes before adding 150 μl H_2O_2. The sample tubes were then heated for an additional 30 minutes, observed to be colorless, and subsequently returned to ambient temperature. After adding 3.9 ml deionized water to each sample tube, 0.5 ml of a 10% (w/v) ascorbic

acid solution was added, and the samples were mixed by vortex 5 times. Sample tubes were then capped with a glass marble and heated to 100 °C for 7 minutes, after which they were returned to ambient temperature. Absorbance for each sample was determined at 820 nm.

Spin Labeling of SecA Variants

Immediately before labeling with the nitroxide reagent (1-oxyl-2,2,5,5-tetramethylpyrroline-3-methyl)-methanethiosulfonate (Toronto Research Chemicals Inc.), the reducing agent, DTT, was removed by exchange from the usual storage buffer (10 mM HEPES-KOH, 50% ethylene glycol, 1.5 M NaCl, 2 mM DTT (pH 7.6)) into 10 mM HEPES-HAc, 300 mM KOAc (pH 6.7) using a Nap10 column (Amersham). The proteins were concentrated using a Nanosep Centrifugal Device with Omega membrane, 30K MWCO (Pall). Typically 0.2 mL of each SecA variant, at a concentration of approximately 440 μM monomer, was incubated with a 2.5 fold molar excess of the spin labeling reagent. The reagent was prepared as a stock of 100 mM in acetonitrile and stored in the dark at -80 °C. Acetonitrile was not allowed to exceed 2% of the total volume in the incubation reaction. The reaction was allowed to proceed on ice in the dark for 2-3 h. To remove excess spin label, the entire reaction mixture was applied to a Nap5 column (Amersham) equilibrated in 10 mM HEPES-HAc, 300 mM KOAc, 5 mM $Mg(OAc)_2$, 1 mM EGTA (pH 6.7) and eluted in ten 90 μL fractions. The fractions were examined by EPR spectroscopy and were pooled to maximize the absorbance spectrum intensity and minimize free spin. The proteins were concentrated using a Nanosep Centrifugal Device with Omega membrane, 30K MWCO (Pall) to a final concentration between 200 – 400 μM SecA monomer and stored at -80 °C. Spin-labeled protein

concentrations were determined spectrophotometrically at 280 nm using an extinction coefficient of 0.77 mL mg^{-1} cm^{-1}. The spin-labeled variants are designated by the amino acid and residue number that has been substituted by cysteine and modified by the nitroxide side-chain, R1. Thus, S350R1 indicates that serine at position 350 was converted to cysteine and reacted with the spin label reagent.

Activity Assay

High performance liquid size exclusion chromatography was performed using a TSK G3000SW column (7.5 mm i.d. x 60 cm) (TosoHaas) in 10 mM HEPES-KOH, 300 mM KOAc, 5 mM $Mg(OAc)_2$, pH 7.6, at a flow rate of 0.6 mL / min and temperature of 7 °C. SecA and SecB were applied to the column at concentrations of 6 μM and 12 μM, respectively, both separately or as a mixture. A miniDAWN Tristar multiangle laser light scatter detector (Wyatt Technologies), an Optilab DSP differential interferometric refractometer (Wyatt Technologies), and a UV detector (Model 116, Gilson) were used to analyze the eluent on-line. Eluent was collected in 0.24 mL fractions for subsequent analysis by gel electrophoresis. All SecA variants were folded and demonstrated a monomer-dimer equilibrium. All species were shown to bind SecB, with the exception of SecAI642R1. SecAI642R1, however, was well-behaved and did bind precursor ligand.

Calculation of Timescale of Tumbling

EPR is sensitive to motion of the nitroxide side-chain in the timescale of 0.1 ns to 20 ns. The molecular tumbling of SecA (τ_c = 104 ns) is too slow to be averaged into the spectra reported here, and thus the spectra are interpreted in terms of local fluctuations of the backbone and internal motion of the nitroxide side-chain. The timescale of tumbling

(τ_c) for SecA was calculated from the rotational diffusion constant (D_r) of the protein as follows:

$$\tau_c = \frac{1}{6 D_r}; D_r = \frac{kT}{8\pi\eta a^3},$$

where k is Boltzmann's constant (1.3807 x 10^{-16} erg·K^{-1}), T is temperature (279 K), η is the viscosity of the solvent (1.74 kg·m^{-1}·s^{-1}) at 279 K, and a is the radius of hydration. The radius of hydration of SecA, determined prior to this study by quasi-elastic light scatter, is 3.8 nm. The centimeter-gram-second system of units was used, and all values were converted as necessary.

Electron Paramagnetic Resonance Spectroscopy

EPR spectroscopy was performed on an X-band Bruker EMX spectrometer with a high sensitivity resonator. Reaction mixtures of 5 µL (60 µM spin label) were loaded into synthetic silica capillaries (0.6 mm i.d. x 0.84 mm o.d.) sealed at one end. Spectra were acquired using incident microwave power at 20 mW and a 100 kHz field modulation of 1 to 4 gauss as appropriate. Spectra were recorded with a scan width of 100 gauss centered at 3356 gauss. For each spectral line, 15 scans were averaged. All spectra were normalized and further analyzed using programs built on the LabVIEW Application Framework (National Instruments) by Christian Altenbach (UCLA).

Molecular Structure Images

All protein structure images use the crystal coordinates for *E. coli* SecA (PDB ID: 2FSF) and were generated using the PyMOL Molecular Graphics System.

Chapter Three

Results

Results

We have created a collection of 48 SecA variants, each containing a single paramagnetic label. Using this collection of labeled proteins with electron paramagnetic resonance spectroscopy, we have defined a surface on SecA that interacts with its binding partners.

Our approach involves introducing a nitroxide side-chain at a specific site on SecA by using cysteine substitution mutagenesis, followed by attachment of the nitroxide label to this cysteine residue through sulfhydryl-specific chemistry. The spin label reagent (1-oxyl-2,2,5,5-tetramethyl pyrroline-3-methyl)-methanethiosulfonate used in this research, and the nitroxide side-chain it generates, is designated R1 and is shown in Figure 1A.

The line shape of an electron paramagnetic resonance spectrum of spin-labeled SecA contains information about the mobility of the nitroxide side-chain on the nanosecond timescale, the origin of the mobility being rotation about the bonds within the nitroxide side-chain or local backbone fluctuations (Columbus 2002). If, while in complex with SecA, a binding partner makes direct contact with the nitroxide or is in close proximity, it is reasonable to expect the motion of the nitroxide to be constrained. As the mobility of the nitroxide side-chain goes from mobile to constrained, two readily visible features of an EPR spectrum change. First, the central line width broadens (Figure 1B, ΔH_{pp}), which can also be seen as a decrease in the central line intensity, since all spectra collected are normalized. Second, the total spectral intensity is spread over a wider range of the magnetic field, which presents itself as an overall increase of spectral breadth.

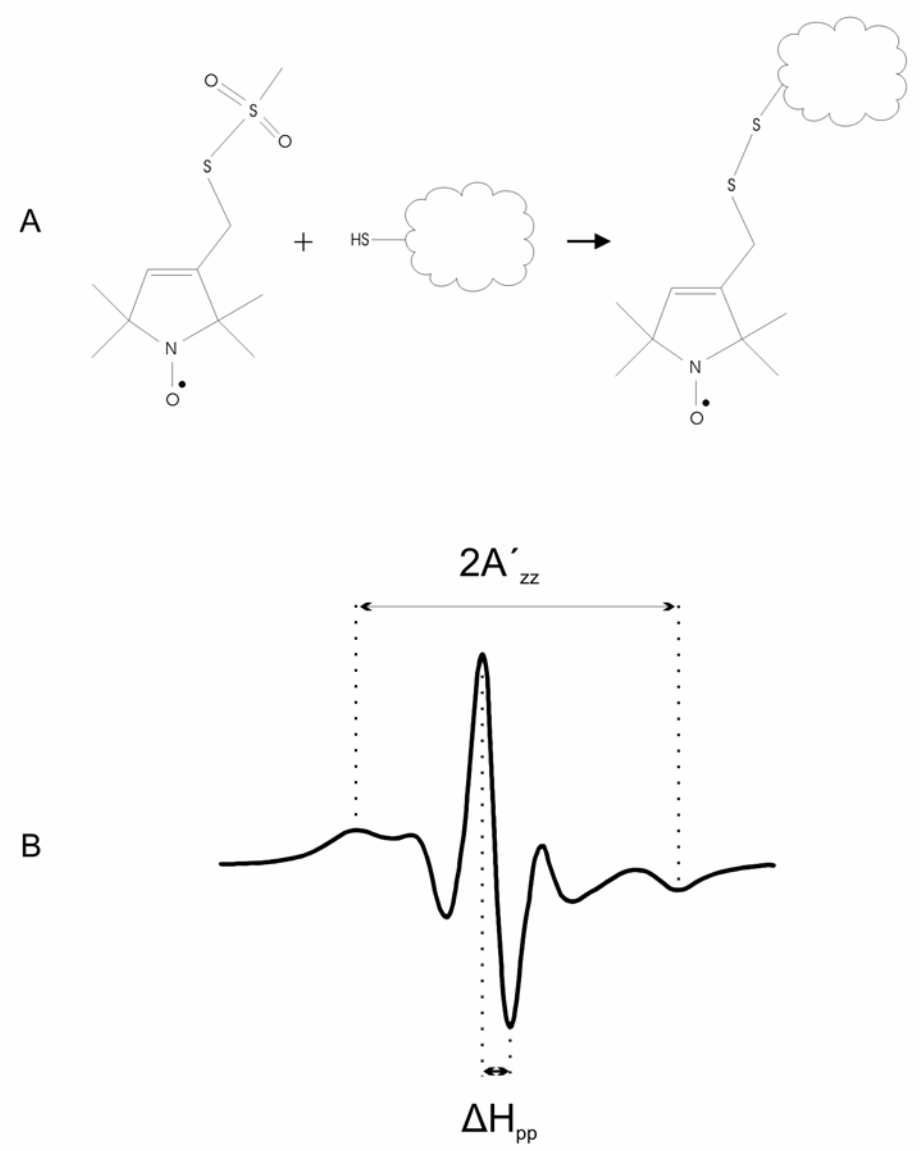

Figure 1. Schematic of protein labeling and spectral characteristics. A) The nitroxide label reagent is attached to a cysteine residue in the protein through sulfhydryl chemistry. B) A typical EPR spectrum showing the spectral breadth ($2A'_{zz}$) and central line width (ΔH_{pp}).

One may use the separation of the hyperfine extrema (Figure 1B, $2A'_{zz}$) as a measurement of spectral breadth when the hyperfine extrema are well resolved and the protein is of sufficient size that its movement is invisible to EPR. By contrast, if contacts are made with a structural element of SecA, possibly inducing conformational changes nearby or propagated over distance which released constraints that exist in the free protein, this increase in nitroxide mobility would present itself as a narrowing of the spectral breadth and an increase in central line intensity. Considering that both spectral changes are apparent by visual inspection, we use them here as simple indicators of mobility to determine which areas on the surface of SecA interact with its ligands. Although it is a formal possibility that constraints placed on the nitroxide side-chain could result, not from direct contact, but from a conformational change, or from contact with an immediate neighbor, with careful examination of all sites showing decreased mobility, we will be able to determine surfaces of SecA that interact with its binding partners.

We conducted our survey by random selection of amino acids on the surface of SecA to modify. When a spectral change was observed while SecA was in complex with one of its binding partners, we expanded the search to the neighboring amino acid residues to reveal patterns of mobilization or constraint on the surface of SecA. Labeled SecA variants were examined in complex with each of its binding partners: the molecular chaperone SecB, precursor forms of two natural ligands of the general secretory system, the periplasmic galactose-binding protein (pGBP) and the outer membrane protein OmpA (proOmpA), a mature, but unfolded form of galactose-binding protein, and the translocon of the Sec system, SecYEG. To distinguish the binding effects of SecY, carried by inverted membrane vesicles, from the effects of SecA binding phospholipids, spectra

gleaned from examination of SecA in complex with SecYEG were compared to spectra resulting from SecA in complex with liposomes.

Five dimeric structures of SecA have been solved through X-ray crystallography, each differing in the interfacial contacts between the two SecA protomers (Hunt et al. 2002; Sharma et al. 2003; Osborne et al. 2004; Vassylyev et al. 2006; Papanikolau et al. 2007). The protomer structures of SecA are related to great degree, and show only two different conformations: an open state (Osborne et al. 2004) and a closed state (Hunt et al. 2002). The crystal structure of the SecA protomer from *E. coli* (Papanikolau et al. 2007) was used as a guide in selection of solvent-exposed side chains for labeling to maximize the probability of observing interactions while minimizing the risk of disrupting the native structure of SecA.

We examined the spin-labeled SecA species with size-exclusion chromatography to ensure they were folded and functional. Interpretation of these results was confounded by the complexity of the system. Not only does SecA undergo monomer-dimer equilibrium, but free SecA and SecB re-equilibrate with the complexes they form. To overcome these difficulties, it was necessary to determine the absolute molar mass at protein concentrations above the dissociation constant, so as to push the equilibria towards formation of complex. The elution position of a protein during size exclusion chromatography depends on both mass and hydrodynamic radius. It is the latter characteristic that underlies the danger of judging mass from position of elution alone, as conformational changes in a protein will alter elution position. Therefore, absolute molar masses of eluted protein species or complexes were determined by coupling a detector of protein concentration with a multi-angle light scattering detector. Refractive index was

used because it changes as a function of concentration (dn / dc), and this change is constant for all proteins. Intensity of light scatter by a particle is proportional to the product of concentration and weight average molar mass of the light-scattering particle.

An experimental series performed on a single spin-labeled SecA species comprises 2 chromatography runs: Application of the spin-labeled protein on the column alone, followed by application of a mixture of spin-labeled SecA and wild-type SecB. The base SecA protein from which the cysteine mutants are made does not contain the native cysteines in the C-terminal tail, thus eliminating the zinc binding site and monomerizing SecA when in complex with SecB. It is for this reason that SecB is included in the mixture at two-fold molar excess tetramer over SecA dimer so that all SecA proteins have an available binding partner. When applied separately to a TSK-G3000SW size exclusion column, the unmodified SecA and SecB proteins elute separately (Fig. 2A, green and red). The molar mass determined for SecB was 69 kDa, which is in agreement with that of the tetrameric SecB (Randall et al. 2005). Consistent with a self-associating species, the mass of SecA was greatest at the apex of the peak, decreasing over the tailing edge. Fractions corresponding to the elution profile of SecA and SecB applied separately were analyzed by SDS-14% polyacrylamide gel electrophoresis, indicating the fractions in which they elute (Figs. 2B, 2C). When applied in a mixture, SecA and SecB yield a single peak (Fig. 2A, blue) with a molar mass of 168 kDa at the apex, where the complex would be most populated. This mass is consistent with an equilibrating mixture which has a stoichiometry of a single SecA protomer (102 kDa) bound to a tetrameric SecB (69 kDa). Fractions corresponding to the elution profile of the mixture of SecA and SecB were analyzed by SDS-14% polyacrylamide gel

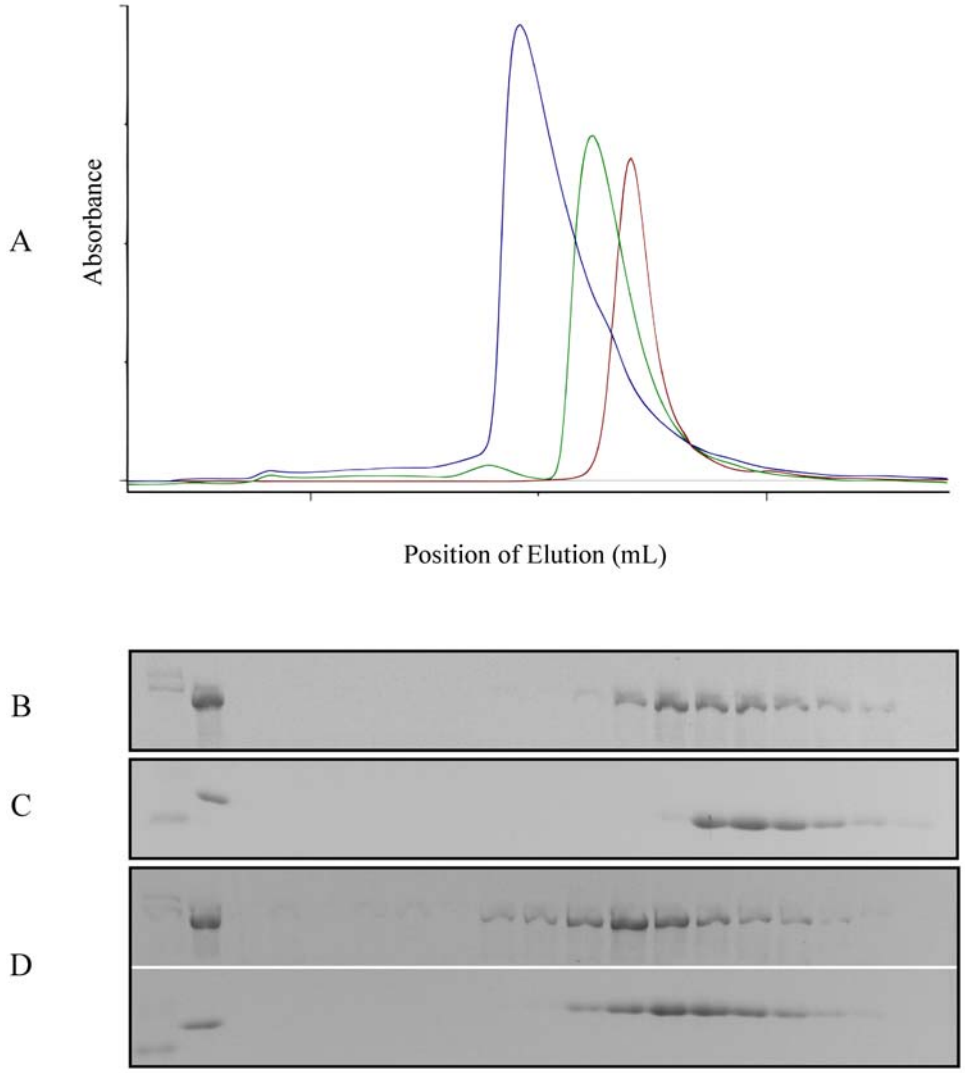

Figure 2. Analysis of SecA by size-exclusion chromatography and SDS-polyacrylamide gel electrophoresis. A) Size-exclusion chromatography of SecB, applied alone (red), SecA, applied alone (green), and SecA and SecB, applied in a mixture (blue). Stained gels of chromatography fractions of SecA, applied alone (B), SecB, applied alone (C), and SecA and SecB, applied in a mixture (D).

electrophoresis, revealing both proteins co-eluted earlier than either eluted separately (Fig. 2D).

All spin-labeled SecA species constructed were folded and exhibited an equilibrium between monomer and dimer forms, as does wild-type. Only one spin-labeled species did not show interaction with SecB during size-exclusion chromatography. The remaining competent SecA species were subsequently used in electron paramagnetic resonance spectroscopy studies.

EPR experiments conducted in this study used spin-labeled SecA at 30 μM dimer, yielding 60 μM spin label in each reaction. To this mixture, a ligand of SecA was added to the following final concentration: precursor ligands, 60 μM; SecB, 60 μM tetramer; inner membrane vesicles containing SecYEG or liposomes, 7.5 mM lipids. In all experiments, the buffer was 10 mM HEPES-KOH, 300 mM KAc, 5 mM $Mg(OAc)_2$, pH 6.7.

Additional components were introduced to the reaction mixtures with the addition of the precursor ligands. This was compensated for by addition of the same components to the SecA alone mixtures, so as to impose the same solution conditions on both the SecA-ligand and SecA alone experiments.

To form complexes between SecA and precursors, the ligands, unfolded in denaturant (either 1M GnHCl or 4M urea), were added by rapid dilution into a solution containing SecA held on ice so the final concentration of the denaturant was either 0.17 M GnHCl or 0.4 M urea. Galactose-binding protein was an ideal ligand for use in these studies because of the exquisite way its rate of folding can be modulated by the presence or absence of calcium. In the absence of calcium, GBP folding rate is markedly

decreased (Topping and Randall 1997), thus experiments using galactose-binding protein contained EGTA (1 mM) in the buffers to sequester calcium away from GBP. Finally, all spectra were collected at 6 °C to slow the rate of folding.

The EPR data collected are summarized by a Venn diagram with seven sets (Fig. 3) to illustrate the effects seen at residues with the respective binding partner. The three most right sets (Fig. 3A) contain residues that show a spectral line shape change indicating a constraint when mixed with a binding partner. The three most left sets (Fig. 3C) contain residues that show spectral line shape changes indicating mobility. Residues for which no spectral line shape change was observed with any binding partner are shown in the central set (Fig. 3B). Additionally, structural diagrams of the *E. coli* SecA protomer are displayed as CPK models to show how the examined residues are distributed on the surface of SecA.

The color scheme of the Venn diagram and the structural models are coordinated so the residue number in the Venn diagram indicates the structural subdomain in which the residue resides. The subdomains of SecA include two nucleotide-binding folds, NBF1 and NBF2 (shown in light brown), a long α-helix, the helical scaffold domain, HSD (blue), a precursor binding domain, PDB (pink), a helical wing domain, HWD (purple), an intramolecular regulator of ATPase, IRA1 (dark red), and a short α-helix composed of 10 residues from 600 to 609 (green) that connects NBF2 to HSD (Fig 4). The N-terminal residues 1 through 8 and C-terminal domain (residues 836-901) were not resolved in this crystal structure. We have elected to show the sites of interaction on the open form of the *E. coli* SecA protomer, on the basis that some residues that show

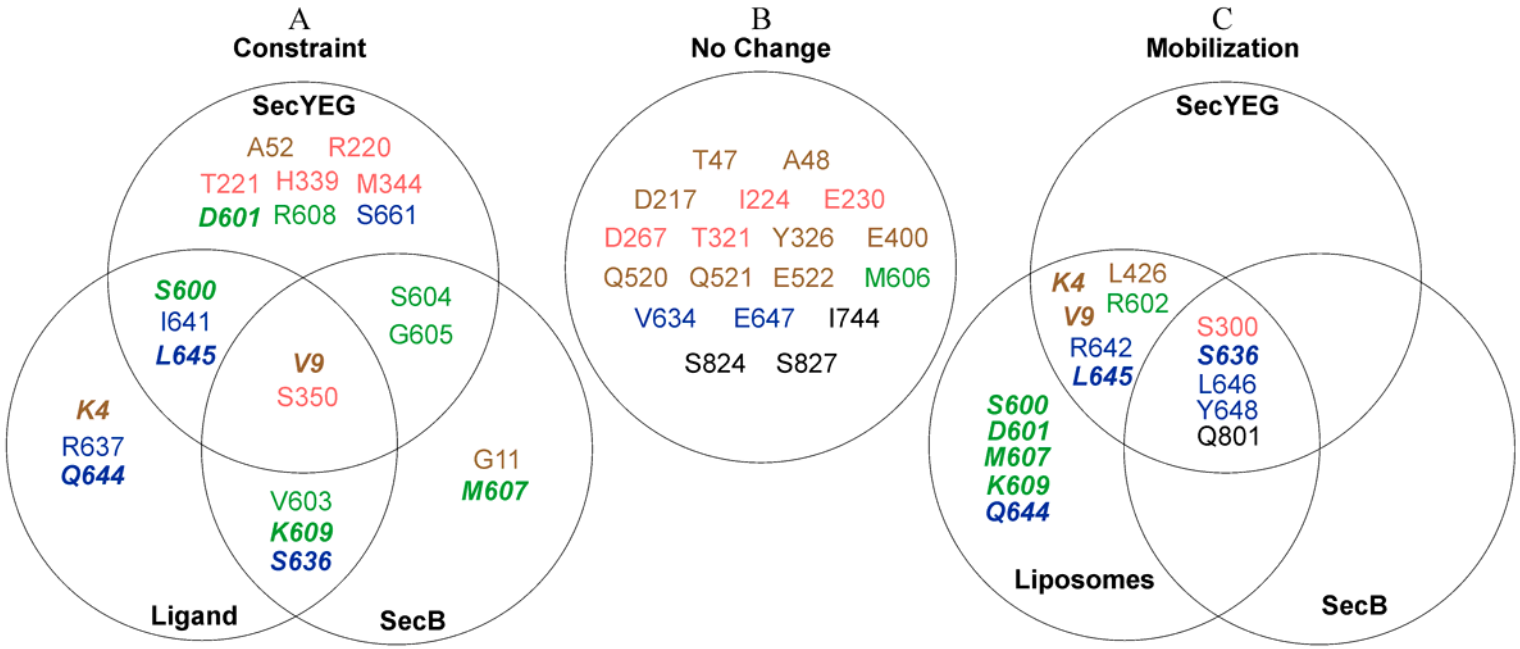

Figure 3. Venn diagram of SecA residues and the change observed. Residues are color coordinated by SecA domain: N-terminal domain (brown), small linking α-helix (green), helical scaffold domain (blue), and precursor cross-linking domain (red). Residues in bold italics showed both constraint and mobilization.

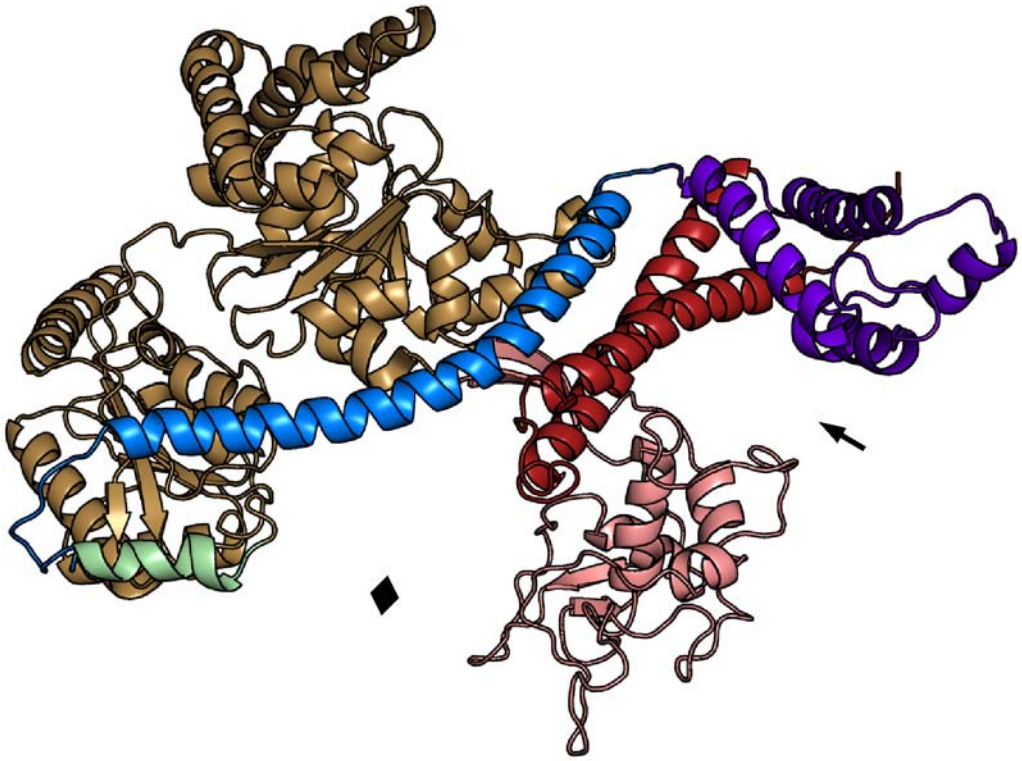

Figure 4. Structure of SecA protomer. The bottom structure is rotated 90° about the x-axis. The domains are colored as follows: NBF1 and NBF2 (light brown), small linking α-helix (green), HSD (blue), HWD (purple), IRA1 (dark red), PBD (pink). The arrow shows the cleft proposed by Osborne et al. The diamond shows the cleft found in this study.

constraint with a binding partner are buried in the closed state, but accessible in the open state. The structural movement that relates the open and closed conformations is a 60° rigid body rotation of the PBD, breaking the interface between the precursor binding domain and the helical scaffold domain and helical wing domain, resulting in the formation of a cleft (Fig. 4, arrow) that comprises these structural elements. This cleft is the same that Osborne and Rapoport propose, after structural examination, binds precursor polypeptides. Our observations, however, define a surface on the opposite side of the PBD that interacts with all ligands we have examined: precursor polypeptides, SecB, and SecY. This large cleft (Fig. 4, diamond) is formed by surfaces of the precursor-binding domain, helical scaffold domain, the small linking α-helix (residues 600-609), and both nucleotide-binding folds.

The spectra for all spin-labeled SecA species showing constraints with precursor, SecB, and SecYEG are shown in Figures 6, 8 and 10, respectively, and are summarized in Table 1. The important spectral changes caused by a constraint of the nitroxide can be seen when looking at residue R637, with and without precursor galactose-binding protein, residue K609, with and without SecB, and residue S350, with and without SecYEG (Fig. 5). The essential spectral features that arise from a constraint can be seen as a decrease in central line amplitude and broadening of the hyperfine extrema, more apparent at the low-field side. Of the residues showing constraint, 17 of 23 lie on the same face of SecA, located along the α-helix of the HSD, the small linker α-helix, or near the amino terminus, leading us to the conclusion that SecA has a single surface that interacts with all of its binding partners.

Sites of contact for precursor polypeptide ligand were found in the N-terminal region of SecA, the PBD, the small linker α-helix, and most numerously, the HSD. To define these sites for unfolded polypeptide ligands, we used two proteins that are known exports of the general secretory pathway: galactose-binding protein (Powers and Randall 1995) and outer membrane protein A (Collier et al.1988). As precursors, both preGBP and proOmpA carry N-terminal signal sequences. In addition to the precursor form of GBP, the mature form was used, which lacks the 23 residue long signal sequence. The degree of change in spectral line shape was the same for all SecA residues examined, whether the precursor or mature form of polypeptide ligand was examined in complex with SecA. Therefore, the site we have defined as binding unfolded polypeptide ligand is not specific for the leader sequence, but interacts with the mature portion of the ligand. When folded, all polypeptide ligands showed no interaction with SecA, seen as no change in spectral line shape, whether the signal sequence was present or absent. This specific binding of polypeptide in an unfolded state is similar to the interaction between the molecular chaperone SecB and unfolded polypeptide ligands, which has been well characterized (Randall and Hardy 1995).

When SecB was added alone to the spin-labeled SecA variants, the data defined a SecB binding site (Fig. 9). A majority of the residues that show contact with SecB are located on the small linker α-helix, while the other residues are located in the the N-terminal region of SecA, the PBD and HSD. Of the 9 residues that showed interaction with SecB, only M607 bound specifically, while the remaining residues showed interaction with other ligands. The N-terminal residue G11 also serves as a contact site for phospholipids and two residues, V9 and S350, showed constraint with SecB as well as

all other ligands used. Additionally, a collection of residues demonstrated mobilizations when SecB was added (S300, S636, L646, Y648, Q801). These residues are a subset of the residues showing mobilization with phospholipids (described below) and produced the same extent of change.

Addition of SecY-containing inverted membrane vesicles to spin-labeled SecA revealed 15 constrained residues (Fig. 11). Notably, there is a strong constraint at residue S350. Additionally, four other residues that lie within the large cleft we define make contact with SecY at positions R220, T221, H339, and M344. Constraints imposed by SecY are also seen along the opening of the cleft on the HSD (I641, L645, S661), and at the small linker α-helix (S600, D601, S604, G605, R608).

The effects of phospholipids in the absence of SecYEG translocon were tested on spin-labeled SecA in the form of liposomes. Constraint of two residues, G11 and K609, was observed at 6 °C. At 27 °C, G11 remained constrained, while K609 became mobilized. All other residues exhibiting a spectral change with liposomes were characterized as mobilizations, and this population represents one-third of the total number of residues examined (16 out of 48).

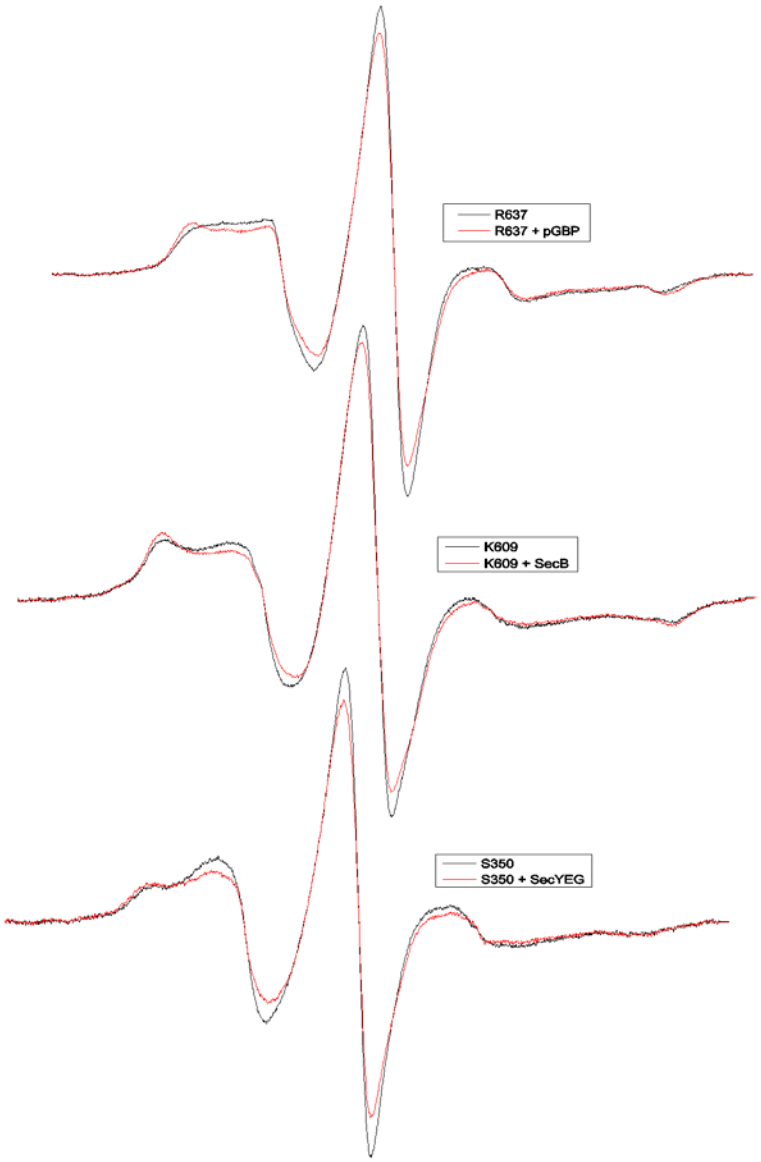

Figure 5. Representative EPR spectra showing constraint on SecA residues while in complex with precursor galactose-binding protein, SecB, or SecYEG.

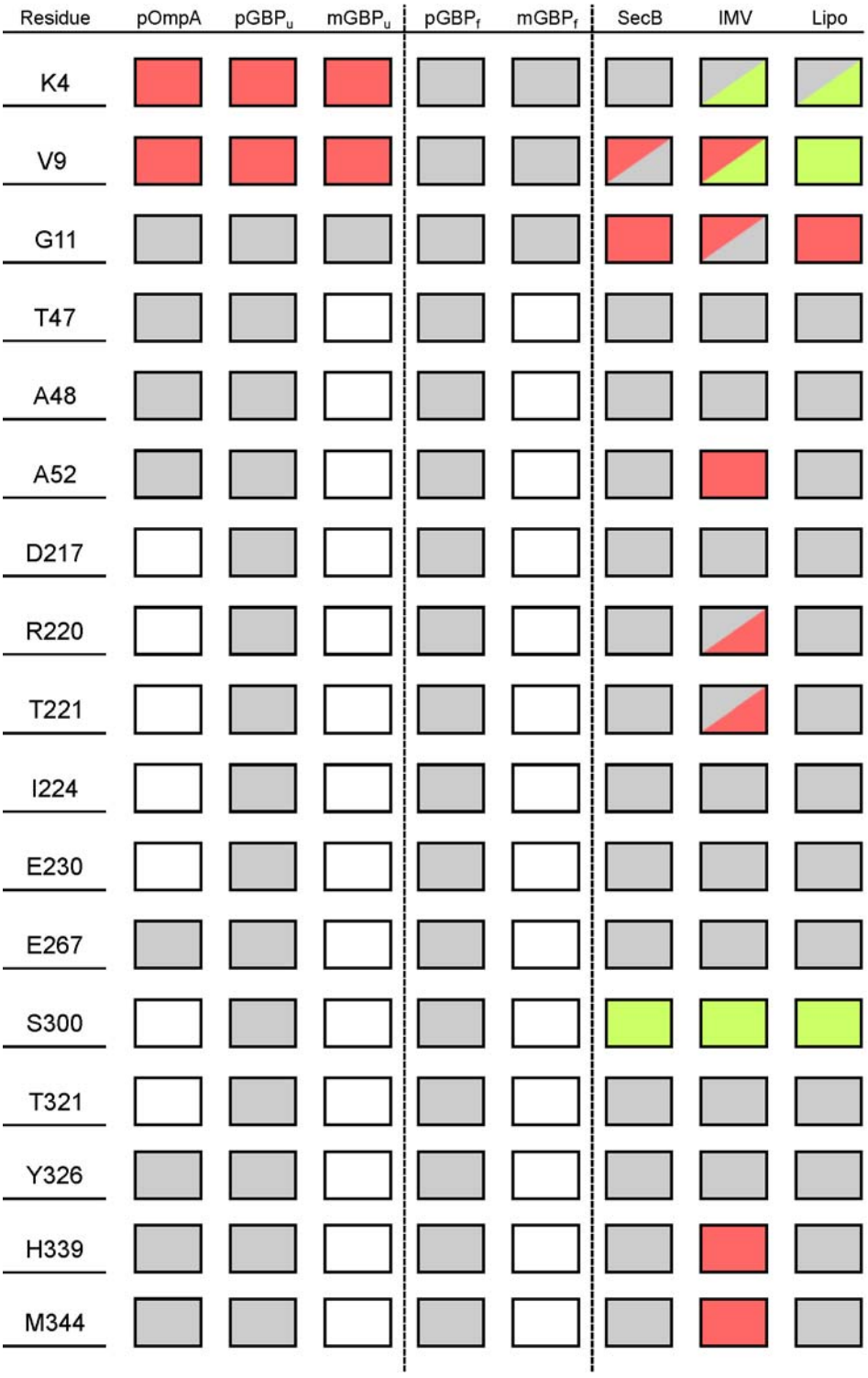

Table 1. Summary of EPR data. Colors indicate result as follows: Red – constraint, Green – mobilization, Grey – no change. Boxes are divided diagonally when results differed at different temperatures: upper half - 23 °C, lower half - 6 °C. White boxes indicate no data was collected.

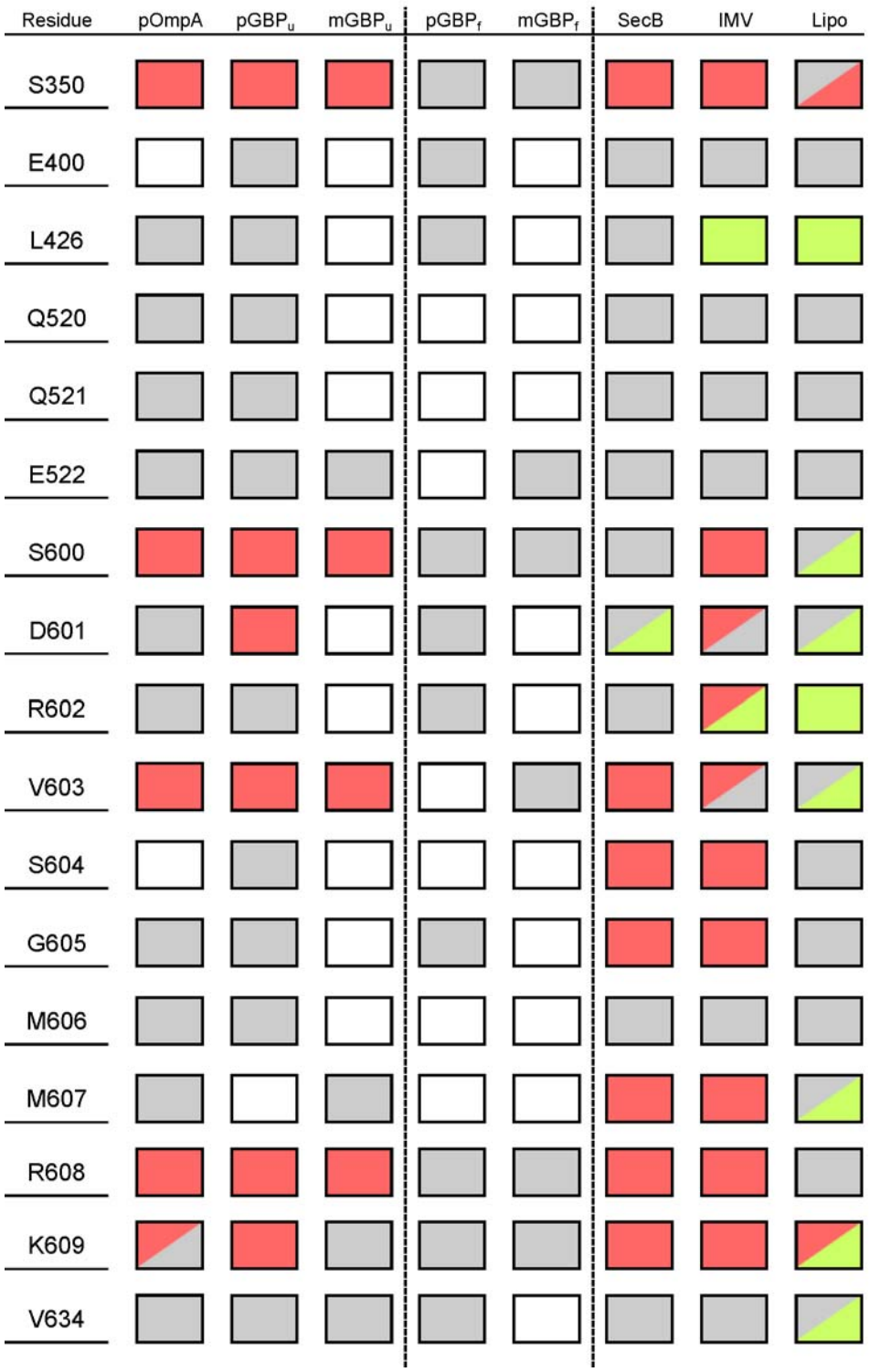

Table 1 (continued). Summary of EPR data. Colors indicate result as follows: Red – constraint, Green – mobilization, Grey – no change. Boxes are divided diagonally when results differed at different temperatures: upper half - 23 °C, lower half - 6 °C. White boxes indicate no data was collected.

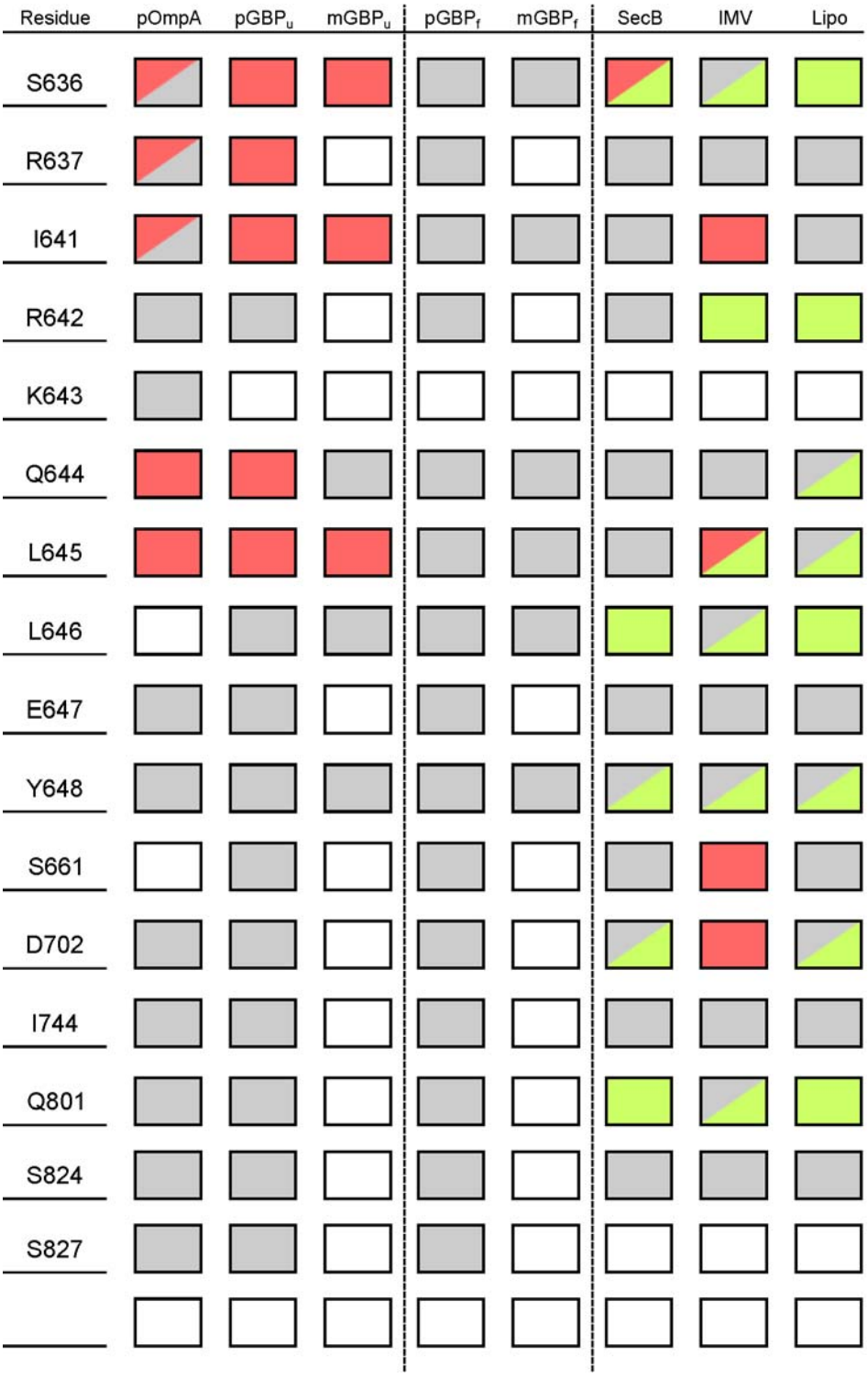

Table 1 (continued). Summary of EPR data. Colors indicate result as follows: Red – constraint, Green – mobilization, Grey – no change. Boxes are divided diagonally when results differed at different temperatures: upper half - 23 °C, lower half - 6 °C. White boxes indicate no data was collected.

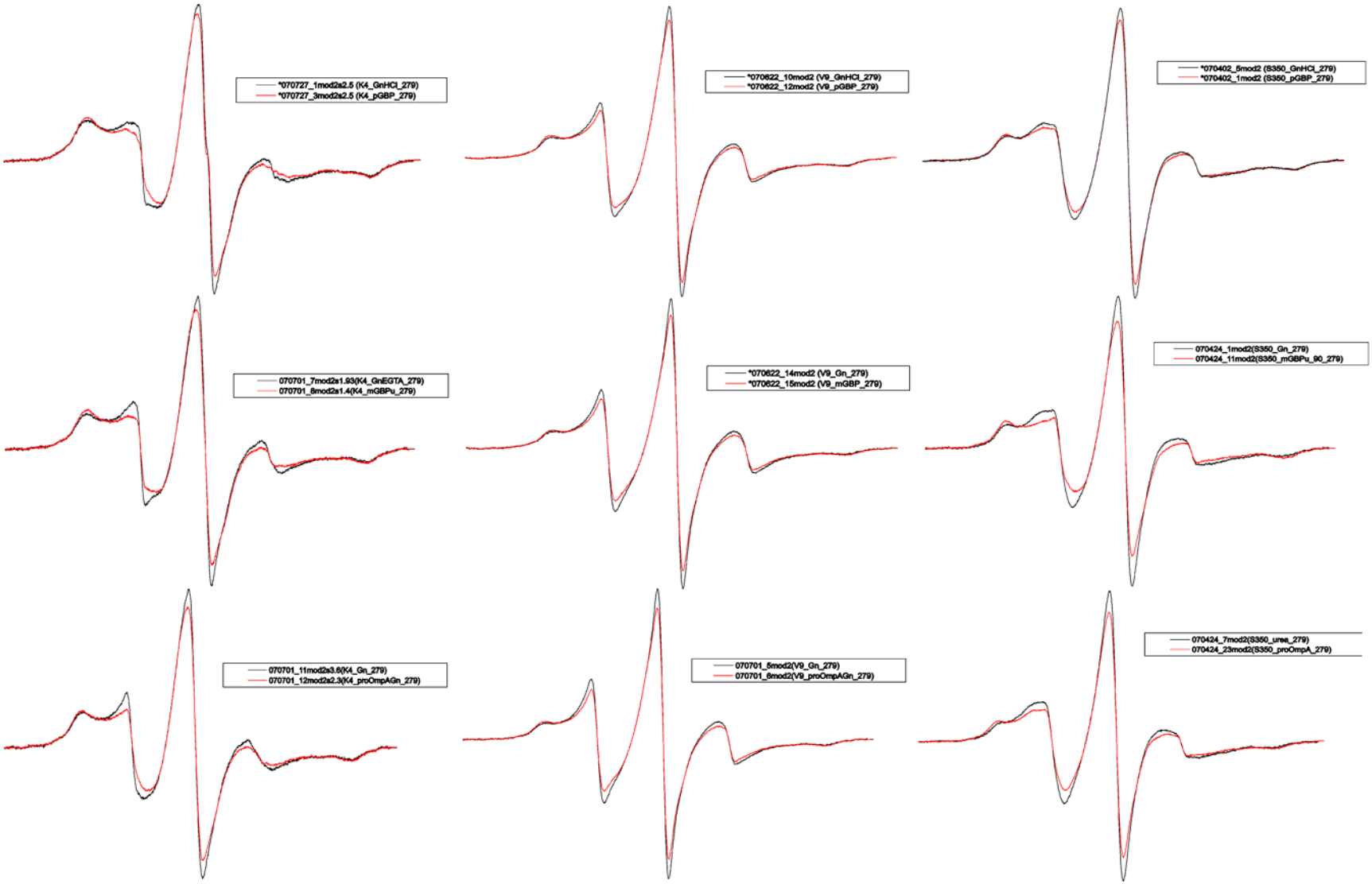

Figure 6. SecA residues showing constraint with precursor.

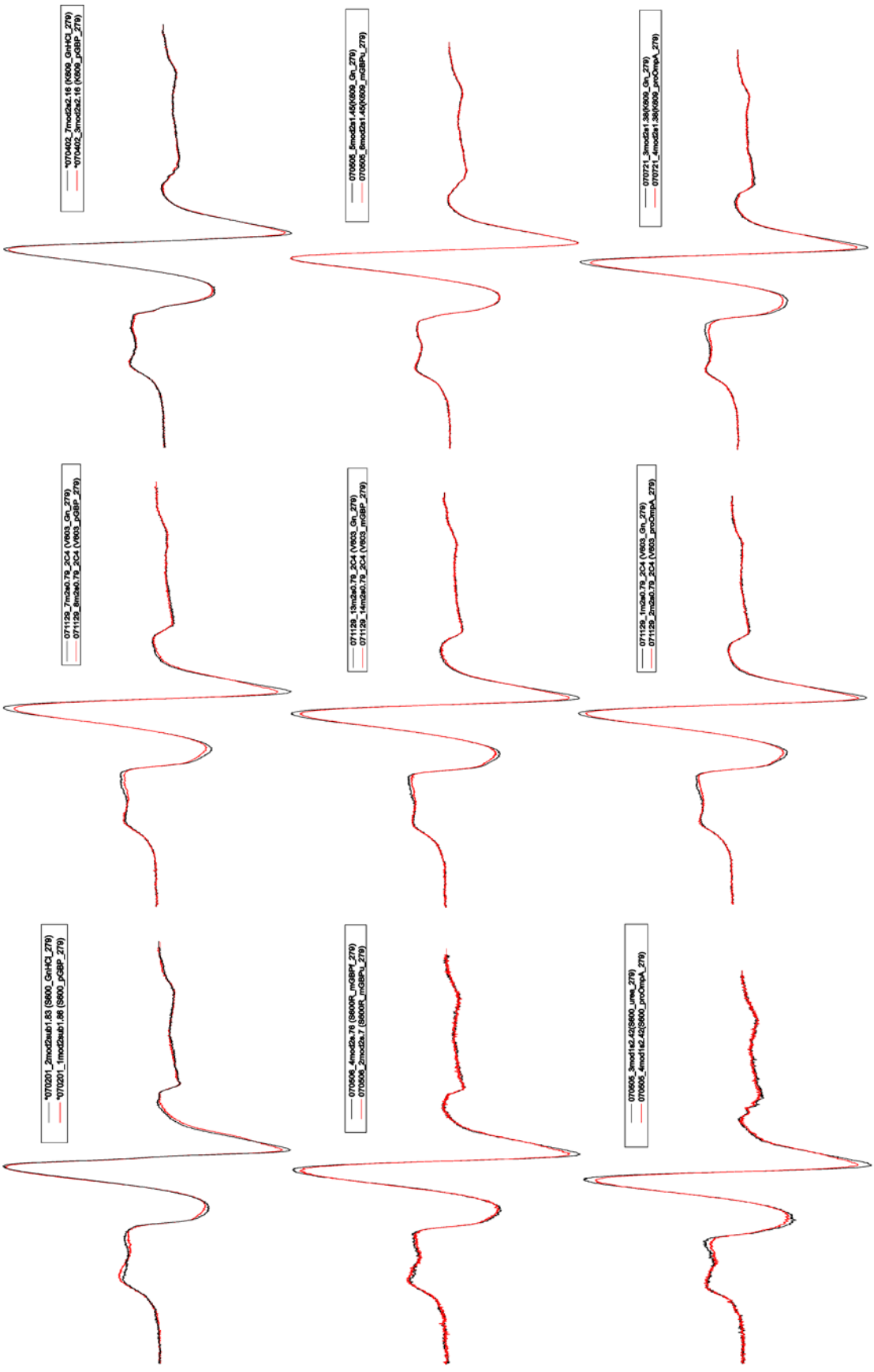

Figure 6 (continued). SecA residues showing constraint with precursor.

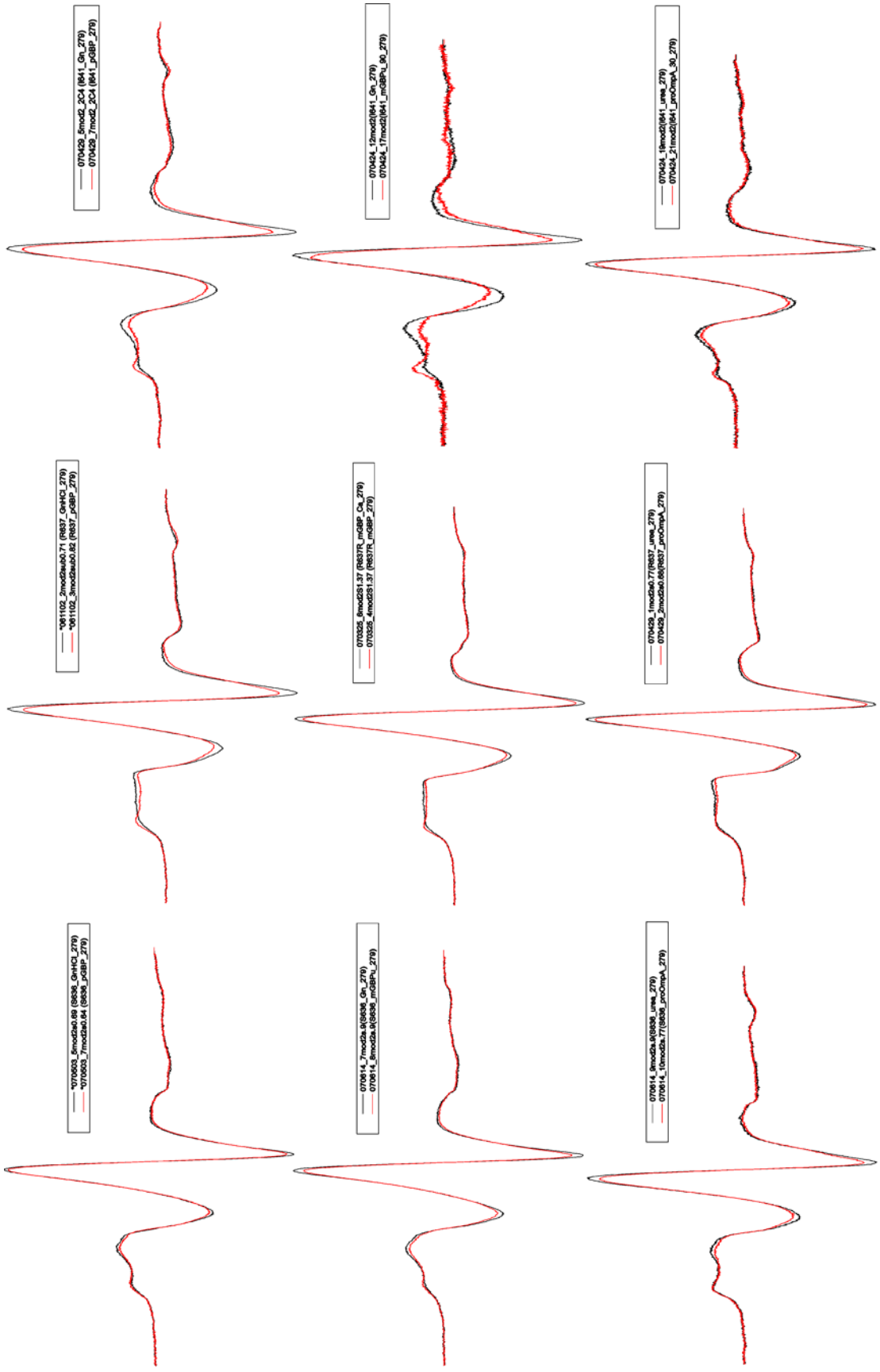

Figure 6 (continued). SecA residues showing constraint with precursor.

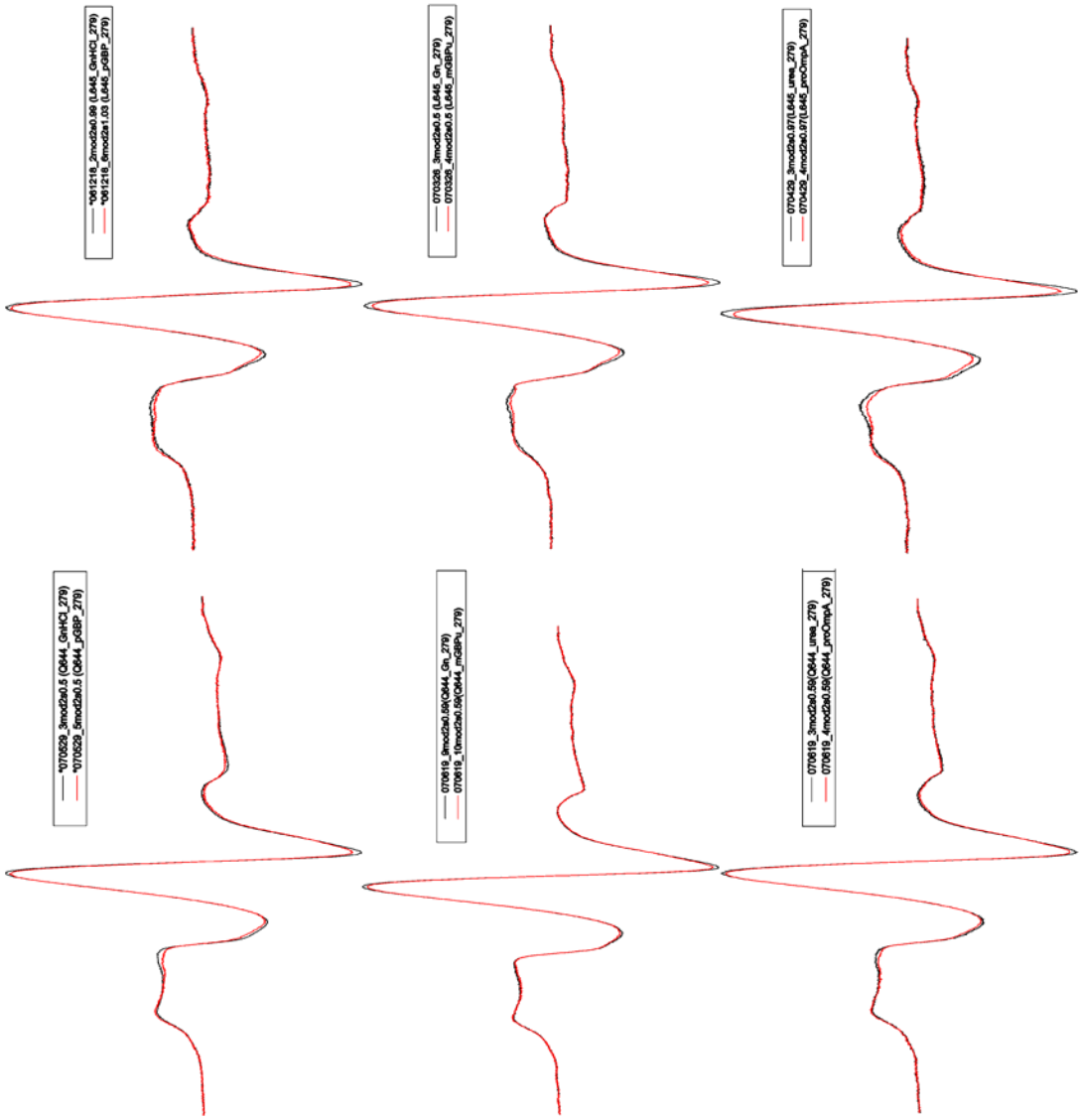

Figure 6 (continued). SecA residues showing constraint with precursor.

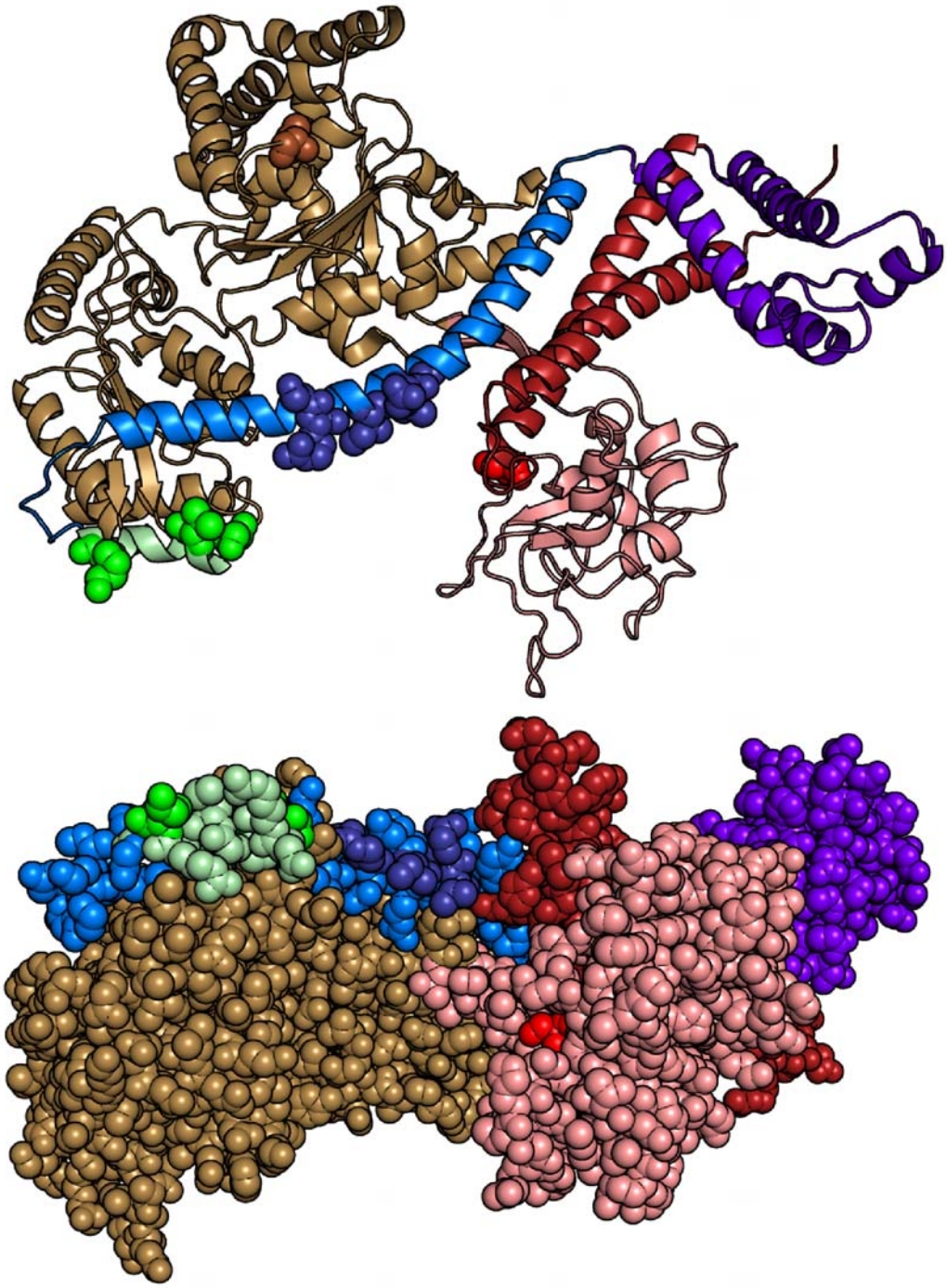

Figure 7. Structures of SecA protomer displaying summary of constraints observed with precursor protein. The bottom structure is rotated 90° about the x-axis. Residues showing constraint are shown in CPK with colors as follows: small linking α-helix (bright green), HSD (dark blue), NBF1 (dark brown), PBD (bright red).

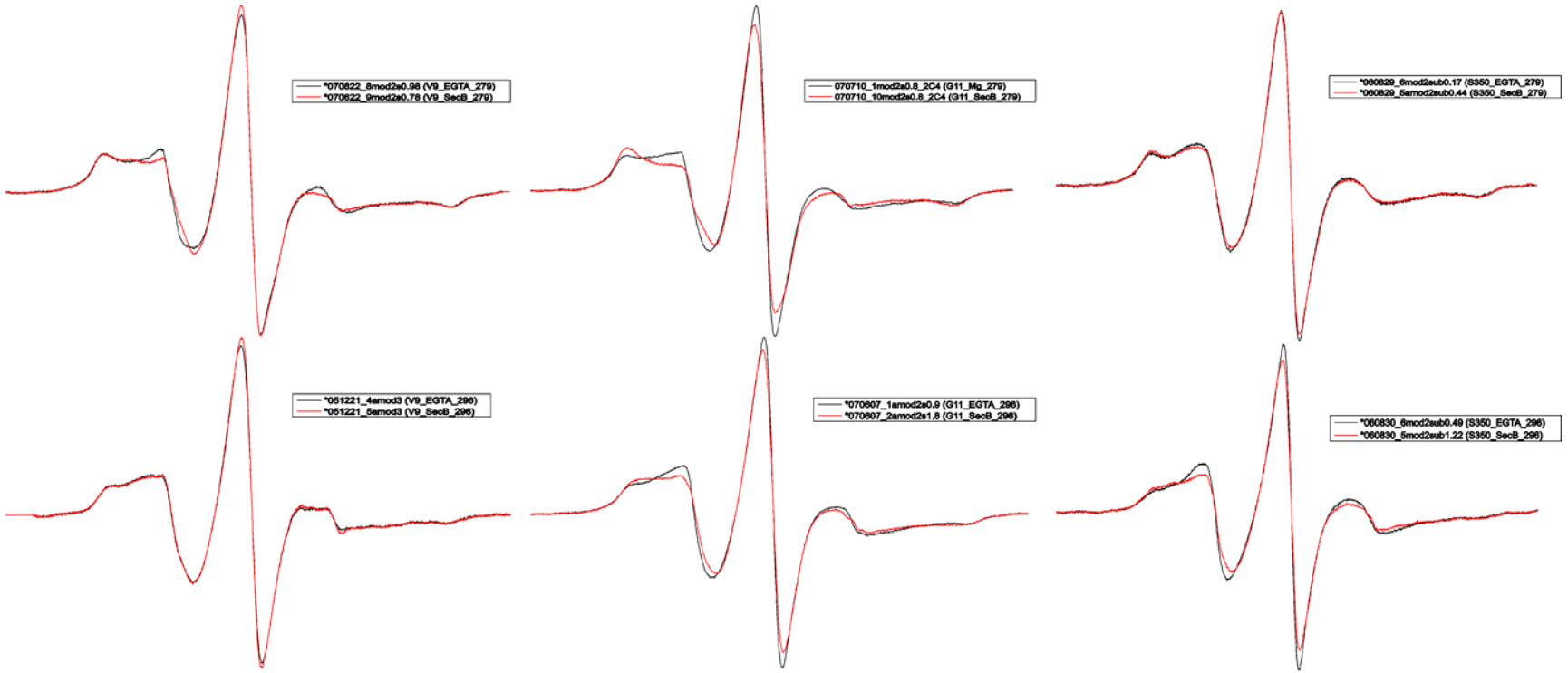

Figure 8. SecA residues showing constraint with SecB.

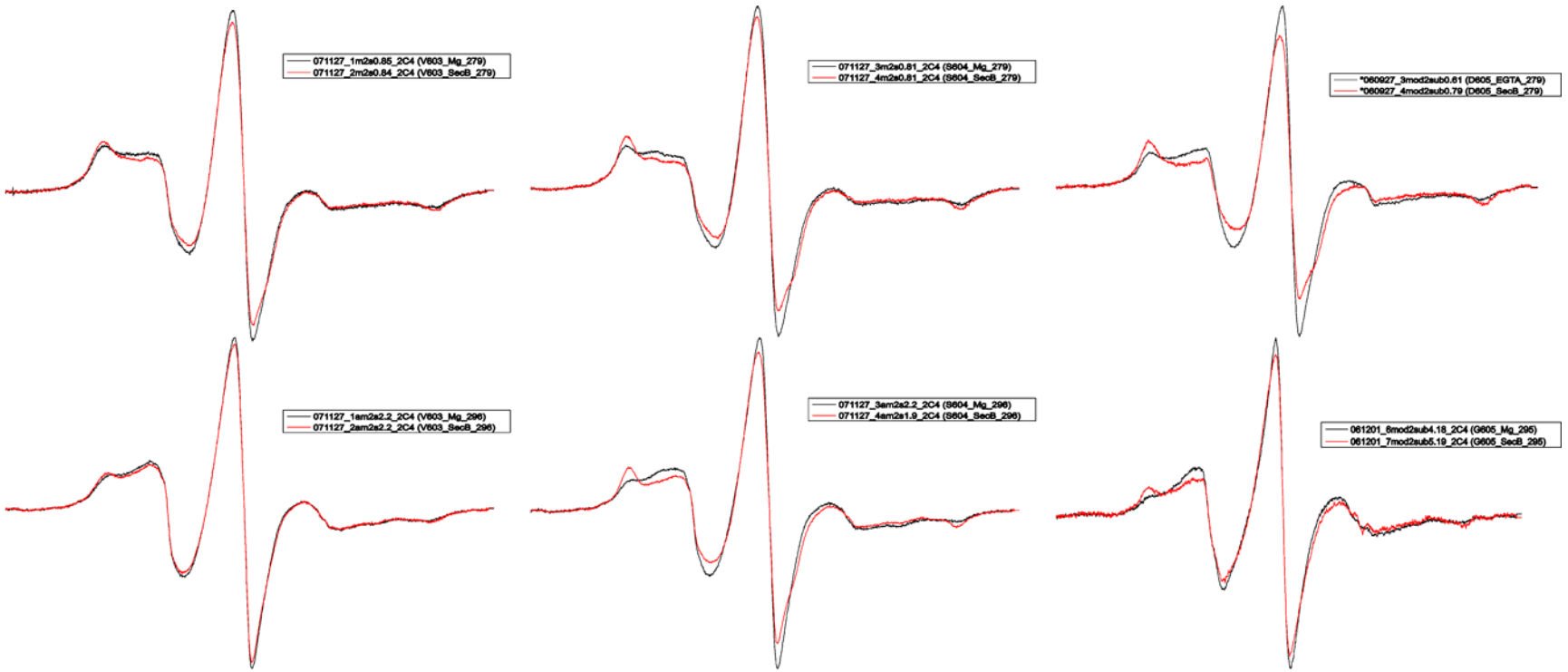

Figure 8 (continued). SecA residues showing constraint with SecB.

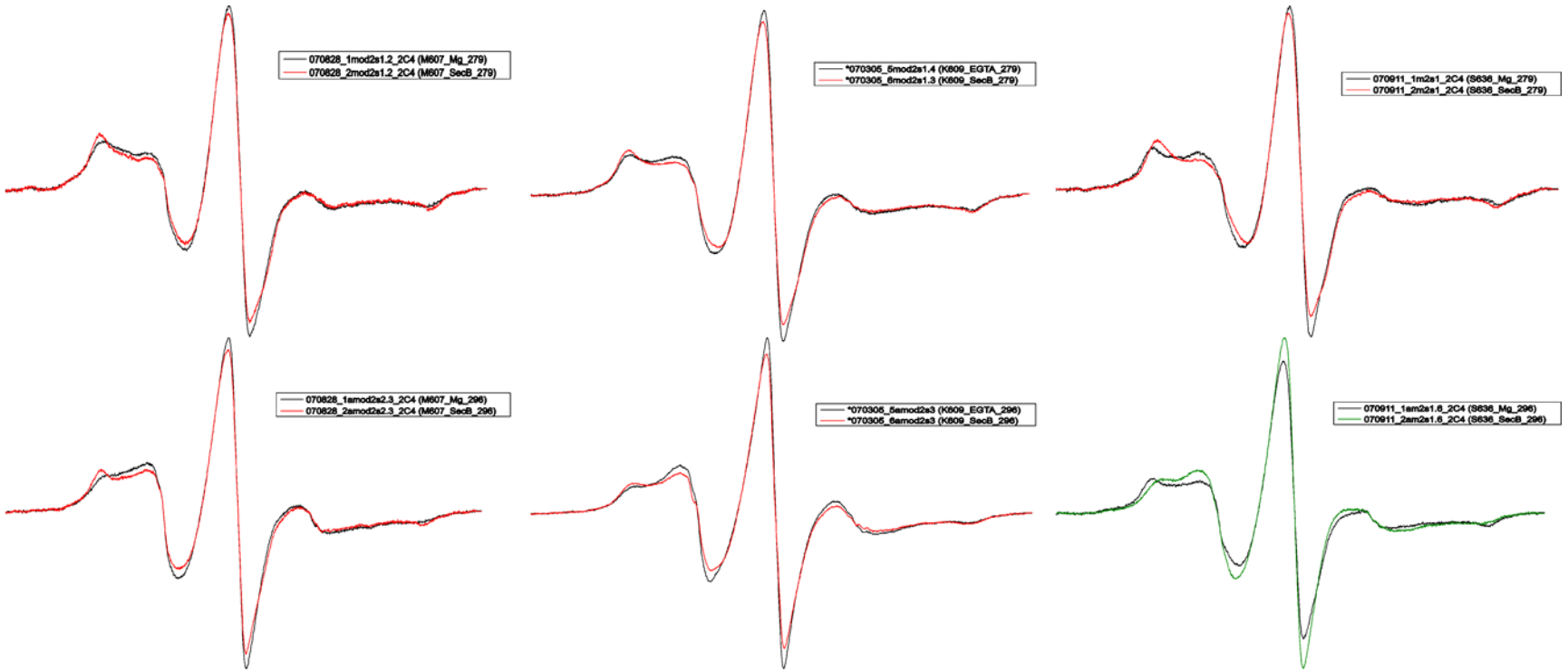

Figure 8 (continued). SecA residues showing constraint with SecB.

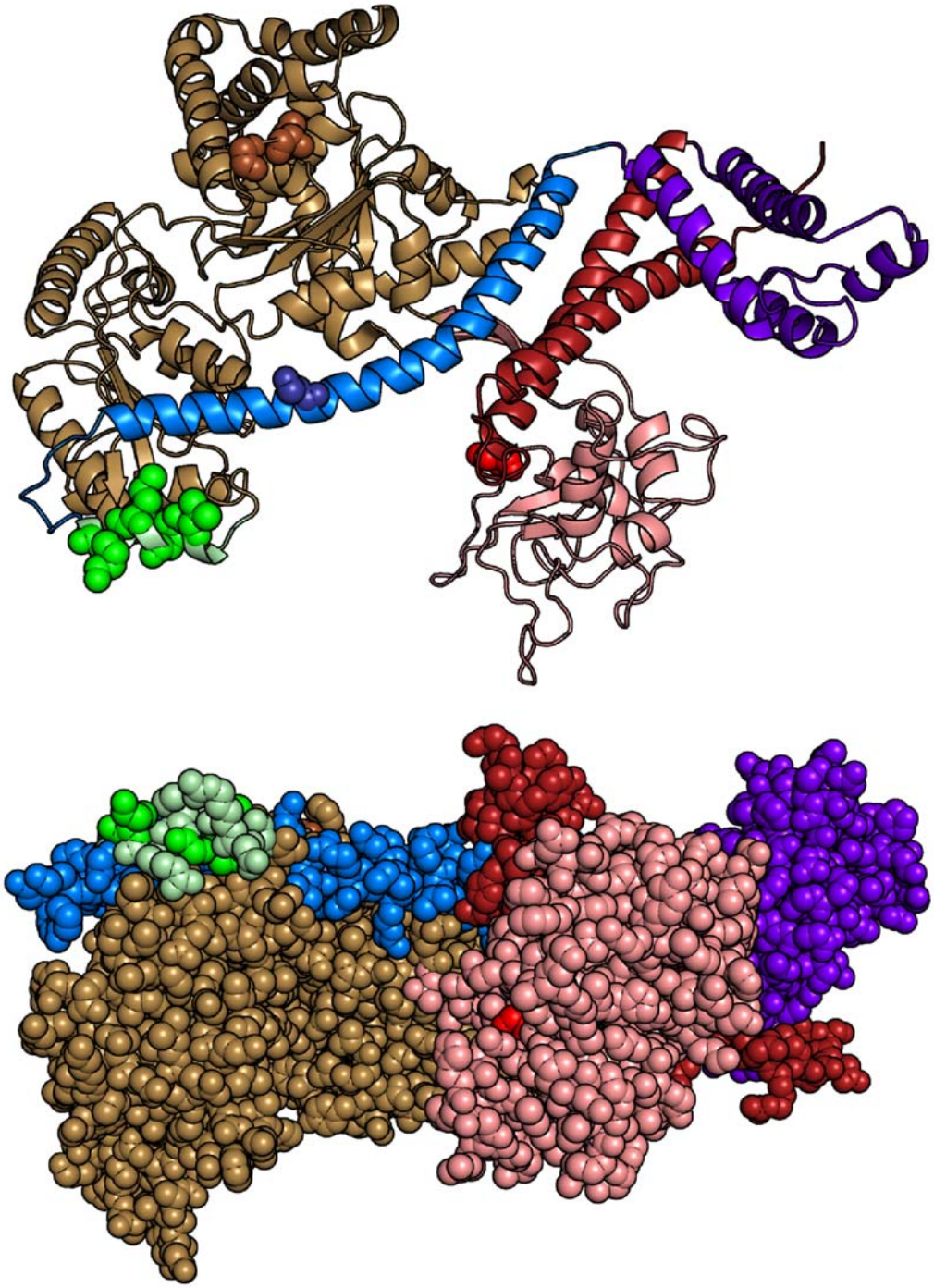

Figure 9. Structures of SecA protomer displaying summary of constraints observed with SecB. The bottom structure is rotated 90° about the x-axis. Residues showing constraint are shown in CPK with colors as follows: small linking α-helix (bright green), HSD (dark blue), NBF1 (dark brown), PBD (bright red).

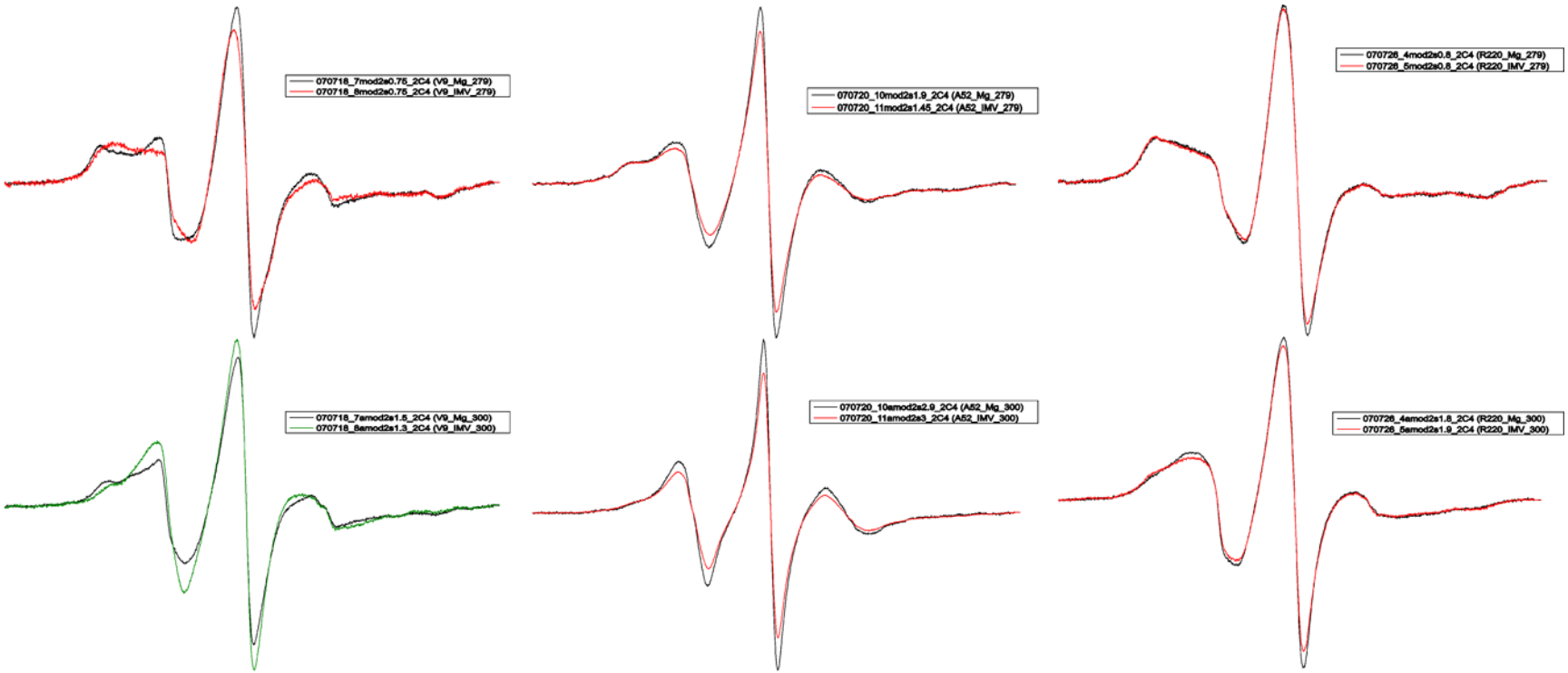

Figure 10. SecA residues showing constraint with SecYEG.

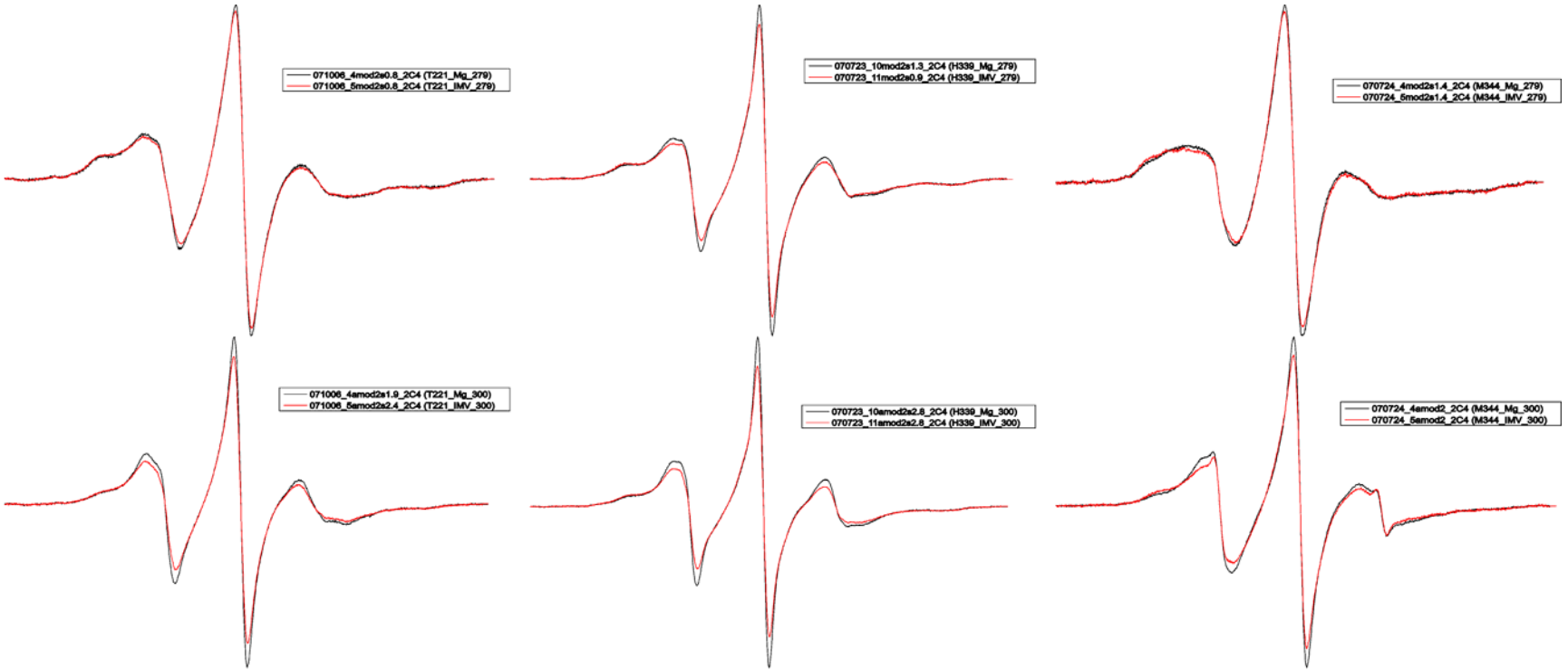

Figure 10 (continued). SecA residues showing constraint with SecYEG.

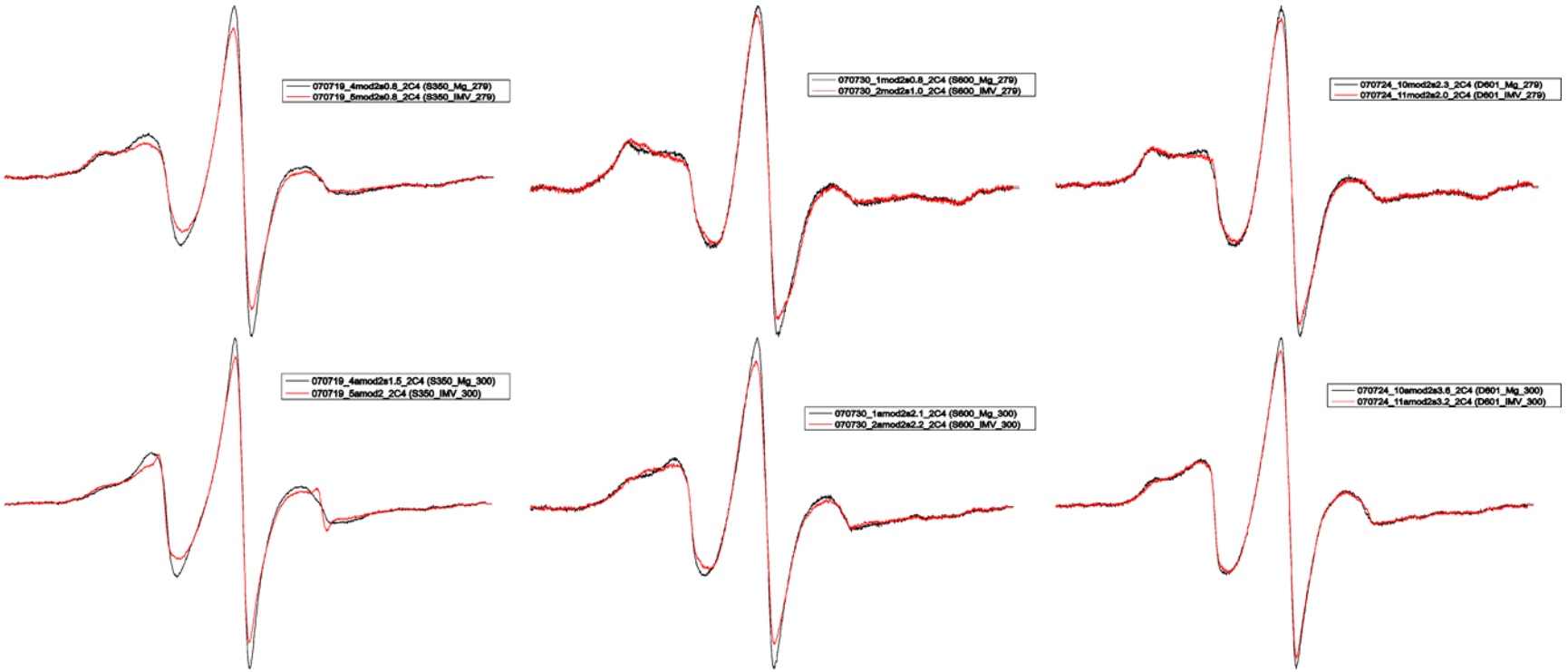

Figure 10 (continued). SecA residues showing constraint with SecYEG.

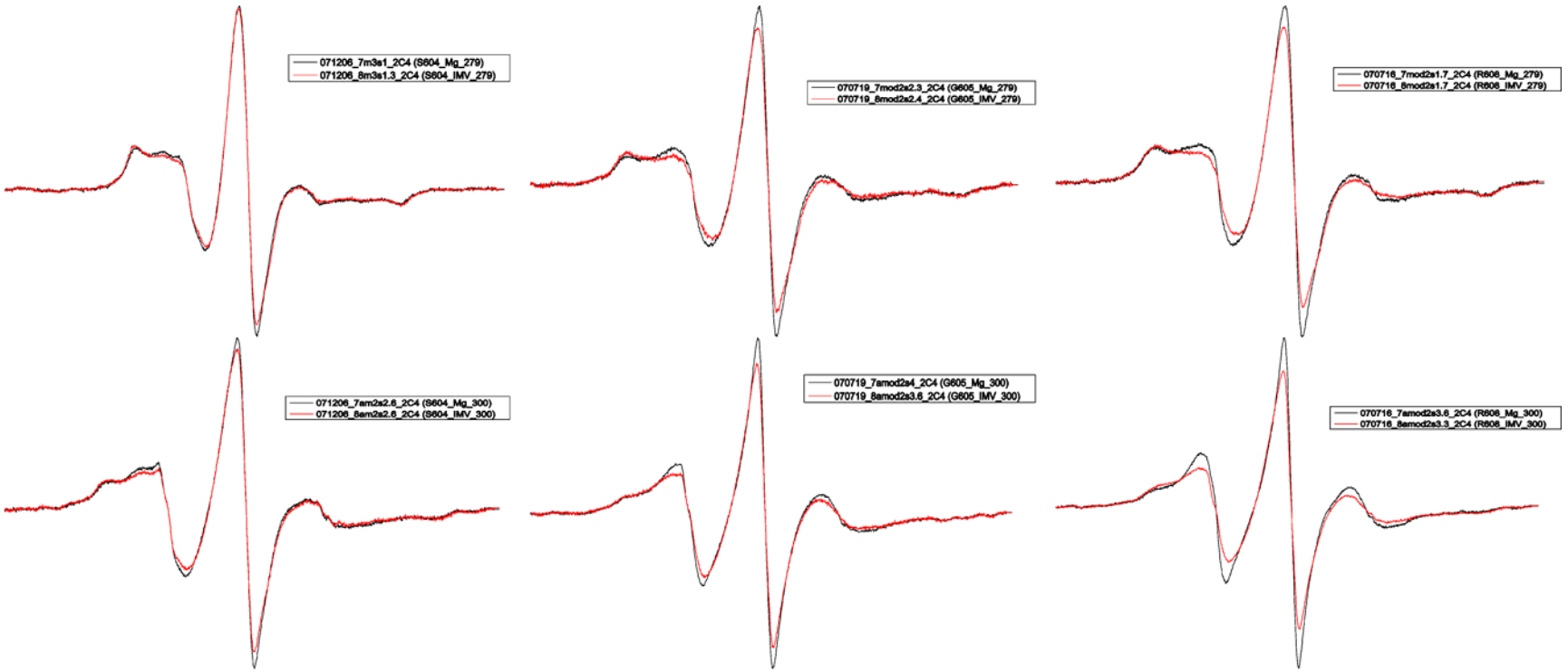

Figure 10 (continued). SecA residues showing constraint with SecYEG.

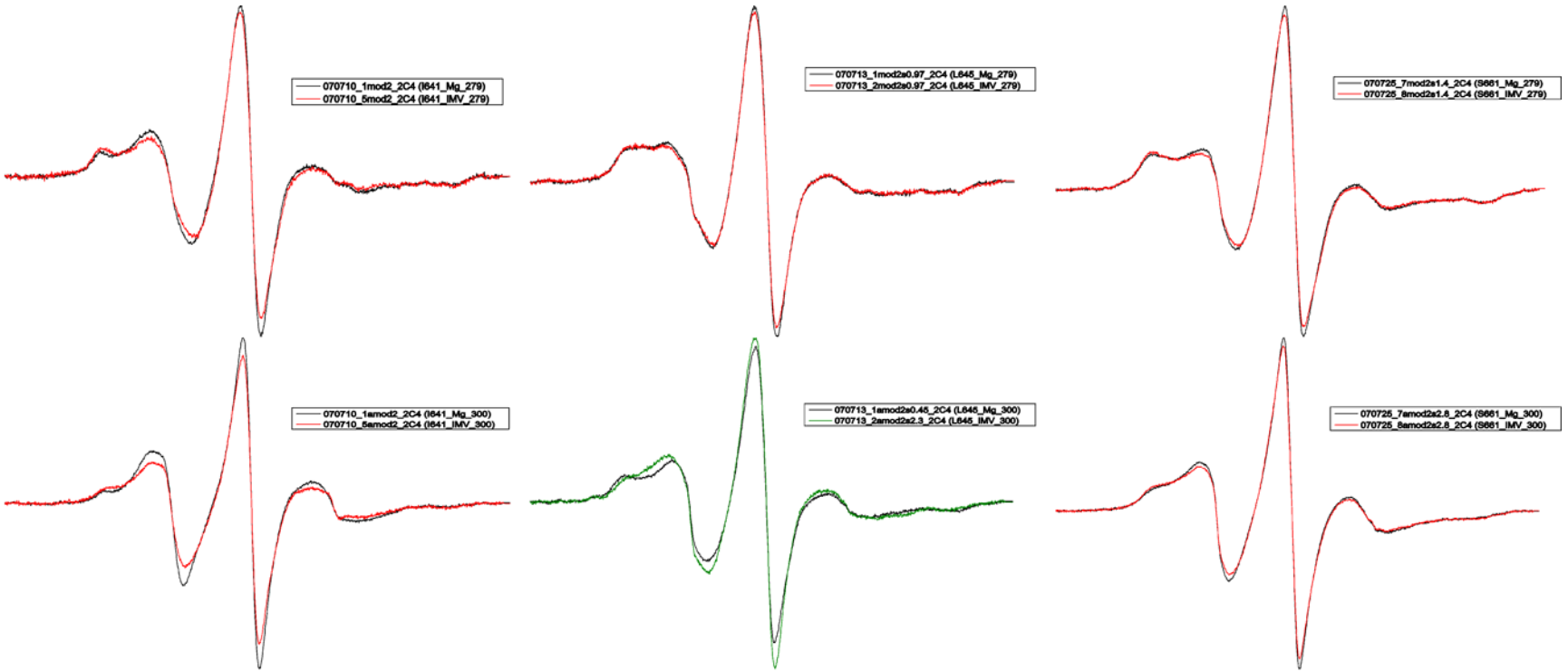

Figure 10 (continued). SecA residues showing constraint with SecYEG.

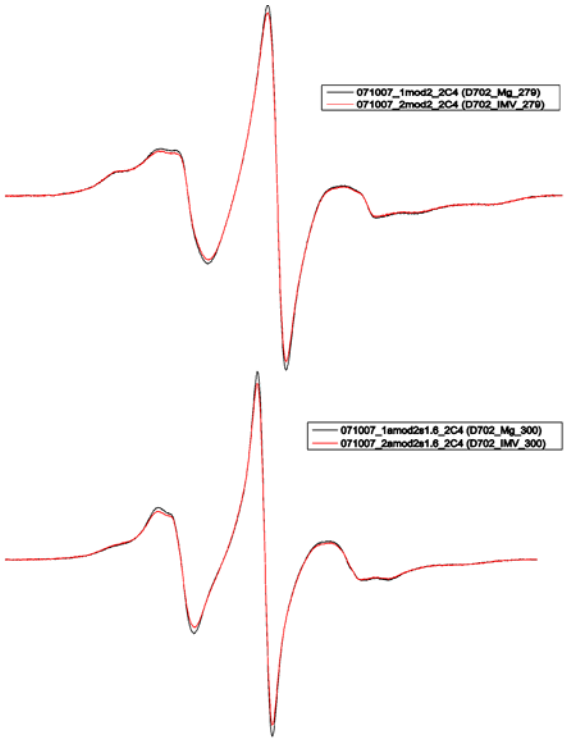

Figure 10 (continued). SecA residues showing constraint with SecYEG.

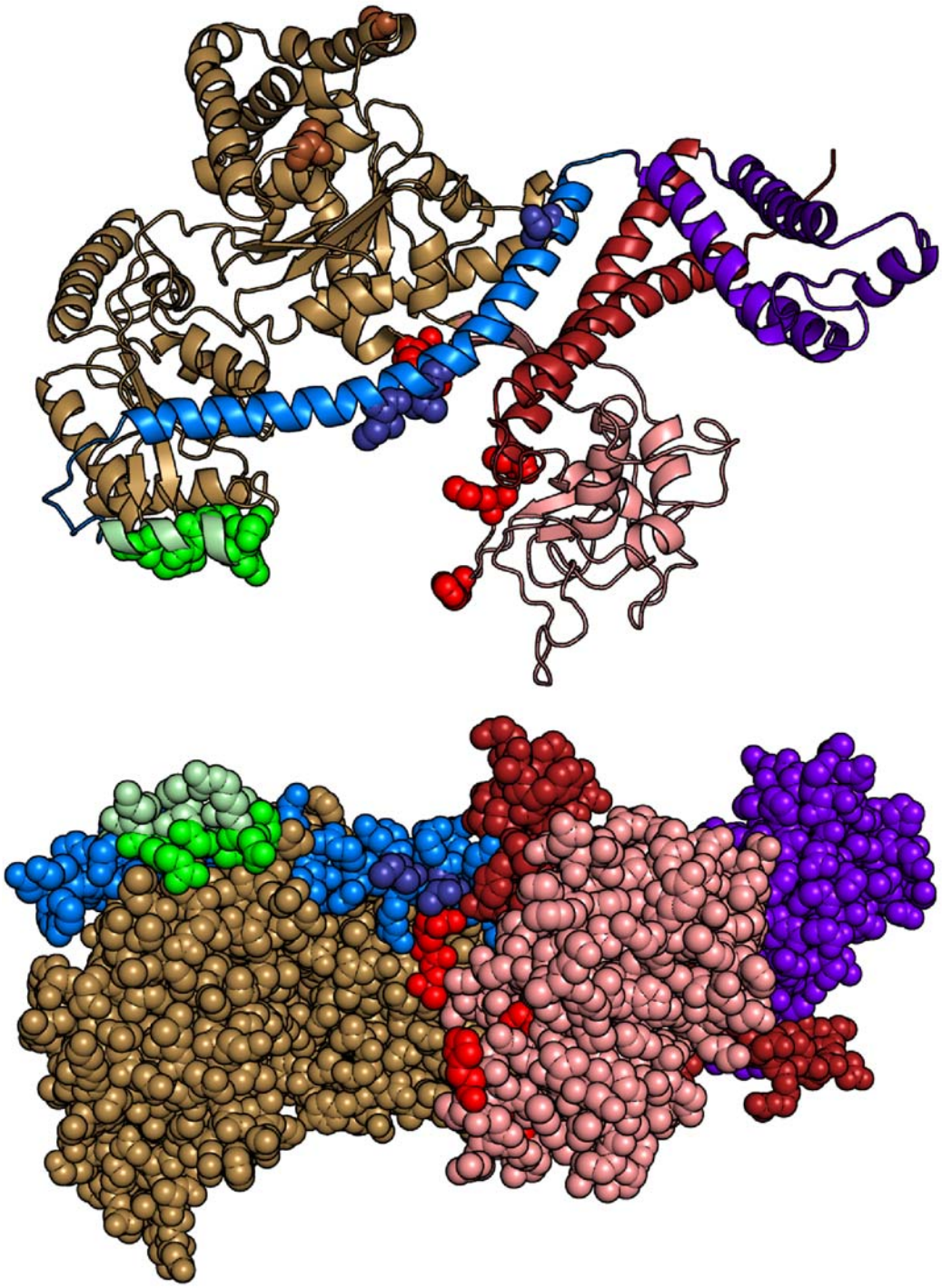

Figure 11. Structures of SecA protomer displaying summary of constraints observed with SecYEG. The bottom structure is rotated 90° about the x-axis. Residues showing constraint are shown in CPK with colors as follows: small linking α-helix (bright green), HSD (dark blue), NBF1 (dark brown), PBD (bright red).

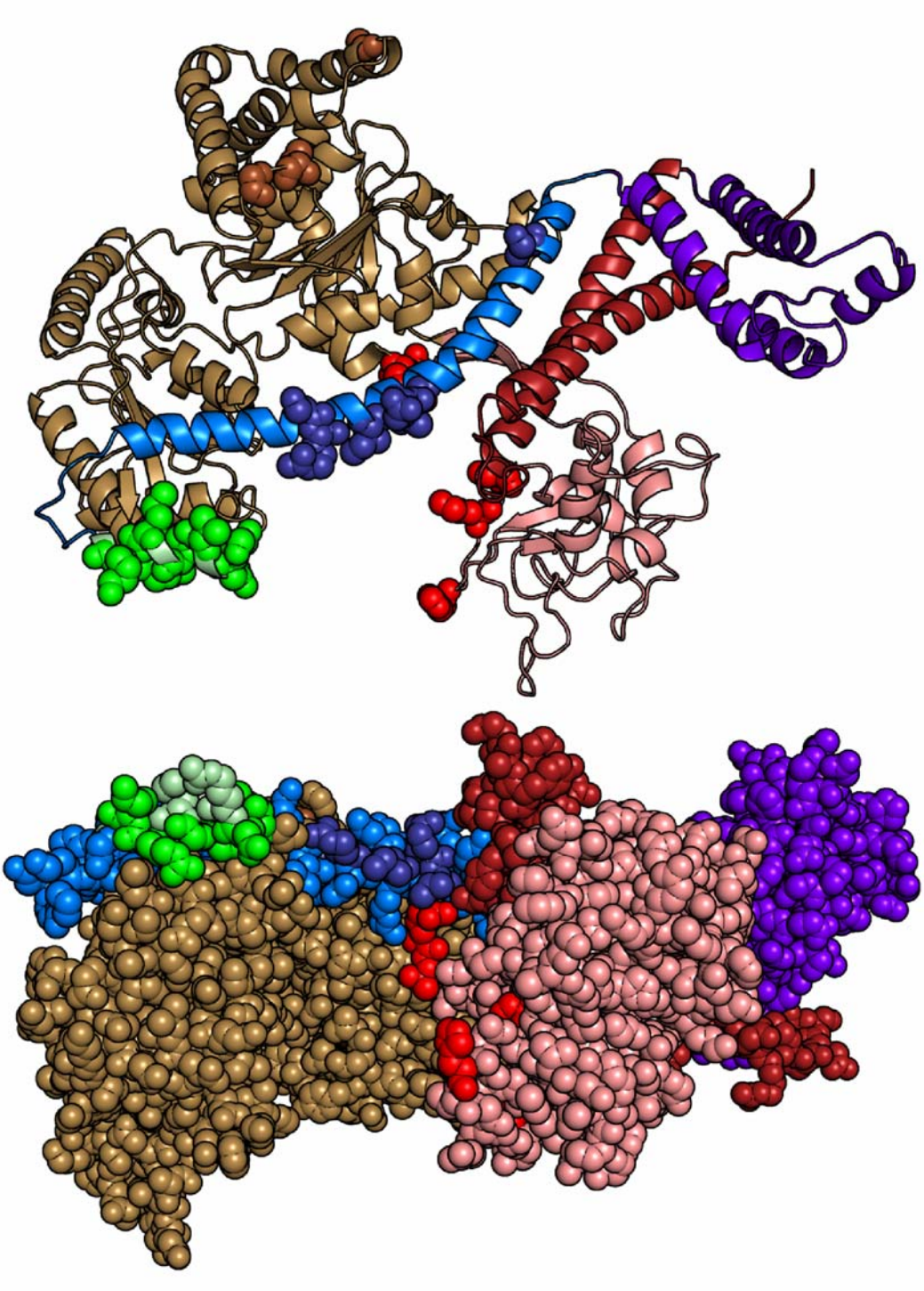

Figure 12. Structures of SecA protomer displaying summary of all constraints observed. The bottom structure is rotated 90° about the x-axis. Residues showing constraint are shown in CPK with colors as follows: small linking α-helix (bright green), HSD (dark blue), NBF1 (dark brown), PBD (bright red).

Chapter Four

Discussion

Discussion

Our data contribute to an existing body of knowledge, and this must be considered when proposing a model for interaction between SecA and its ligands. Gelis and Economou conducted NMR studies of a complex between SecA and a signal peptide and show contact with 13 aminoacyl residues (Fig. 13, aqua residues) that lie along a groove (Gelis et al. 2007) Osborne and Rapoport suggest is a potential binding site (Osborne et al. 2004) (Fig. 13, arrow). Additionally, a peptide of SecA in this region (residues 269-322) has been labeled with a signal sequence carrying a photoreactive group (Musial-Siwek et al. 2007) (Fig. 13, orange ribbon). Contact sites we have identified define the opening to a large cleft that lies opposite the groove defined above, and to the side of the PBD. The floor of this cleft is visible in Figure 13, which is a 90° rotation about the x-axis. Also visible are two β-strands, which connect the bulb of the PBD to the ATP binding fold in NBD2 and have been suggested by several groups to bind signal peptides (Hunt et al. 2002; Papanikolau et al. 2007; Papanikou et al. 2005). Residues in addition to these β-strands which reside nearby have been postulated by Chou and Gierasch to interact with signal sequences (Fig 13, light purple residues). Our data show strong constraint at residue S350, located on the wall of the cleft formed by the PBD, opposite the wall formed by the NBD2. We propose that the signal sequence of precursor peptide ligands interacts with the narrow groove and that the mature region of the polypeptide makes contact with the HSD and small linking α-helix, after crossing over the IRA1 and entering the wide cleft. Although it is currently controversial whether SecA functions as a dimer during export, if one considers the SecA dimer to be functional for a moment *arguendo*, a polypeptide

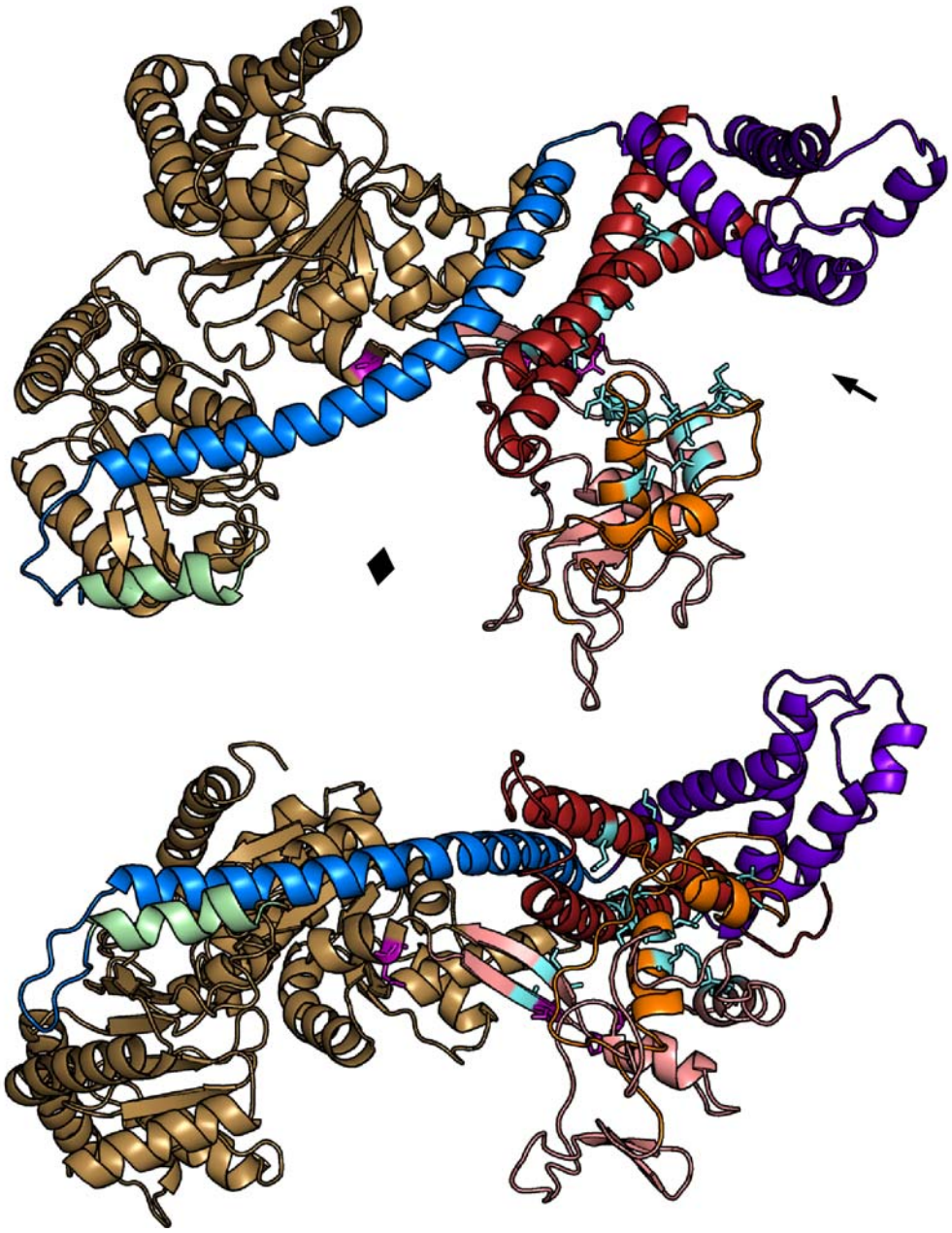

Figure 13. Structures of SecA protomer displaying summary of precursor protein signal binding data. The bottom structure is rotated 90° about the x-axis. Residues in the PBD are indicated as follows: Chou and Gierasch (light purple ball and stick), Musial-Siwek et al. (orange ribbon), Gelis et al. (aqua ball and stick). The arrow indicates the cleft proposed by Osborne et al. The diamond indicates the cleft found by this study.

ligand might occupy the binding site shown here on one protomer and extend into the corresponding site on the second protomer.

That the SecB binding site on SecA overlaps that of polypeptide ligands is not surprising when one considers that SecB delivers the unfolded polypeptide ligand to the same surface on SecA that SecA uses to bind precursors directly. One residue in the PBD, S350, shows constraint by SecB that varies with temperature. When measured at 6 °C, the constraint seen is small, whereas at 23 °C, the observed change is as large as that seen for contact with either polypeptide ligands or SecY. This temperature dependence may reflect the need for mobility of the PBD for contact with its ligands, since S350 lies within the cleft, not at an edge. Additionally, when the PBD is in the closed conformation S350 appears shielded from ligand contact. It is possible that the rigid structure of SecB can only reach S350 after the PDB has undergone the rotational translation seen in the open conformation, while a long unstructured precursor polypeptide could extend into the cleft, gaining access to S350 and yielding the constraint seen at 6 °C.

Residues showing constraint with SecY on SecA indicate that SecY interacts with SecA on the same surface as other ligands. An elegant *in vivo* study (Jilaveanu and Oliver 2007) identified this same face as the side of SecA that is in contact with the aqueous periplasmic compartment by means of the translocon pore, and our conclusion is in agreement with this study. During cotranslational export the cytoplasmic loops on SecY residing between helices TM6 and TM7 and between TM8 and TM9 insert into the polypeptide exit site of the ribosome (Menetret et al. 2007). These loops in SecY are likely candidates for binding the cleft (Mori and Ito 2001; Mori and Ito 2006) and may

function analogously to capture precursor from either the ribosome or SecA. These conclusions do not necessarily mean that in order for SecY and SecA to form a complex, SecB must be released from SecA. Indeed, there is experimental evidence to the contrary, as SecA has high affinity for SecB while SecA is bound to the translocon (den Blaauwen et al. 1997), and only when SecA binds ATP is SecB released (Fekkes et al. 1997).

Both SecB and SecY interact with SecA on the same surface, as emphasized by the fact that four residues examined (V9, S350, S604, G605) are used by both. Although this seems contradictory in cases other than simple mixtures of SecA:SecB or SecA:SecY, this dissonance can be resolved by two observations: 1) binding interactions between SecA and SecB while in complex are asymmetric even though both components have two-fold symmetry (Randall et al. 2005), and 2) interfacial contacts that stabilize the SecA antiparallel dimer are blocked from forming (Randall et al. 2005). Stepwise translocation consistent with our observations could be accomplished in the following fashion. A single protomer of SecA could be released from the complex formed with SecB by breaking a subset of interactions and freeing the sites on SecA for interaction with SecY. If this release of a SecA protomer were accompanied with a transfer of the precursor from SecB to SecA, this protomer could be free to bind the translocon and deliver the precursor while the other protomer stays in complex with SecB in order to bind the next portion of the precursor to be translocated.

In the absence of the SecYEG translocon, SecA binds phospholipids. This property of lipid binding is thought to be of physiological significance since *E. coli* strains depleted of acidic phospholipids are defective in protein export (Fekkes et al.

1997). Candidate lipid-binding residues on SecA are G11, near the amino terminus and K609, in the small linking α-helix. Constraint of these residues was observed at 6 °C, when the lipid bilayer would be in an ordered, condensed state. Therefore, contact is expected to be with the lipid head groups.

Not all changes observed on SecA were constraints. Of the 48 residues examined, a total of 16 demonstrated mobilization with the either the addition of SecB, inner membrane vesicles containing SecYEG or liposomes. The spectra are displayed in Figure 14 (SecB), Figure 15 (SecYEG), and Figure 16 (liposomes). All residues mobilized by SecYEG were also mobilized by liposomes, so it is not possible to conclude that mobilization seen with SecYEG liposomes is exclusively due to interactions between SecA and the translocon. Interaction of SecA with SecB increases mobility of a subset of the residues mobilized by lipids, suggesting a conformational change occurs. Although binding between SecA and SecB does not appear to mobilize the small linking α-helix, because SecB makes contact with five of the ten residues that make up the helix, the mobilization resulting from conformational change could be masked by constraints imposed by SecB.

Conformational changes in SecA resulting from ligand binding could be caused either by direct propagation of movement from sites of binding to the structural elements mobilized or by indirectly disrupting interfacial contacts between the SecA dimers. Further, the disruption of the SecA dimer interface could cause additional mobilizations. Presently, we cannot distinguish between these possibilities. Both residues identified as contact sites for SecB and lipids (G11 and K609) are involved in interfacial contacts in the reported dimeric SecA structures crystallized from *B. subtilis*: G11 in the antiparallel

dimer (Hunt et al. 2002) and K609 in the intertwined dimer (Zimmer et al. 2006). SecB has been reported to disrupt interfacial contacts in SecA (Randall et al. 2005) and at low concentrations of SecA, binding liposomes renders SecA monomeric (Or et al. 2005). It should be noted that, at concentrations near those used in this study, SecA remained dimeric while associated with lipids, unless nucleotides were present (Bu et al. 2003).

The observed pattern of mobilization (Fig. 17) might be explained by a rolling movement along the long α-helix in the HSD away from the NBDs, freeing the residues within that helix, as well as residues L426 and Q801, which make contact with the HSD. Also, movements of the small linking α-helix away from direct contact with the body of the protein would relieve constraints at S600, D601 and M607. Interestingly, residues R602 and K609, which point away from NBF1, are also mobilized. The mobility of all residues in the small linking α-helix would increase if one considers that the conformational change disrupts the helical nature of this region, thus rendering the backbone more flexible.

The rolling movement we observe in the HSD is similar to that proposed by Mori and Ito (Mori and Ito 2006). Their data show that variants of SecA with substitutions at E400 and R642 were unable to form a salt bridge at those residues and were defective in export both *in vivo* and *in vitro* and that this defect was suppressed by the mutational change M607T in the small linking α-helix. As a result of these observations, they proposed that a crucial conformational change involved movement of the HSD and the small linking α-helix away from the NBDs.

Additional support for the relevance of the movement observed here can be found in an NMR study (Keramisanou et al. 2006) demonstrating the coupling of ATP binding

and hydrolysis to translocation involves a shift in equilibrium between order and disorder of the nucleotide-binding cleft. This shift is allosterically propagated to the PBD. The ordered state of the interface of NBD1 and NBD2 favors the binding of ATP while the disordered state favors the binding of ADP, subsequent to hydrolysis. The high ATPase activity property of SecA prior to translocation is suppressed by interactions between the NBDs and both the HSD and the IRA1 (Karamanou et al. 1999). Therefore, the rolling movement of HSD away from the NBDs induced by binding SecB or lipids could account for their demonstrated ability to activate the ATPase activity of SecA (Lill et al. 1990; Miller et al. 2002). It is possible that once translocation is initiated, the order-disorder transition cycle coupled to ATP binding and hydrolysis result in the cyclic rolling away of the HSD followed by rebinding. These movements of the HSD and small linking α-helix, which are binding sites for both precursors and SecY, could serve as the structural transducer of the chemical energy of ATP hydrolysis to the mechanical work of moving precursors from SecA to SecY and ultimately through the translocon.

Crucial to the function of SecA is that one interactive surface serves to bind multiple partners. Transfer of the precursor polypeptide captured by the molecular chaperone SecB to SecA occurs in a ternary complex at the interface between SecA and SecB (Crane et al. 2006). Subsequent delivery of the precursor from SecA to SecY would efficiently occur if SecY were bound over the same surface on SecA that holds the precursor polypeptide. The presence of residues specific for each partner on a common surface of interaction give rise to characteristic patterns that would allow for simultaneous binding of precursor and either SecB or SecY to facilitate transfer. Most contact residues for SecB point upward from the surface of the small linking α-helix, and

only two residues lie in the same plane as residues which bind precursor and SecY. Contacts for precursor and SecY in the HSD point into the cleft. Residues tested that lie deep within the cleft on the floor (R220) or on the wall (T211, H339, M344) interact only with SecY, with the exception of S350, which makes contact with all binding partners. Incorporating all available data, the model for precursor binding suggests that the signal is held in the narrow groove and the polypeptide crosses over the IRA1 to interact at the HSD and the small linking α-helix at the mouth of the groove. When SecY binds SecA on this same surface the precursor would lie at the interface, as it did in the SecA:SecB complex. As SecA undergoes a conformational change the rolling of the HSD and the coupled movements of the small linking α-helix, IRA1 and the PBD might bring the precursor further into the cleft and alter the accessibility of sidechains resulting in release of the precursor from SecA and transfer to SecY.

These findings establish the location of binding sites on SecA and the nature of interaction between SecA and its natural ligands. This is the foundation for further investigation of the dynamic interplay between SecA and its binding partners during conversion of the chemical energy of ATP hydrolysis to the mechanical work of protein translocation.

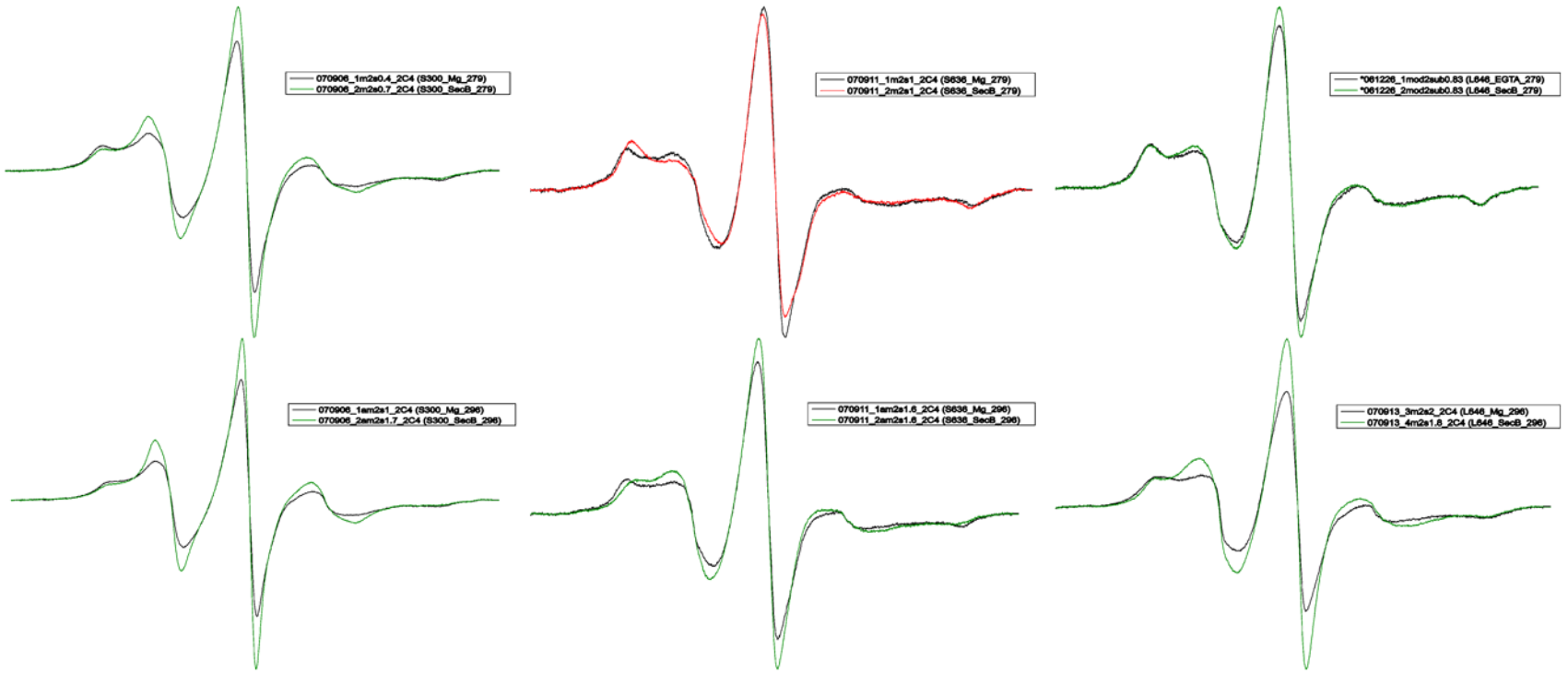

Figure 14. SecA residues showing mobilization with SecB.

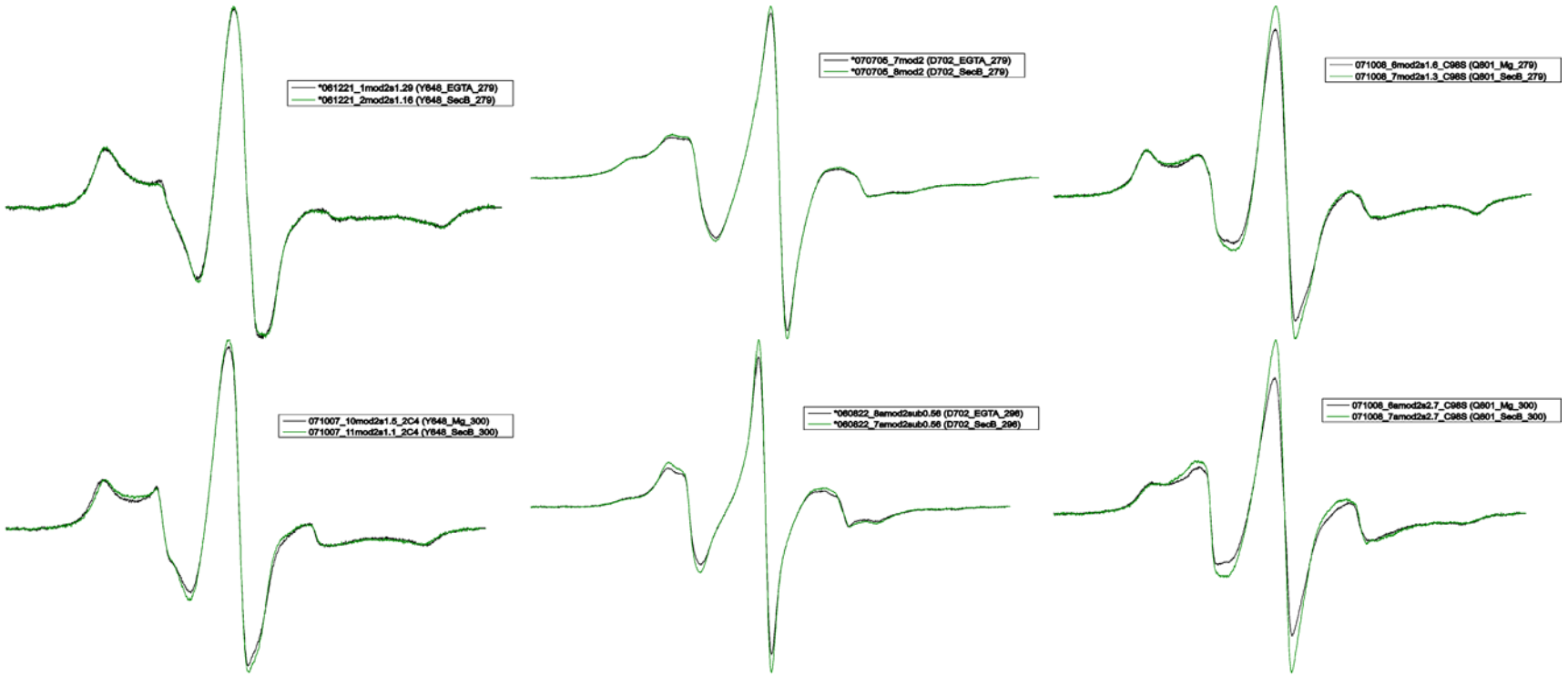

Figure 14 (continued). SecA residues showing mobilization with SecB.

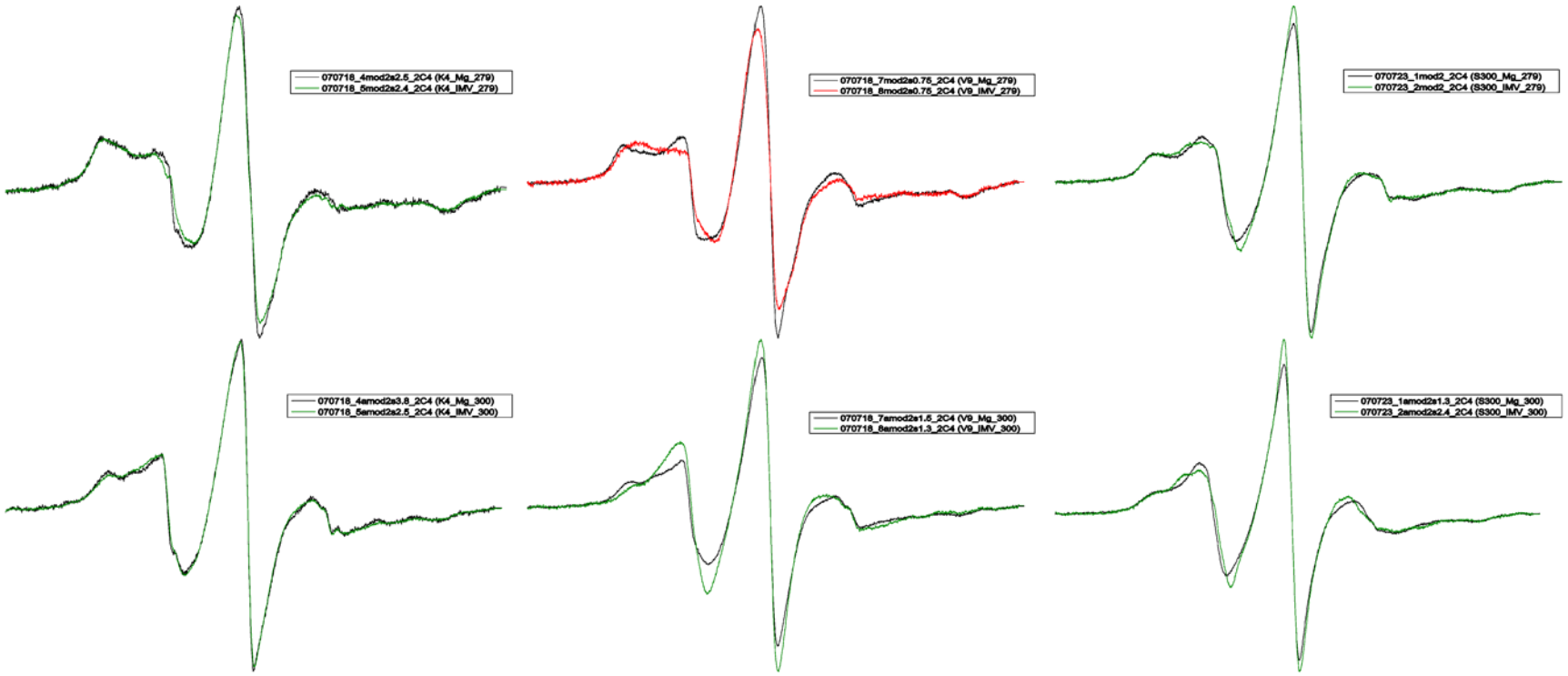

Figure 15. SecA residues showing mobility with SecYEG.

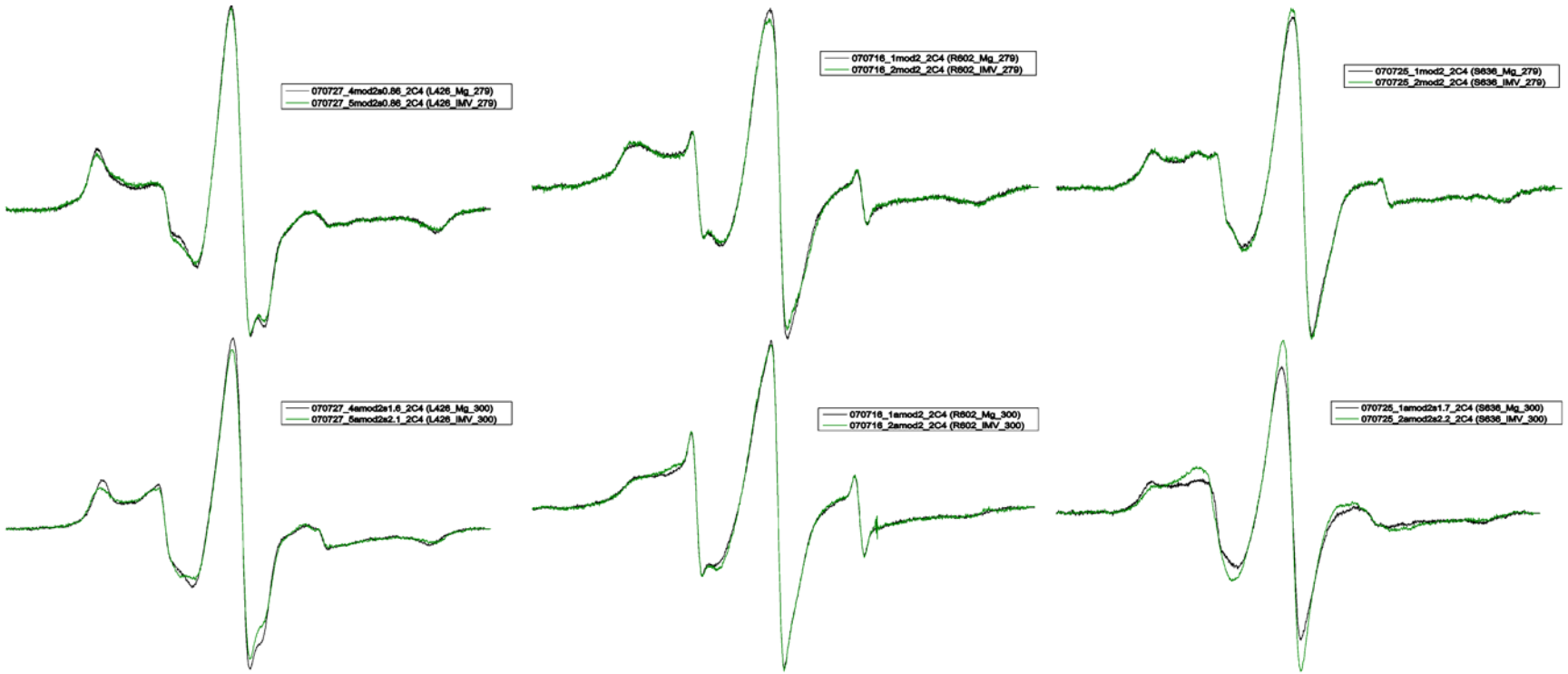

Figure 15 (continued). SecA residues showing mobility with SecYEG.

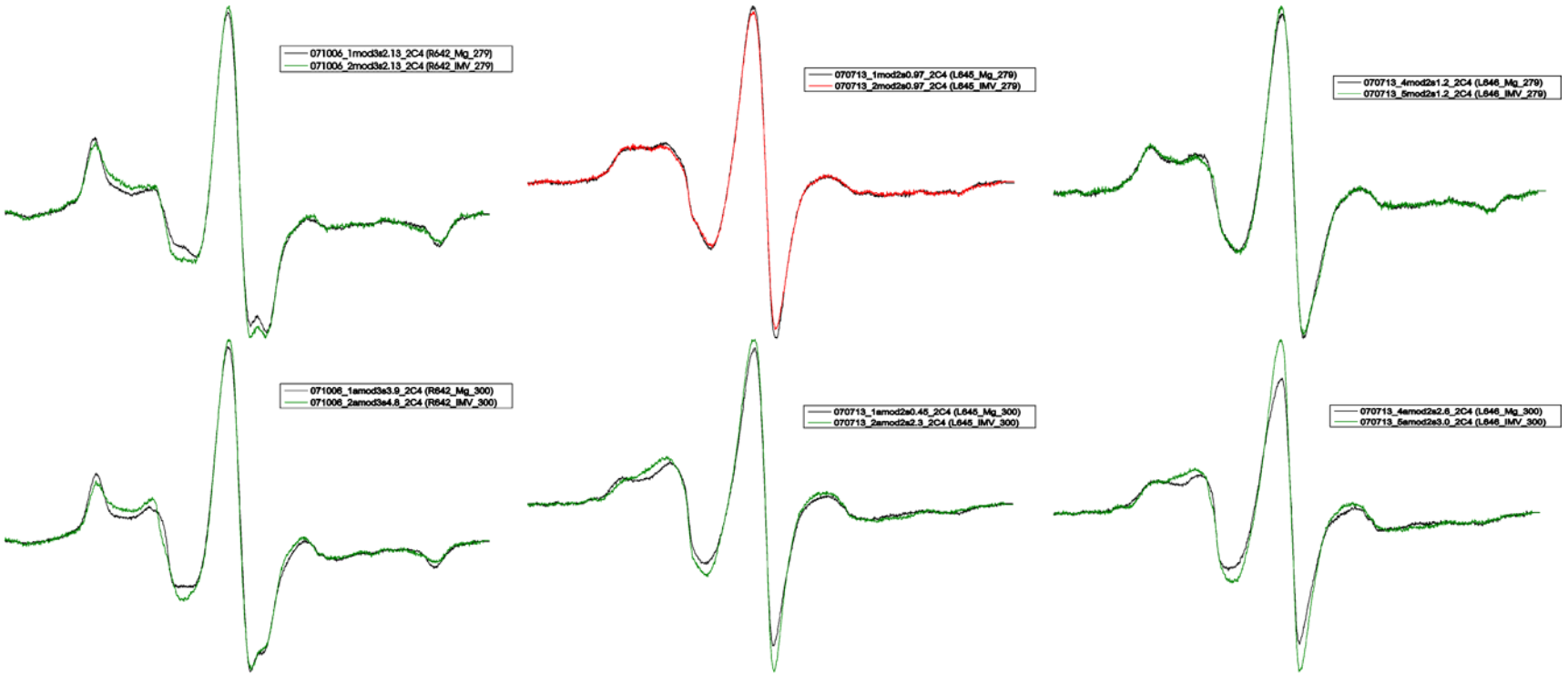

Figure 15 (continued). SecA residues showing mobility with SecYEG.

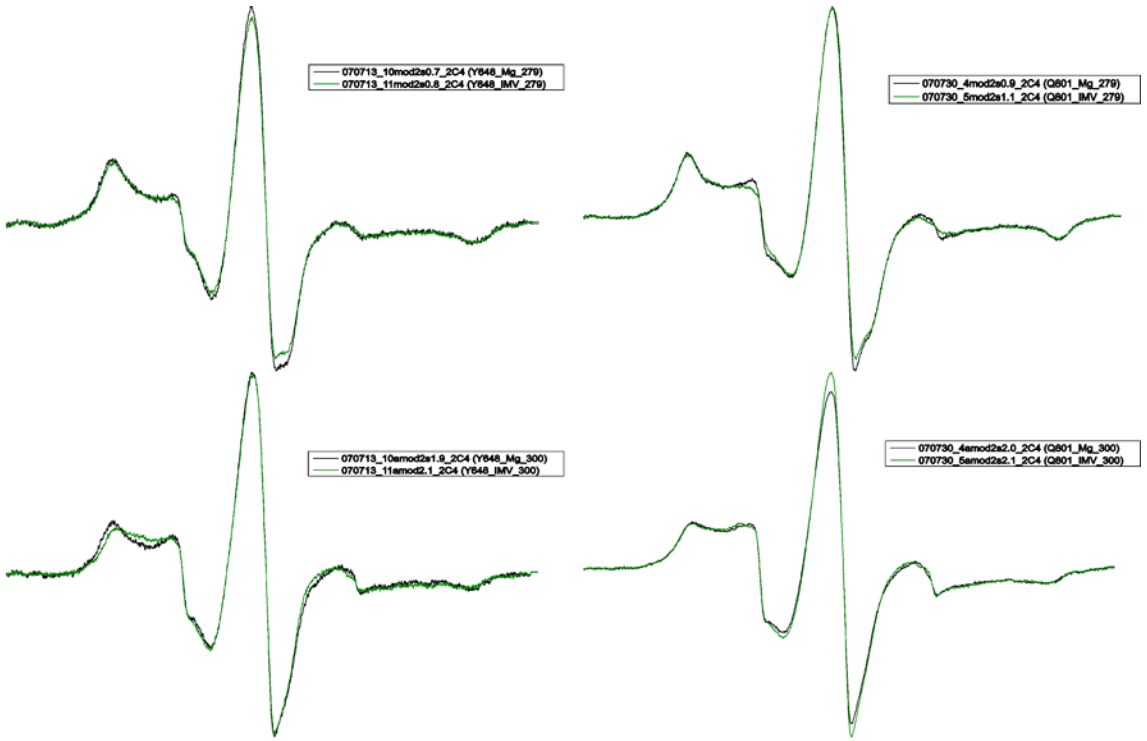

Figure 15 (continued). SecA residues showing mobility with SecYEG.

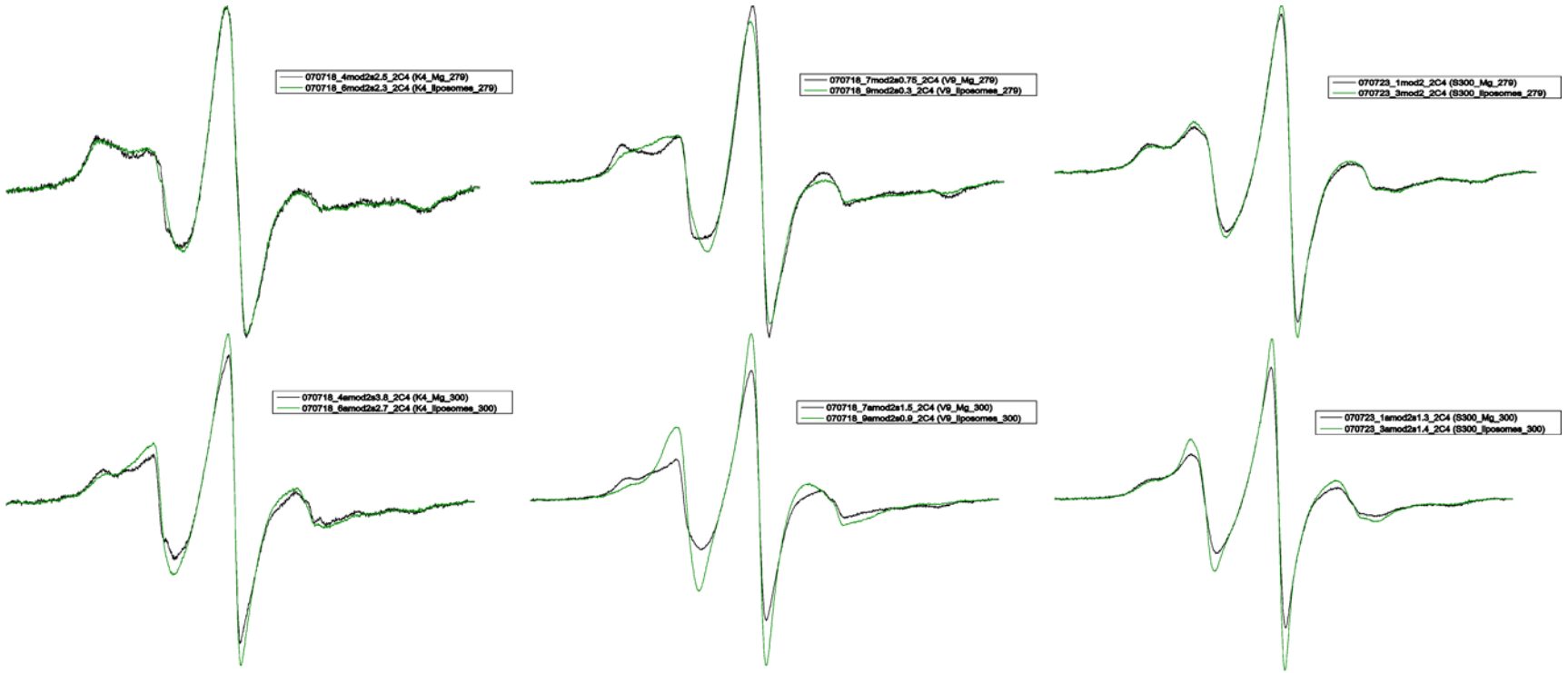

Figure 16. SecA residues showing mobilization with Liposomes.

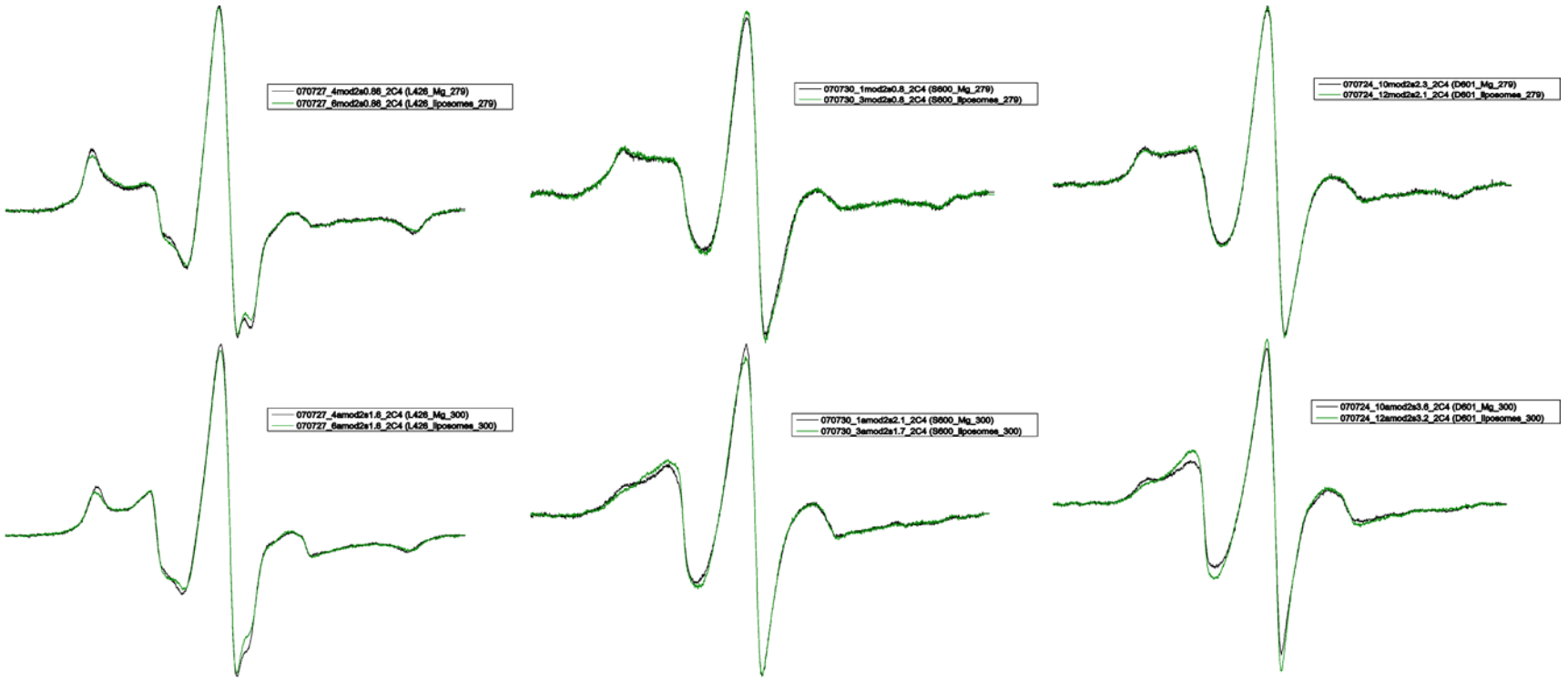

Figure 16 (continued). SecA residues showing mobilization with Liposomes.

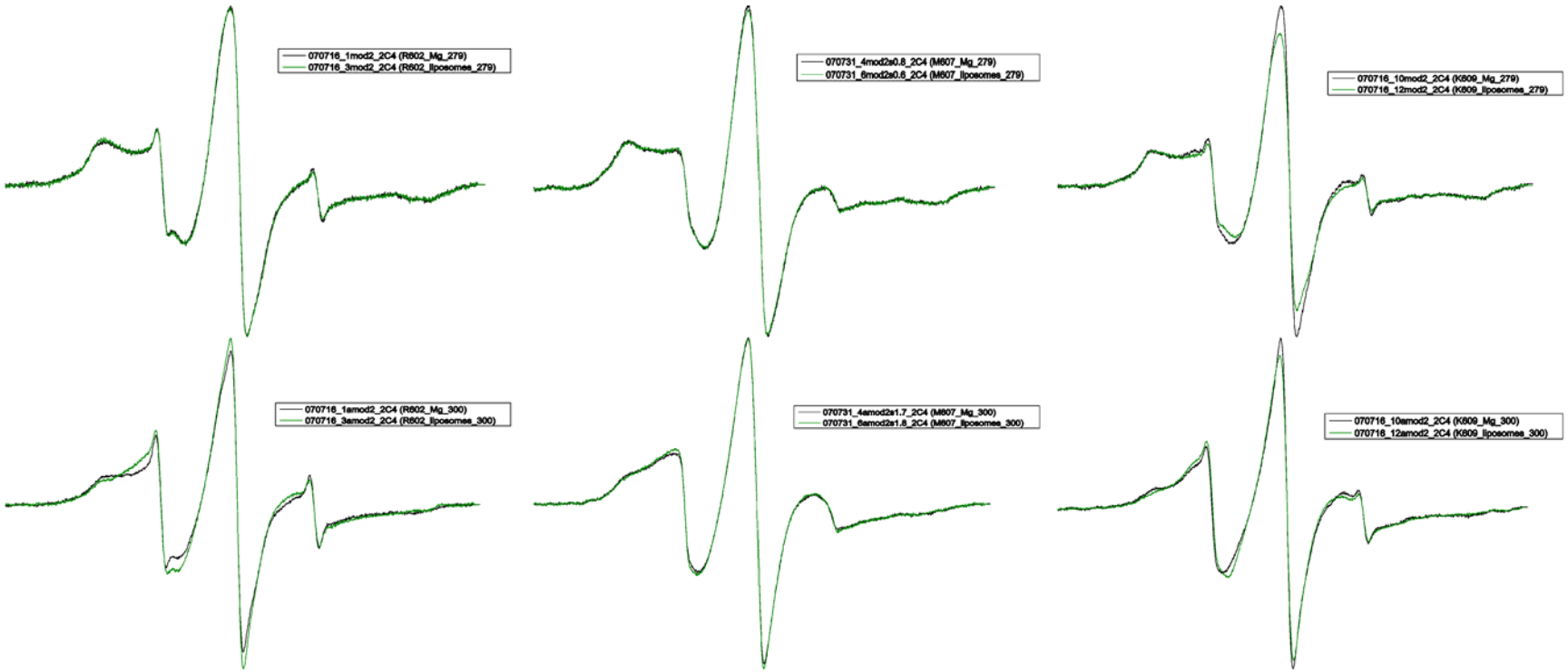

Figure 16 (continued). SecA residues showing mobilization with Liposomes.

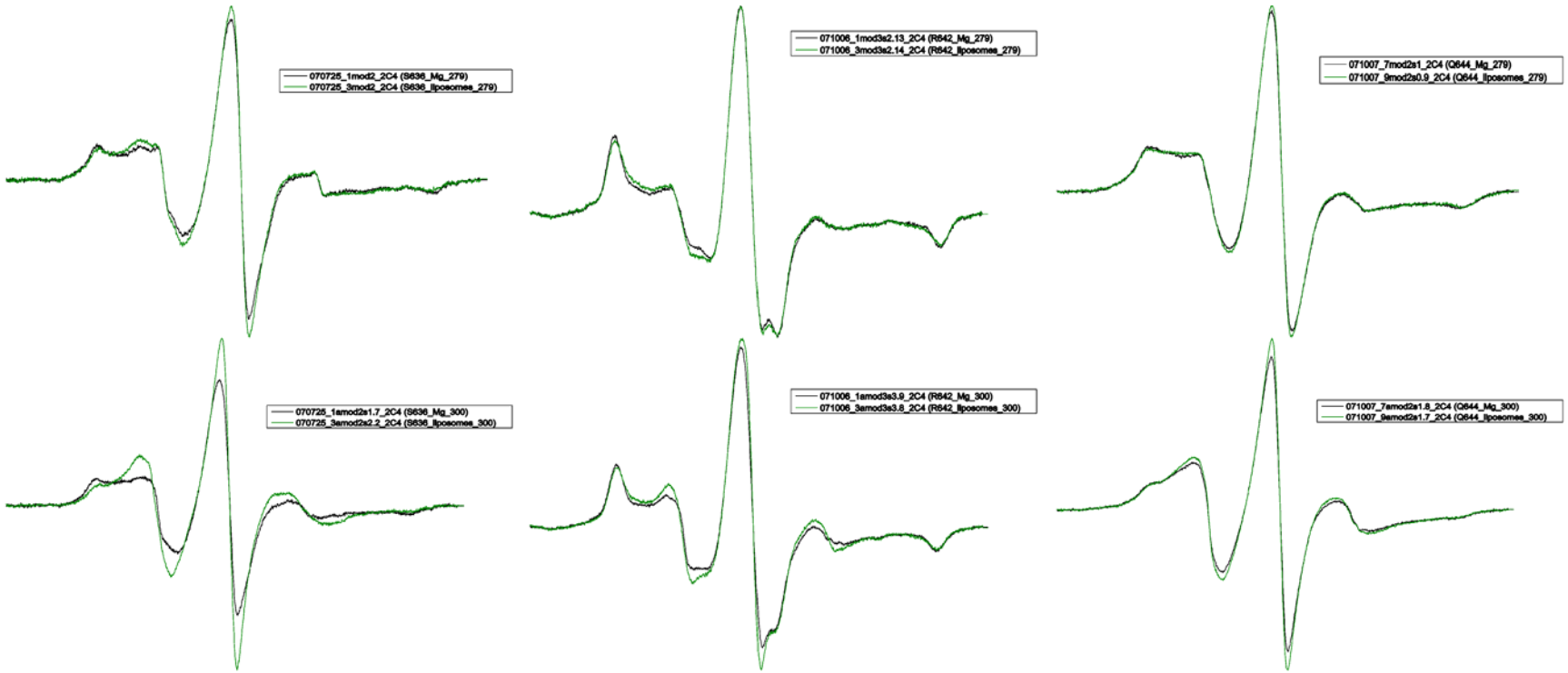

Figure 16 (continued). SecA residues showing mobilization with Liposomes.

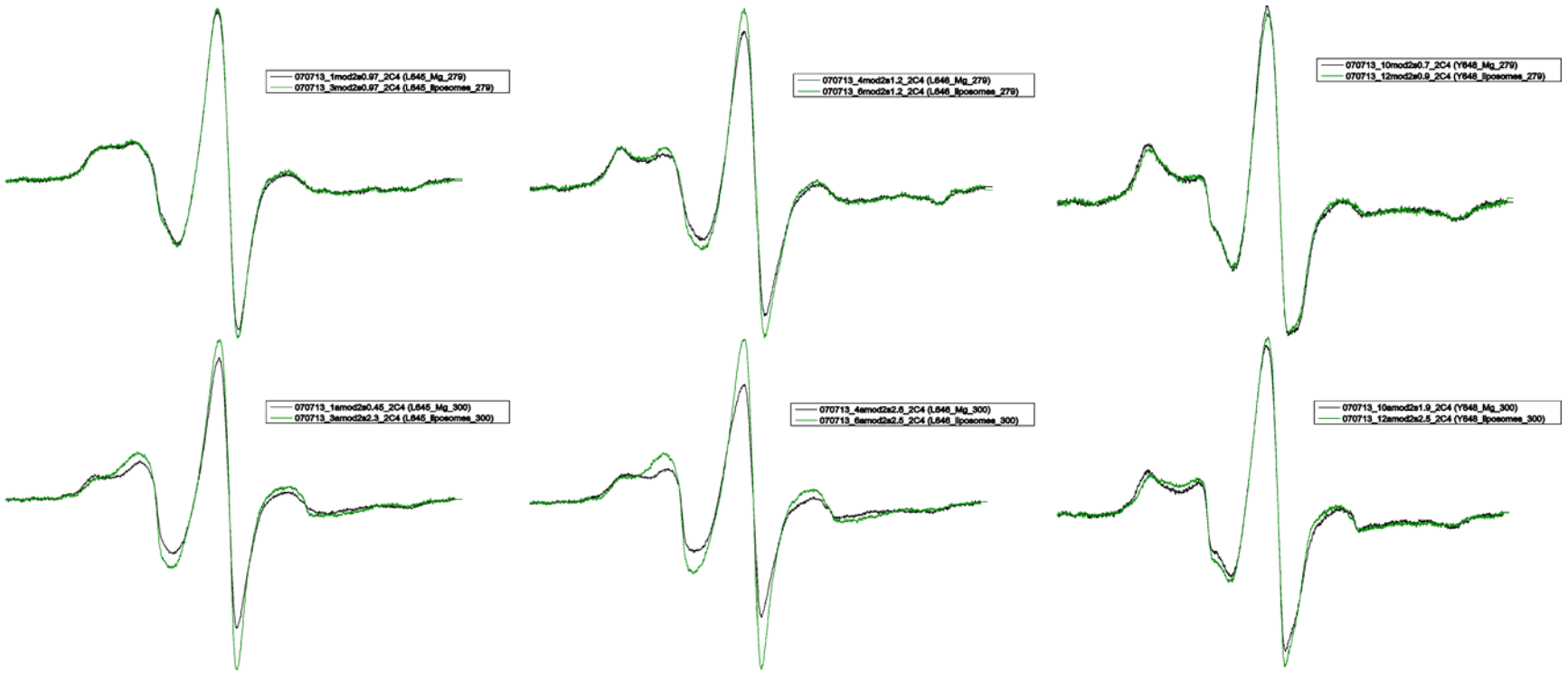

Figure 16 (continued). SecA residues showing mobilization with Liposomes.

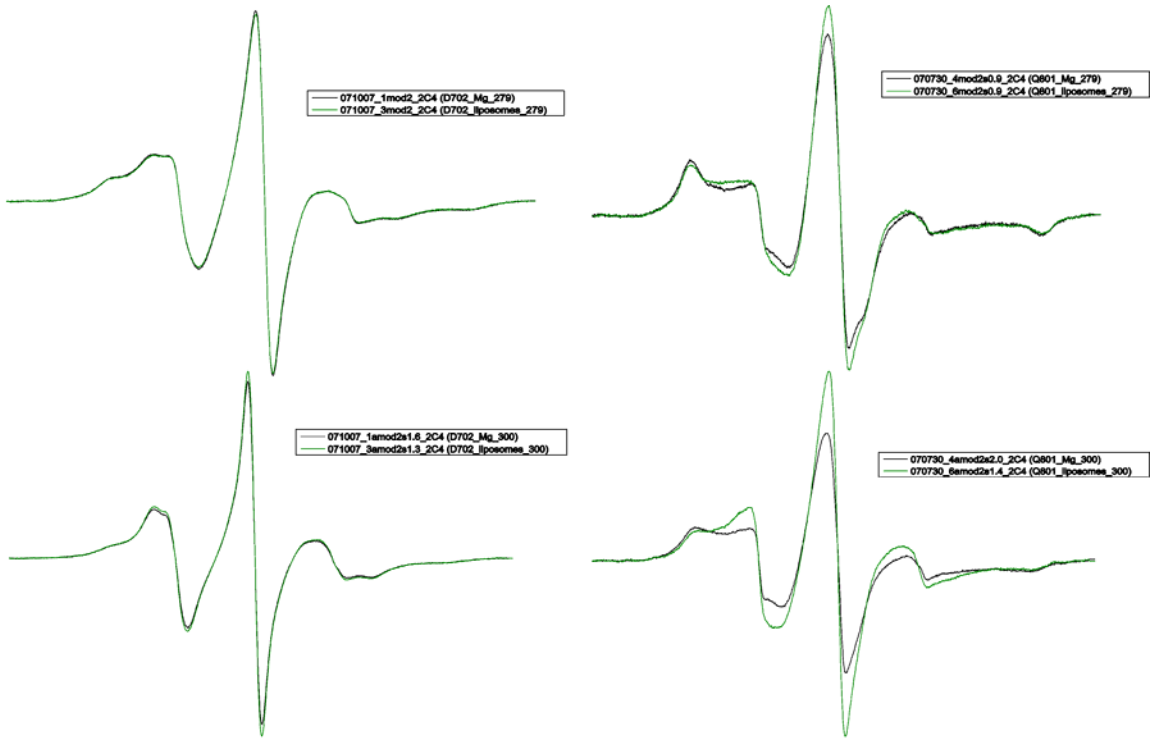

Figure 16 (continued). SecA residues showing mobilization with Liposomes.

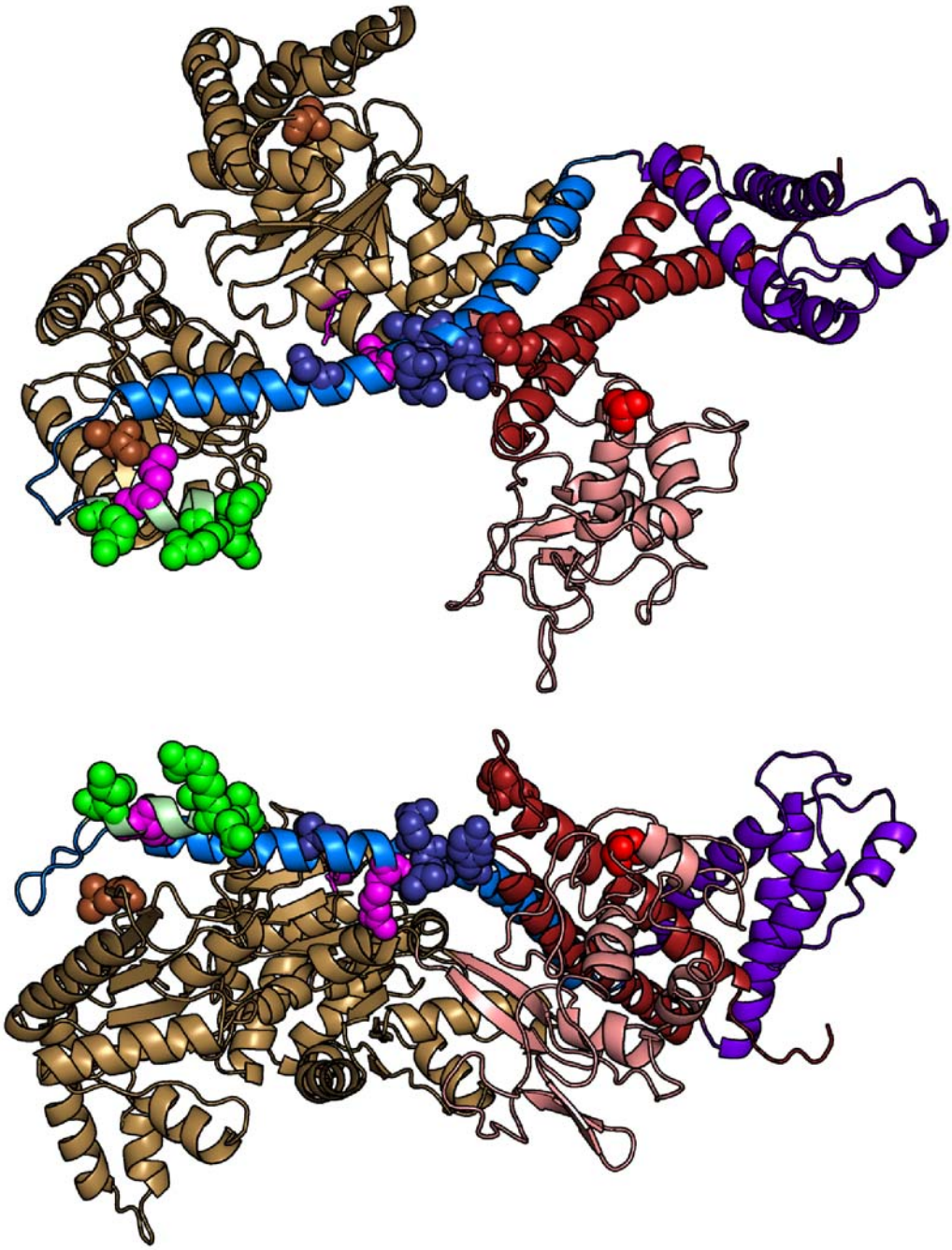

Figure 17. Structures of SecA protomer displaying summary of mobilizations in complex with binding partners. The bottom structure is rotated 90° about the x-axis. Residues mobilized are displayed in CPK. Substitutions at residues in light purple were found by Mori and Ito to cause export defects (E400, ball and stick; R642, CPK) or suppress the defect (M607, CPK).

Appendix

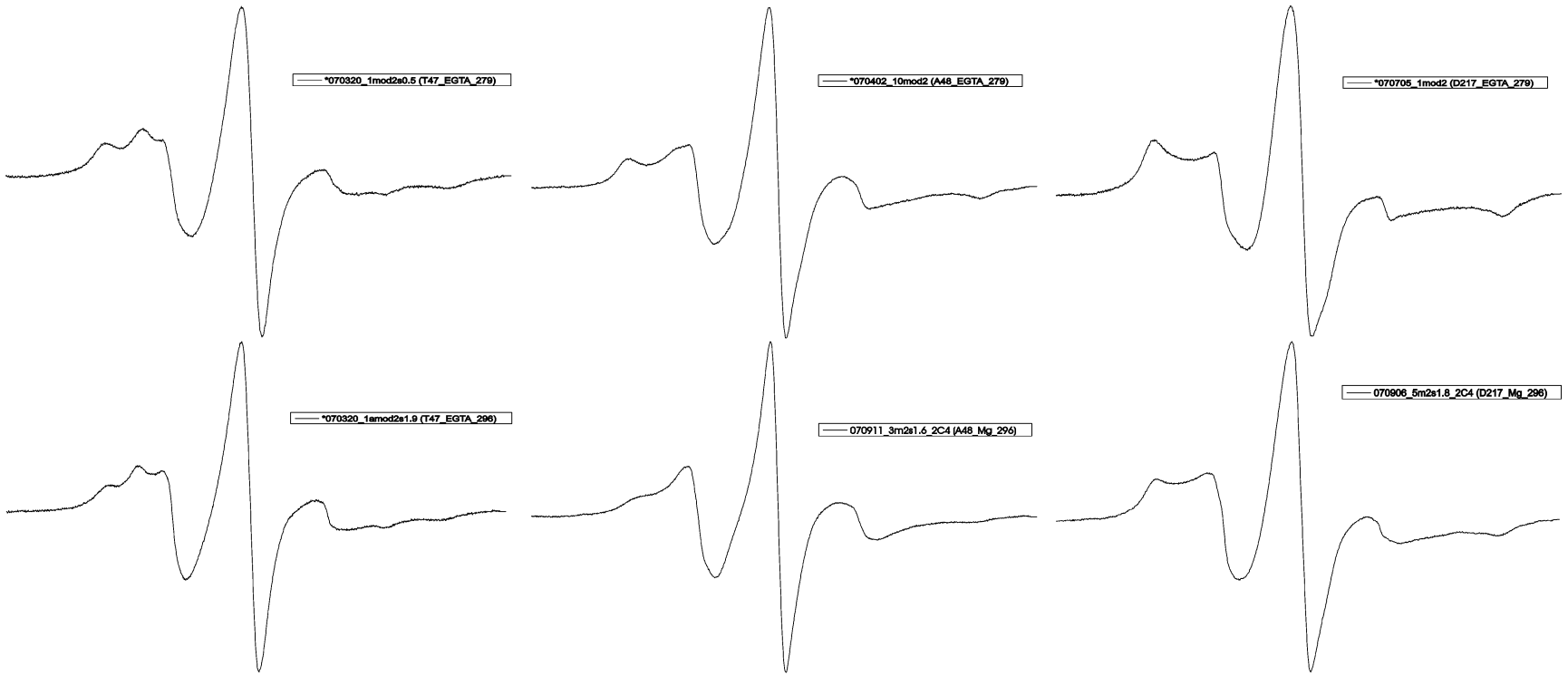

Appendix 1. SecA residues showing no change with precursor, SecB, or SecYEG.

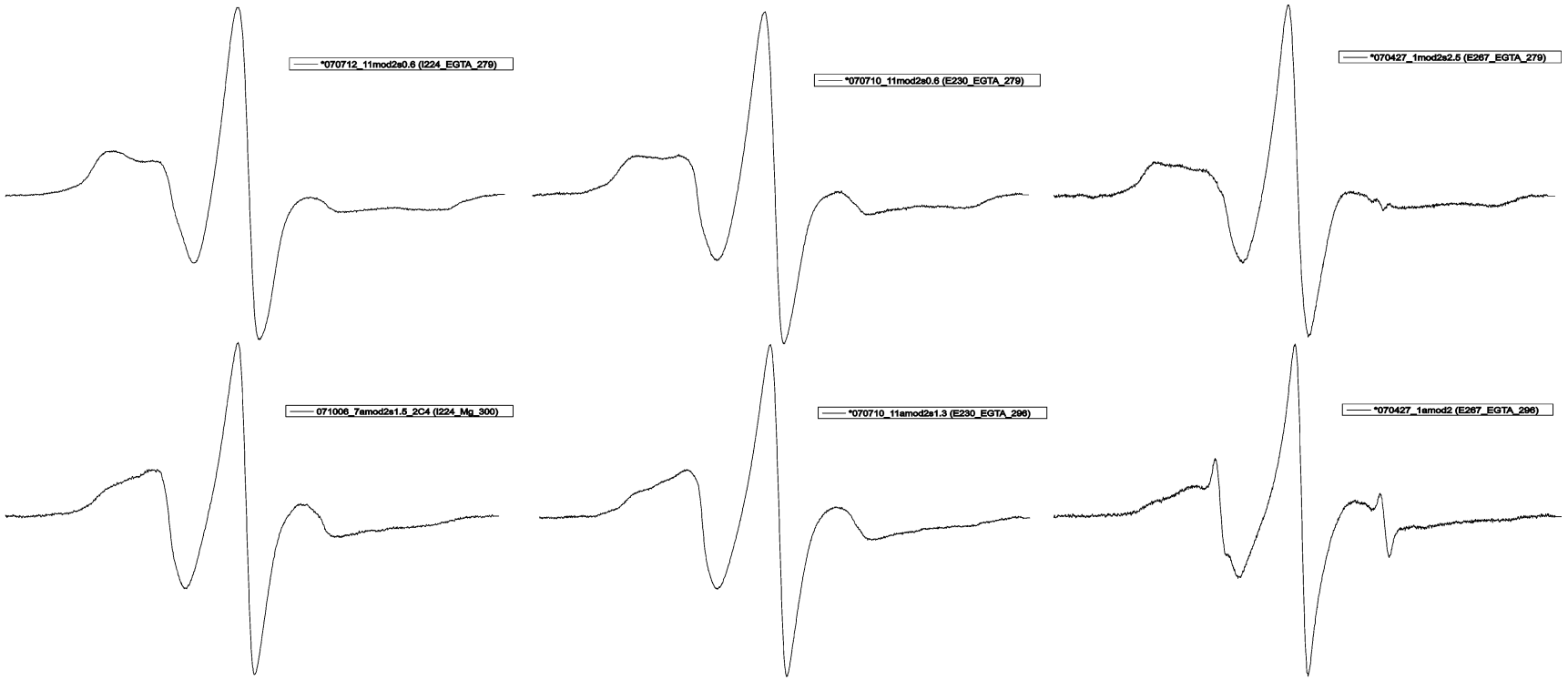

Appendix 1 (continued). SecA residues showing no change with precursor, SecB, or SecYEG.

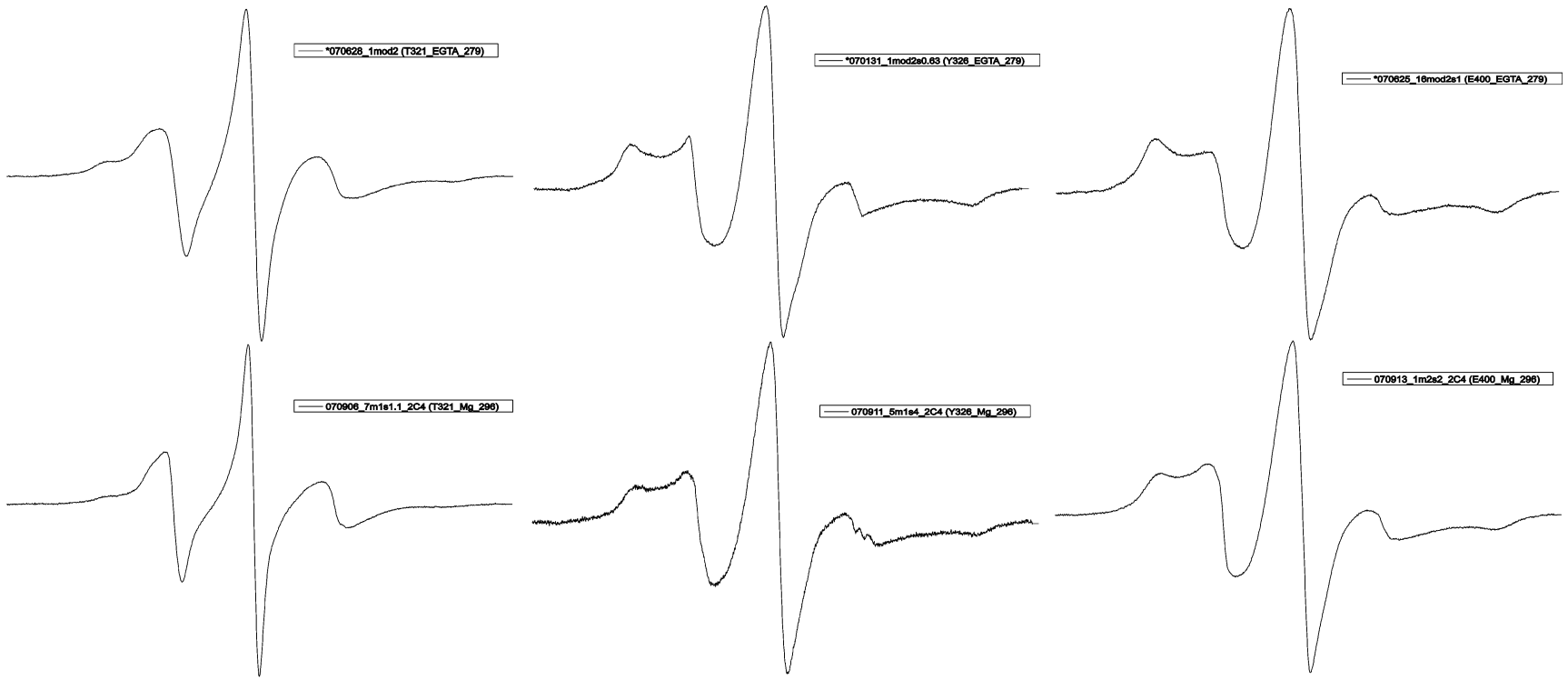

Appendix 1 (continued). SecA residues showing no change with precursor, SecB, or SecYEG.

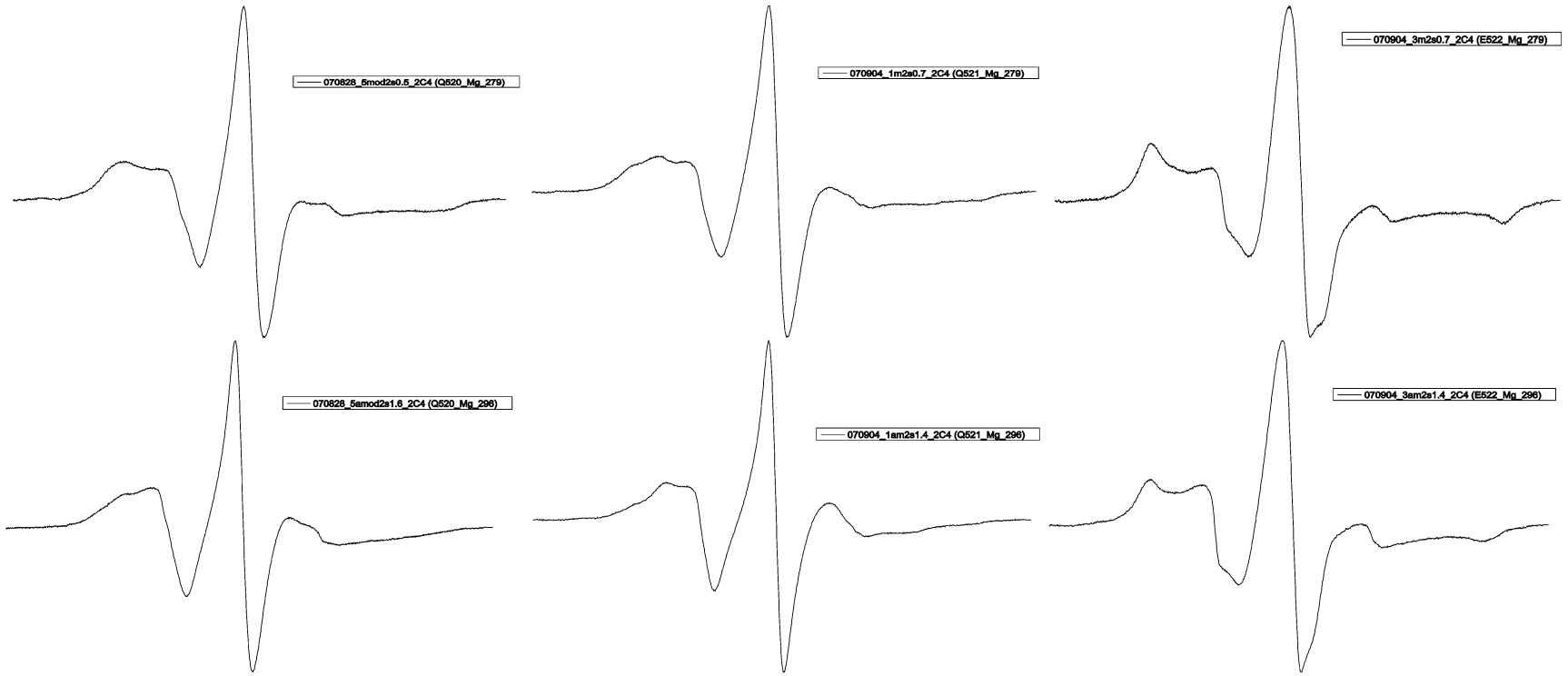

Appendix 1 (continued). SecA residues showing no change with precursor, SecB, or SecYEG.

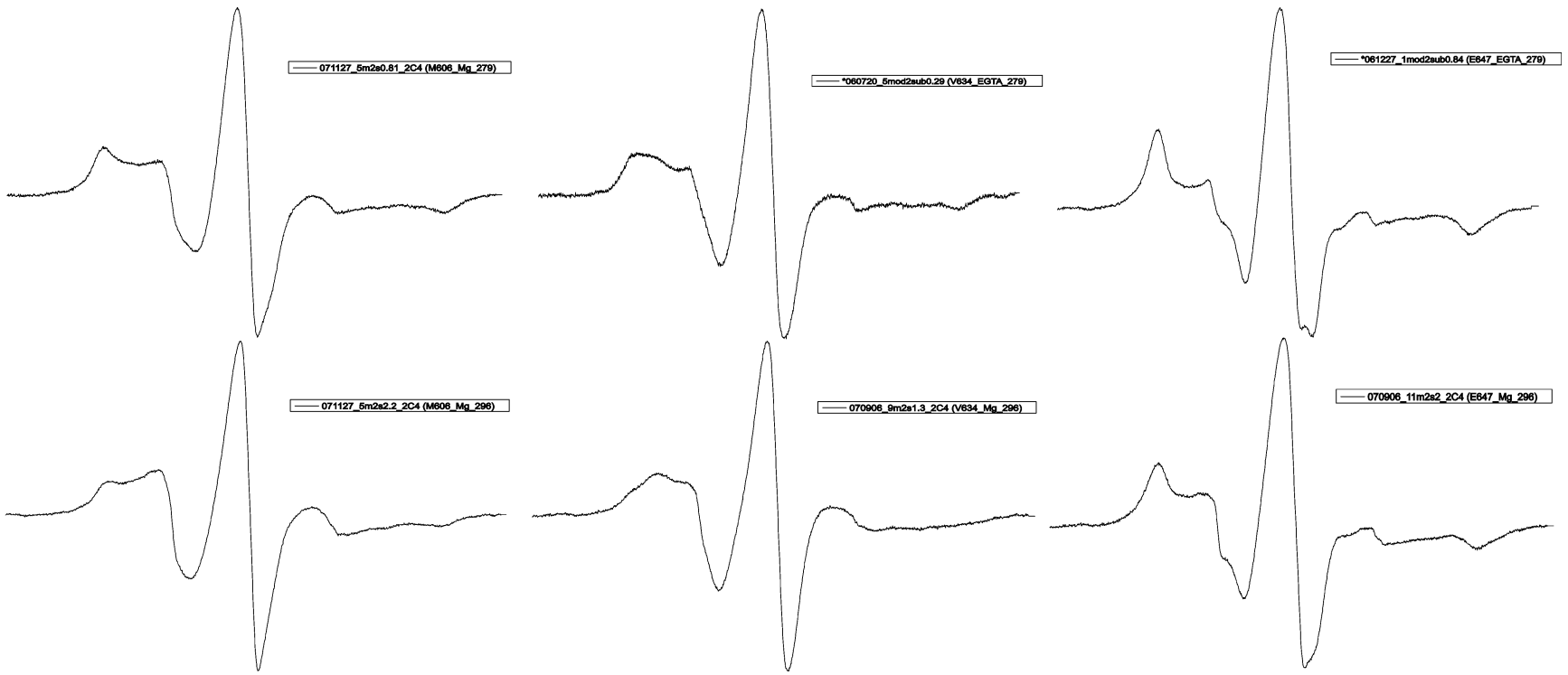

Appendix 1 (continued). SecA residues showing no change with precursor, SecB, or SecYEG.

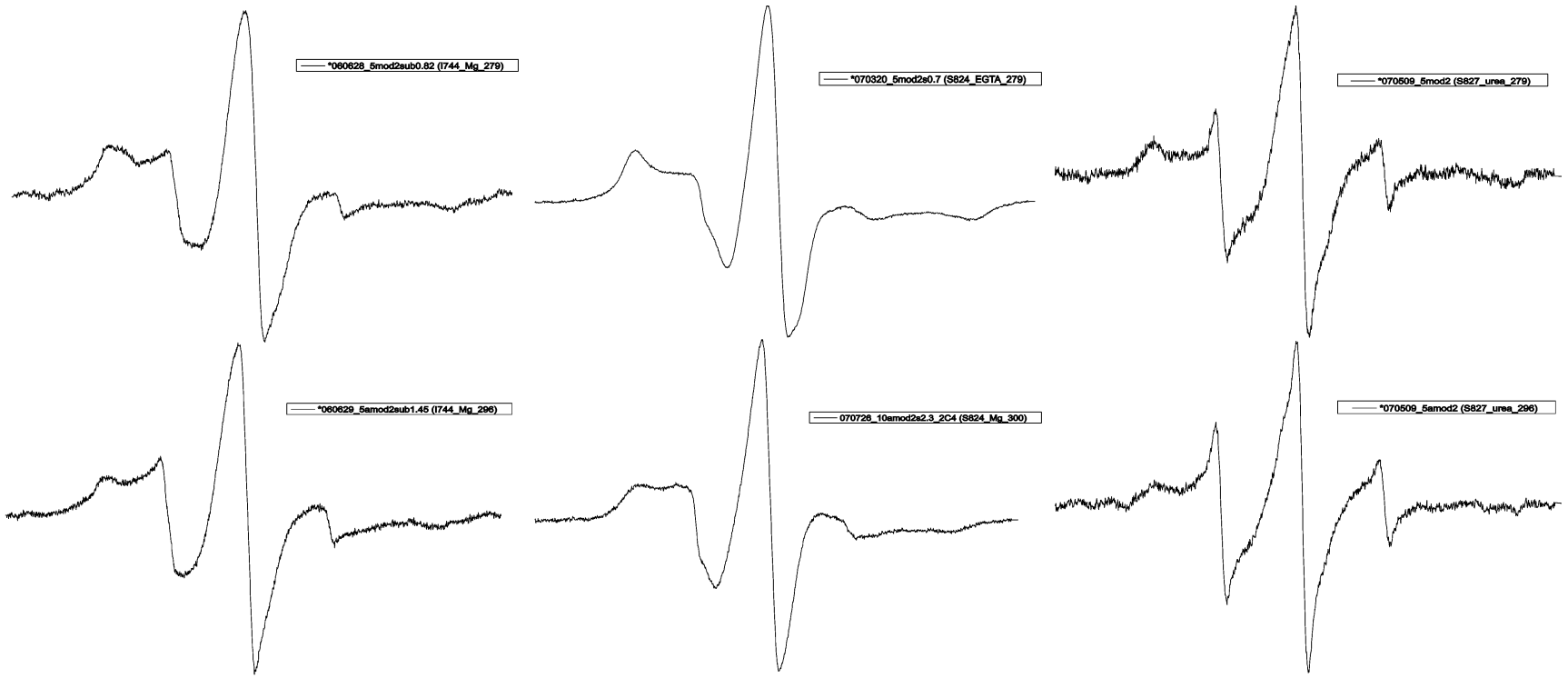

Appendix 1 (continued). SecA residues showing no change with precursor, SecB, or SecYEG.

References

Akimaru, J., Matsuyama, S., Tokuda, H., and Mizushima, S. 1991. Reconstitution of a protein translocation system containing purified SecY, SecE, and SecA from Escherichia coli. *Proc. Natl. Acad. Sci. U S A.* **88:** 6545-6549.

Akita, M., Sasaki, S., Matsuyama, S., and Mizushima, S. 1990. SecA interacts with secretory proteins by recognizing the positive charge at the amino terminus of the signal peptide in Escherichia coli. *J. Biol. Chem.* **265:** 8164-8169.

Brink, S., Bogsch, E.G., Edwards, W.R., Hynds, P.J., and Robinson, C. 1998. Targeting of thylakoid proteins by the delta pH-driven twin-arginine translocation pathway requires a specific signal in the hydrophobic domain in conjunction with the twin-arginine motif. *FEBS Lett.* **434:** 425-430.

Breukink, E., Nouwen, N., van Raalte, A., Mizushima, S., Tommassen, J., and de Kruijff, B. 1995. The C terminus of SecA is involved in both lipid binding and SecB binding. *J. Biol. Chem.* **270:** 7902-7907.

Brundage, L., Hendrick, J.P., Schiebel, E., Driessen, A.J., and Wickner, W. 1990. The purified E. coli integral membrane protein SecY/E is sufficient for reconstitution of SecA-dependent precursor protein translocation. *Cell.* **62:** 649-657.

Brüser, T. 2007. The twin-arginine translocation system and its capability for protein secretion in biotechnological protein production. *Appl. Microbiol. Biotechnol.* **76:** 35-45.

Bu, Z., Wang, L., and Kendall, D.A. 2003. Nucleotide binding induces changes in the oligomeric state and conformation of SecA in a lipid environment: a small-angle neutron-scattering study. *J. Mol. Biol.* **332:** 23-30.

Cabelli, R.J., Chen, L., Tai, P.C., and Oliver, D.B. 1988. SecA protein is required for secretory protein translocation into E. coli membrane vesicles. *Cell* **55:** 683-692.

Chen, X., Xu, H., and Tai, P.C. 1996. A significant fraction of functional SecA is permanently embedded in the membrane. SecA cycling on and off the membrane is not essential during protein translocation. *J. Biol. Chem.* **271:** 29698-29706.

Chou, K.C. 1990. Applications of graph theory to enzyme kinetics and protein folding kinetics. Steady and non-steady-state systems. *Biophysical Chemistry.* **35:** 1-24.

Chou, Y.T., and Gierasch, L.M. 2005. The conformation of a signal peptide bound by Escherichia coli preprotein translocase SecA. *J. Biol. Chem.* **280:** 32753-32760.

Chun, S.Y., and Randall, L.L. 1994. In vivo studies of the role of SecA during protein export in Escherichia coli. *J. Bacteriol.* **176:** 4197-4203.

Collier, D.N., Bankaitis, V.A., Weiss, J.B., Bassford Jr., P.J. 1988. The antifolding activity of SecB promotes the export of the E. coli maltose-binding protein. *Cell.* **53:** 273-283.

Columbus, L., and Hubbell, W.L. 2002. A new spin on protein dynamics. *Trends Biochem. Sci.* **27:** 288-295.

Crane, J.M., Mao, C., Lilly, A.A., Smith, V.F., Suo, Y., Hubbell, W.L., and Randall, L.L. 2005. Mapping of the docking of SecA onto the chaperone SecB by site-directed spin labeling: insight into the mechanism of ligand transfer during protein export. *J. Mol. Biol.* **353:** 295-307.

Crane, J.M., Suo, Y., Lilly, A.A., Mao, C., Hubbell, W.L., and Randall, L.L. 2006. Sites of interaction of a precursor polypeptide on the export chaperone SecB mapped by site-directed spin labeling. *J. Mol. Biol.* **363:** 63-74.

Cunningham, K., and Wickner, W. 1989. Specific recognition of the leader region of precursor proteins is required for the activation of translocation ATPase of Escherichia coli. *Proc. Natl. Acad. Sci. U S A* **86:** 8630-8634.

Dalbey, R.E., Lively, M.O., Bron, S., and van Dijl, J.M. 1997. The chemistry and enzymology of the type I signal peptidases. *Protein Sci.* **6:** 1129-1138.

Dalbey, R.E., and Wickner, W. 1985. Leader peptidase catalyzes the release of exported proteins from the outer surface of the Escherichia coli plasma membrane. *J. Biol. Chem.* **260:** 15925-15931.

Dekker, C., de Kruijff, B., and Gros, P. 2003. Crystal structure of SecB from Escherichia coli. *Journal of Structural Biology* **144:** 313-319.

DeLano, W.L. 2002. The PyMOL Molecular Graphics System. DeLano Scientific, Palo Alto, CA, USA.

den Blaauwen, T., Terpetschnig, E., Lakowicz, J.R., and Driessen, A.J. 1997. Interaction of SecB with soluble SecA. *FEBS Lett.* **416:** 35-38.

Driessen, A.J. 1993. SecA, the peripheral subunit of the Escherichia coli precursor protein translocase, is functional as a dimer. *Biochemistry* **32:** 13190-13197.

Economou, A., Pogliano, J.A., Beckwith, J., Oliver, D.B., and Wickner, W. 1995. SecA membrane cycling at SecYEG is driven by distinct ATP binding and hydrolysis events and is regulated by SecD and SecF. *Cell.* **83:** 1171-1181.

Economou, A., and Wickner, W. 1994. SecA promotes preprotein translocation by undergoing ATP-driven cycles of membrane insertion and deinsertion. *Cell* **78:** 835-843.

Fekkes, P., de Wit, J.G., Boorsma, A., Friesen, R.H., and Driessen, A.J. 1999. Zinc stabilizes the SecB binding site of SecA. *Biochemistry* **38:** 5111-5116.

Fekkes, P., de Wit, J.G., van der Wolk, J.P., Kimsey, H.H., Kumamoto, C.A., and Driessen, A.J. 1998. Preprotein transfer to the Escherichia coli translocase requires the co- operative binding of SecB and the signal sequence to SecA. *Mol. Microbiol.* **29:** 1179-1190.

Fekkes, P., van der Does, C., and Driessen, A.J. 1997. The molecular chaperone SecB is released from the carboxy-terminus of SecA during initiation of precursor protein translocation. *EMBO J.* **16:** 6105-6113.

Gelis, I., Bonvin, A.M., Keramisanou, D., Koukaki, M., Gouridis, G., Karamanou, S., Economou, A., and Kalodimos, C.G. 2007. Structural basis for signal-sequence recognition by the translocase motor SecA as determined by NMR. *Cell* **131:** 756-769.

Gennity, J., Goldstein, J., and Inouye, M. 1990. Signal peptide mutants of Escherichia coli. *Journal of Bioenergetics & Biomembranes.* **22:** 233-269.

Hardy, S.J.S., and Randall, L.L. 1991. A kinetic partitioning model of selective binding of nonnative proteins by the bacterial chaperone SecB. *Science.* **251:** 439-443.

Hartmann, E., Sommer, T., Prehn, S., Gorlich, D., Jentsch, S., and Rapoport, T.A. 1994. Evolutionary conservation of components of the protein translocation complex. *Nature.* **367:** 654-657.

Hikita, C., and Mizushima, S. 1992. The requirement of a positive charge at the amino terminus can be compensated for by a longer central hydrophobic stretch in the functioning of signal peptides. *J. Biol. Chem.* **267:** 12375-12379.

Hunt, J.F., Weinkauf, S., Henry, L., Fak, J.J., McNicholas, P., Oliver, D.B., and Deisenhofer, J. 2002. Nucleotide control of interdomain interactions in the conformational reaction cycle of SecA. *Science* **297:** 2018-2026.

Jilaveanu, L.B., and Oliver, D. 2006. SecA dimer cross-linked at its subunit interface is functional for protein translocation. *J. Bacteriol.* **188:** 335-338.

Jilaveanu, L.B., and Oliver, D. 2007. In vivo membrane topology of Escherichia coli SecA ATPase reveals extensive periplasmic exposure of multiple functionally important domains clustering on one face of SecA. *J. Biol. Chem.* **282:** 4661-4668.

Jilaveanu, L.B., Zito, C.R., and Oliver, D. 2005. Dimeric SecA is essential for protein translocation. *Proc. Natl. Acad. Sci. U S A.* **102:** 7511-7516.

Joly, J.C., and Wickner, W. 1993. The SecA and SecY subunits of translocase are the nearest neighbors of a translocating preprotein, shielding it from phospholipids. *EMBO Journal* **12:** 255-263.

Karamanou, S., Vrontou, E., Sianidis, G., Baud, C., Roos, T., Kuhn, A., Politou, A.S., and Economou, A. 1999. A molecular switch in SecA protein couples ATP hydrolysis to protein translocation. *Mol. Microbiol.* **34:** 1133-1145.

Keramisanou, D., Biris, N., Gelis, I., Sianidis, G., Karamanou, S., Economou, A., and Kalodimos, C.G. 2006. Disorder-order folding transitions underlie catalysis in the helicase motor of SecA. *Nat. Struct. Mol. Biol.* **13:** 594-602.

Kim, Y.J., Rajapandi, T., and Oliver, D. 1994. SecA protein is exposed to the periplasmic surface of the E. coli inner membrane in its active state. *Cell* **78:** 845-853.

Kimura, E., Akita, M., Matsuyama, S., and Mizushima, S. 1991. Determination of a region in SecA that interacts with presecretory proteins in Escherichia coli. *J Biol Chem* **266:** 6600-6606.

Kuhn, A., and Wickner, W. 1985. Conserved residues of the leader peptide are essential for cleavage by leader peptidase. *J. Biol. Chem.* **260:** 15914-15918.

Lill, R., Dowhan, W., and Wickner, W. 1990. The ATPase activity of SecA is regulated by acidic phospholipids, SecY, and the leader and mature domains of precursor proteins. *Cell* **60:** 271-280.

Liu, G., Topping, T.B., and Randall, L.L. 1989. Physiological role during export for the retardation of folding by the leader peptide of maltose-binding protein. *Proc. Natl. Acad. Sci. U S A* **86:** 9213-9217.

Matsumoto, G., Yoshihisa, T., and Ito, K. 1997. SecY and SecA interact to allow SecA insertion and protein translocation across the Escherichia coli plasma membrane. *EMBO Journal* **16:** 6384-6393.

Menetret, J.F., Schaletzky, J., Clemons Jr., W.M., Osborne, A.R., Skanland, S.S., Denison, C., Gygi, S.P., Kirkpatrick, D.S., Park, E., Ludtke, S.J., Rapoport, T.A., and Akey, C.W. 2007. Ribosome binding of a single copy of the SecY complex: implications for protein translocation. *Mol. Cell.* **28:** 1083-1092.

Miller, A., Wang, L., and Kendall, D.A. 2002. SecB modulates the nucleotide-bound state of SecA and stimulates ATPase activity. *Biochemistry.* **41:** 5325-5332.

Mitchell, C., and Oliver, D. 1993. Two distinct ATP-binding domains are needed to promote protein export by Escherichia coli SecA ATPase. *Mol Microbiol* **10:** 483-497.

Mori, H., and Ito, K. 2001. The Sec protein-translocation pathway. *Trends Micro.* **9:** 494-500.

Mori, H., and Ito, K. 2006. The long alpha-helix of SecA is important for the ATPase coupling of translocation. *J. Biol. Chem.* **281:** 36249-36256.

Múren, E.M., Suciu, D., Topping, T.B., Kumamoto, C.A., and Randall, L.L. 1999. Mutational alterations in the homotetrameric chaperone SecB that implicate the structure as dimer of dimers. *J. Biol. Chem.* **274:** 19397-19402.

Musial-Siwek, M., Rusch, S.L., and Kendall, D.A. 2007. Selective photoaffinity labeling identifies the signal peptide binding domain on SecA. *J. Mol. Biol.* **365:** 637-648.

Oliver, D.B., Cabelli, R.J., and Jarosik, G.P. 1990. SecA protein: autoregulated initiator of secretory precursor protein translocation across the E. coli plasma membrane. *J Bioenerg Biomembr* **22:** 311-336.

Or, E., Boyd, D., Gon, S., Beckwith, J., and Rapoport, T. 2005. The bacterial ATPase SecA functions as a monomer in protein translocation. *J. Biol. Chem.* **280:** 9097-9105.

Or, E., Navon, A., and Rapoport, T. 2002. Dissociation of the dimeric SecA ATPase during protein translocation across the bacterial membrane. *EMBO J.* **21:** 4470-4479.

Or, E., Rapoport, T. 2007. Cross-linked SecA dimers are not functional in protein translocation. *FEBS Lett.* **581:** 2616-2620.

Osborne, A.R., Clemons, W.M., and Rapoport, T.A. 2004. A large conformational change of the translocation ATPase SecA. *Proc. Natl. Acad. Sci. U S A.* **101:** 10937-10942.

Papanikolau, Y., Papadovasilaki, M., Ravelli, R.B., McCarthy, A.A., Cusack, S., Economou, A., Petratos, K. 2007. Structure of dimeric SecA, the Escherichia coli preprotien translocase motor. *J. Mol. Biol.* **366:** 1545-1557.

Papanikou, E., Karamanou, S., Baud, C., Frank, M., Sianidis, G., Keramisanou, D., Kalodimos, C.G., Kuhn, A., and Economou, A. 2005. Identification of the preprotein binding domain of SecA. *J. Biol. Chem.* **280:** 43209-43217.

Park, S., Liu, G., Topping, T.B., Cover, W.H., and Randall, L.L. 1988. Modulation of folding pathways of exported proteins by the leader sequence. *Science* **239:** 1033-1035.

Patel, C.N., Smith, V.F., and Randall, L.L. 2006. Characterization of three areas of interactions stabilizing complexes between SecA and SecB, two proteins involved in protein export. *Protein Sci.* **15:** 1379-1386.

Powers, E.L., and Randall, L.L. 1995. Export of periplasmic galactose-binding protein in Escherichia coli depends on the chaperone SecB. *J. Bacteriol.* **177:** 1906-1907.

Price, A., Economou, A., Duong, F., and Wickner, W. 1996. Separable ATPase and membrane insertion domains of the SecA subunit of preprotein translocase. *J. Biol. Chem.* **271:** 31580-31584.

Randall, L.L. 1983. Translocation of domains of nascent periplasmic proteins across the cytoplasmic membrane is independent of elongation. *Cell.* **33:** 231-240.

Randall, L.L., and Hardy, S.J. 1986. Correlation of competence for export with lack of tertiary structure of the mature species: a study in vivo of maltose-binding protein in E. coli. *Cell.* **46:** 921-928.

Randall, L.L., and Hardy, S.J. 1995. High selectivity with low specificity: how SecB has solved the paradox of chaperone binding. *Trends Biochem. Sci.* **20:** 65-69.

Randall, L.L., Crane, J.M., Lilly, A.A., Liu, G., Mao, C., Patel, C.N., and Hardy, S.J.S. 2005. Asymmetric binding between SecA and SecB two symmetric proteins: implications for function in export. *J. Mol. Biol.* **348:** 479-489.

Randall, L.L., Topping, T.B., and Hardy, S.J. 1990. No specific recognition of leader peptide by SecB, a chaperone involved in protein export. *Science* **248:** 860-863.

Sargent, F., Berks, B.C., Palmer, T. 2006. Pathfinders and trailblazers: a prokaryotic targeting system for transport of folded proteins. *FEMS Microbiol. Lett.* **254:** 198-207.

Schiebel, E., Driessen, A.J., Hartl, F.U., and Wickner, W. 1991. Delta mu H+ and ATP function at different steps of the catalytic cycle of preprotein translocase. *Cell* **64:** 927-939.

Schmidt, M.G., Rollo, E.E., Grodberg, J., and Oliver, D.B. 1988. Nucleotide sequence of the secA gene and secA(Ts) mutations preventing protein export in Escherichia coli. *J. Bact.* **170:** 3404-3414.

Sharma, V., Arockiasamy, A., Ronning, D.R., Savva, C.G., Holzenburg, A., Braunstein, M., Jacobs, W.R., Jr., and Sacchettini, J.C. 2003. Crystal structure of Mycobacterium tuberculosis SecA, a preprotein translocating ATPase. *Proc. Natl. Acad. Sci. U S A.* **100:** 2243-2248.

Smith, V.F., Schwartz, B.L., Randall, L.L., and Smith, R.D. 1996. Electrospray mass spectrometric investigation of the chaperone SecB. *Protein Sci.* **5:** 488-494.

Topping, T.B., and Randall, L.L. 1997. Chaperone SecB from Escherichia coli mediates kinetic partitioning via a dynamic equilibrium with its ligands. *J. Biol. Chem.* **272:** 19314-19318.

Topping, T.B., Woodbury, R.L., Diamond, D.L., Hardy, S.J., and Randall, L.L. 2001. Direct demonstration that homotetrameric chaperone SecB undergoes a dynamic dimer-tetramer equilibrium. *J. Biol. Chem.* **276:** 7437-7441.

van der Does, C., den Blaauwen, T., de Wit, J.G., Manting, E.H., Groot, N.A., Fekkes, P., and Driessen, A.J. 1996. SecA is an intrinsic subunit of the Escherichia coli preprotein translocase and exposes its carboxyl terminus to the periplasm. *Mol. Microbiol.* **22:** 619-629.

van der Wolk, J.P., de Wit, J.G., and Driessen, A.J. 1997. The catalytic cycle of the Escherichia coli SecA ATPase comprises two distinct preprotein translocation events. *EMBO J.* **16:** 7297-7304.

Vassylyev, D.G., Mori, H., Vassylyeva, M.N., Tsukazaki, T., Kimura, Y., Tahirov, T.H., and Ito, K. 2006. Crystal structure of the translocation ATPase SecA from Thermus thermophilus reveals a parallel, head-to-head dimer. *J. Mol. Biol.* **364:** 248-258.

Walter, P., and Johnson, A.E. 1994. Signal sequence recognition and protein targeting to the endoplasmic reticulum membrane. *Annu. Rev. Cell Biol.* **10:** 87-119.

Woodbury, R.L., Topping, T.B., Diamond, D.L., Suciu, D., Kumamoto, C.A., Hardy, S.J., and Randall, L.L. 2000. Complexes between protein export chaperone SecB and SecA. Evidence for separate sites on SecA providing binding energy and regulatory interactions. *J. Biol. Chem.* **275:** 24191-24198.

Zimmer, J., Li, W., and Rapoport, T.A. 2006. A novel dimer interface and conformational changes revealed by an X-ray structure of B. subtilis SecA. *J. Mol. Biol.* **364:** 259-265.

Zwizinski, C., and Wickner, W. 1980. Purification and characterization of leader (signal) peptidase from Escherichia coli. *J. Biol. Chem.* **255:** 7973-7977.